

TURBULENCE MEASURING SYSTEM UTILIZING A  
SONIC ANEMOMETER/THERMOMETER

Peter Douglas Quinton

INTERNALLY  
DISTRIBUTED REPORT

Library  
Naval Postgraduate School  
Monterey, California 93940

INTERVALY INST 1957  
REPORT

NAVAL POSTGRADUATE SCHOOL  
Monterey, California



THESIS

TURBULENCE MEASURING SYSTEM UTILIZING  
A  
SONIC ANEMOMETER/THERMOMETER

by

Peter Douglas Quinton

Thesis Advisor:

K. L. Davidson

March 1973

T 154589



INTERNAIY DISTRICTED  
REPORT

Turbulence Measuring System Utilizing  
a  
Sonic Anemometer/Thermometer

by

Peter Douglas Quinton  
Lieutenant Commander, United States Navy  
B.S., United States Naval Academy, 1963

Submitted in partial fulfillment of the  
requirements for the degree of

MASTER OF SCIENCE IN METEOROLOGY

from the  
NAVAL POSTGRADUATE SCHOOL  
March 1973

1711  
1712  
1713

# ABSTRACT

The general characteristics and the bandwidth response of the Kaijo Denki PAT 313-1 sonic anemometer/thermometer were examined. Measurements were compared to those of a hot wire anemometer system and a one mil thermocouple system. Turbulence data were obtained by all three systems simultaneously in two experiments conducted at a beach site. The sonic anemometer/thermometer system proved to be a reliable, rugged, easily installed system with a bandwidth response of from 0.0 Hz to approximately 12.0 Hz.





## TABLE OF CONTENTS

I.	INTRODUCTION -----	11
A.	PROBLEM -----	11
B.	OBJECTIVES -----	11
II.	GENERAL DESCRIPTION AND OPERATING PROCEDURES OF THE SONIC ANEMOMETER/THERMOMETER MODEL PAT 313-1 -----	12
A.	GENERAL -----	12
B.	COMPONENT PARTS OF THE SONIC ANEMOMETER/THERMOMETER -----	12
1.	Power Supply/Indicator Unit (PR-1) -----	12
2.	Probe (TR-31) -----	13
3.	Junction Box (OA-33H) -----	18
C.	ADVANTAGES/DISADVANTAGES OF THE SONIC ANEMOMETER/THERMOMETER -----	18
D.	MEASUREMENT PROCESS -----	24
1.	Wind Measurement -----	24
2.	Temperature Measurement -----	26
3.	Discussion of Possible Errors in Wind Velocity and Temperature Measurements -----	27
4.	Timing Sequence -----	30
III.	DATA ANALYSIS -----	34
A.	GENERAL -----	34
B.	KOLMOGOROV'S HYPOTHESES -----	35
1.	General -----	35
2.	Kolmogorov's First Hypothesis: Equilibrium Range -----	36



3.	Kolmogorov's Second Hypothesis: Inertial Subrange -----	36
C.	ANALOG TO DIGITAL PROCEDURES -----	37
1.	General -----	37
2.	Considerations Prior to Digitization ----	39
D.	CONVERSION OF SEVEN TRACK TO NINE TRACK -----	41
E.	FOURIER COEFFICIENT COMPUTATIONS -----	42
F.	UBCSCOR PROGRAM -----	43
IV.	FIELD EXPERIMENTS -----	45
A.	PRELIMINARIES -----	45
B.	OBJECTIVE OF EXPERIMENTS -----	45
C.	EXPERIMENTS -----	46
1.	Installation of Instruments -----	46
2.	Experiment I - 14 Dec 1972 -----	46
3.	Experiment II- 27 Feb 1973 -----	51
V.	RESULTS AND CONCLUSIONS -----	54
A.	GENERAL PERFORMANCE OF SONIC ANEMOMETER/THERMOMETER -----	54
B.	SPECTRA PLOTS -----	54
1.	General -----	54
2.	Sonic Anemometer/Thermometer Data Sampled at 390.5 Hz - 14 Dec 1972 (Experiment I) -----	56
3.	Sonic Anemometer/Thermometer Data Sampled at 62.5 Hz - 14 Dec 1972 (Experiment I) -----	56
4.	Hot Wire Anemometer Data Sampled at 200.0 Hz - 10 Jan 1973 -----	56



5.	Sonic Anemometer/Thermometer Data Sampled at 62.5 Hz - 28 Feb 1973 (Experiment II) -----	79
6.	Hot Wire Anemometer Data Sampled at 200.0 Hz - 28 Feb 1973 (Experiment II) -----	79
7.	Thermocouple Data Sampled at 200.0 Hz - 28 Feb 1973 (Experiment II) -----	79
C.	CONCLUSIONS -----	79
APPENDIX A -	Definition of Terms Used in Analog-Digital Data Processing -----	94
BIBLIOGRAPHY	-----	96
INITIAL DISTRIBUTION LIST	-----	97
FORM DD 1473	-----	98



## LIST OF FIGURES

1.	Wind and Sonic Axes -----	14
2.	Power Supply/Indicator Unit (PR-1) -----	15
3.	Wind Unit (PD-11) -----	16
4.	Temperature Unit (PS-11) -----	17
5.	Wind Direction Limits of Probe Type TR-31. Kaijo Denki (1969) -----	19
6.	Probe Head. Kaijo Denki (1969) -----	19
7.	Probe Type, TR-31. Kaijo Denki (1969) -----	20
8.	Junction Box (OA-33H). Kaijo Denki (1969) -----	21
9.	Wiring Diagram of PAT-313-1 System. Kaijo Denki (1969) -----	21
10.	Schematic of Typical Measuring Process and Nomenclature -----	25
11A.	Temperature Compensating Constant. Kaijo Denki (1969) -----	29
11B.	Humidity Compensation Graph. Kaijo Denki (1969) -----	29
12.	Error by Wind Velocity. Kaijo Denki (1969) -----	30
13.	Timing Sequence Schematic. Kaijo Denki (1969) ---	32
14.	Temperature and Time Relationship. Kaijo Denki (1969) -----	33
15.	Schematic Drawing of Spectral Energy Transfer in Free Convection. Lumley and Panofsky (1964) -----	38
16.	Arrangement of Probes for Experiments I and II -----	47
17.	Close-up of Probe Arrangement -----	48





18.	Probe Stand Orientation -----	49
19.	Inside Installation of Equipment -----	50
20.	Strip Chart Recording of the Sonic A and W Channels Indicating Spikes -----	52
21.	Sonic "A" Channel Data Observed 14 December 1972 1st Period (Experiment I) High Sample Rate -----	57
22.	Sonic "B" Channel Data Observed 14 December 1972 1st Period (Experiment I) High Sample Rate -----	58
23.	Sonic "W" Channel Data Observed 14 December 1972 1st Period (Experiment I) High Sample Rate -----	59
24.	Sonic "T" Channel Data Observed 14 December 1972 1st Period (Experiment I) High Sample Rate -----	60
25.	Sonic "A" Channel Data Observed 14 December 1972 2nd Period (Experiment I) High Sample Rate -----	61
26.	Sonic "B" Channel Data Observed 14 December 1972 2nd Period (Experiment I) High Sample Rate -----	62
27.	Sonic "W" Channel Data Observed 14 December 1972 2nd Period (Experiment I) High Sample Rate -----	63
28.	Sonic "T" Channel Data Observed 14 December 1972 2nd Period (Experiment I) High Sample Rate -----	64
29.	Sonic "A" Channel Data Observed 14 December 1972 3rd Period (Experiment I) High Sample Rate -----	65
30.	Sonic "B" Channel Data Observed 14 December 1972 3rd Period (Experiment I) High Sample Rate -----	66
31.	Sonic "W" Channel Data Observed 14 December 1972 3rd Period (Experiment I) High Sample Rate -----	67



32.	Sonic "T" Channel Data Observed 14 December 1972 3rd Period (Experiment I) High Sample Rate -----	68
33.	Sonic "A" Channel Data Observed 14 December 1972 2nd Period (Experiment I) Low Sample Rate -----	69
34.	Sonic "B" Channel Data Observed 14 December 1972 2nd Period (Experiment I) Low Sample Rate -----	70
35.	Sonic "W" Channel Data Observed 14 December 1972 2nd Period (Experiment I) Low Sample Rate -----	71
36.	Sonic "T" Channel Data Observed 14 December 1972 2nd Period (Experiment I) Low Sample Rate -----	72
37.	Sonic "A" Channel Data Observed 14 December 1972 3rd Period (Experiment I) Low Sample Rate -----	73
38.	Sonic "B" Channel Data Observed 14 December 1972 3rd Period (Experiment I) Low Sample Rate -----	74
39.	Sonic "W" Channel Data Observed 14 December 1972 3rd Period (Experiment I) Low Sample Rate -----	75
40.	Sonic "T" Channel Data Observed 14 December 1972 3rd Period (Experiment I) Low Sample Rate -----	76
41.	Hot Wire Data Observed 10 January 1973 1st Period -----	77
42.	Hot Wire Data Observed 10 January 1973 2nd Period -----	78
43.	Sonic "A" Channel Data Observed 28 February 1973 1st Period (Experiment II) -----	80
44.	Sonic "W" Channel Data Observed 28 February 1973 1st Period (Experiment II) -----	81
45.	Sonic "T" Channel Data Observed 28 February 1973 1st Period (Experiment II) -----	82



46.	Sonic "A" Channel Data Observed 28 February 1973 2nd Period (Experiment II)	----- 83
47.	Sonic "W" Channel Data Observed 28 February 1973 2nd Period (Experiment II)	----- 84
48.	Sonic "T" Channel Data Observed 28 February 1973 2nd Period (Experiment II)	----- 85
49.	Sonic "A" Channel Data Observed 28 February 1973 3rd Period (Experiment II)	----- 86
50.	Sonic "W" Channel Data Observed 28 February 1973 3rd Period (Experiment II)	----- 87
51.	Sonic "T" Channel Data Observed 28 February 1973 3rd Period (Experiment II)	----- 88
52.	Hot Wire Data Observed 28 February 1973 2nd Period (Experiment II)	----- 89
53.	Hot Wire Data Observed 28 February 1973 3rd Period (Experiment II)	----- 90
54.	Thermocouple Data Observed 28 February 1973 2nd Period (Experiment II)	----- 91
55.	Thermocouple Data Observed 28 February 1973 3rd Period (Experiment II)	----- 92



## ACKNOWLEDGEMENT

The author acknowledges the generous assistance and advice given by Dr. Kenneth L. Davidson and Dr. Noel E.J. Boston on all phases of this research. A special note of thanks to Dr. Thomas M. Houlihan for his expertise and assistance with the hot wire anemometer and one mil thermocouple systems during the field experiments, Mr. Robert Limes for his assistance during the digitization of data, Miss Sharon Raney for advice in IBM tape procedures and FT1 Jim Nolan USN for his expert maintenance and upkeep of the sonic anemometer/thermometer.

This research project was supported by the Naval Ordnance Systems Command through project order-3-0126 dated 14 September 1972 with the Naval Postgraduate School.





## I. INTRODUCTION

### A. PROBLEM

Turbulent processes in the atmosphere are of interest to meteorologists since it is by these processes that efficient vertical and horizontal transfers of energy, heat and momentum occur. These transfer processes have been experimentally observed to occur within the frequency band from 0.01 Hz to 10.0 Hz. An important method for describing the role of turbulence is through use of a system of instruments capable of measuring over this band. The analog data obtained is then read into computer systems to be digitized into discrete samples and then to be analyzed by spectral or other techniques.

### B. OBJECTIVES

The primary objective of this thesis was to utilize a sonic anemometer/thermometer to measure turbulence and evaluate the band over which it is capable of measuring. A secondary objective was to utilize a Hybrid computer system to digitize the analog data and then to use the IBM-360/67 computer system for spectral analysis of the digitized data. A third objective was to compare a sonic anemometer/thermometer with a hot wire anemometer system and a one mil thermocouple system.



## II. GENERAL DESCRIPTION AND OPERATING PROCEDURES OF THE SONIC ANEMOMETER/THERMOMETER MODEL PAT-313-1

### A. GENERAL

The sonic anemometer/thermometer<sup>1</sup> measures the three velocity components of the wind by detecting accurately the transit time difference (transit time sum for temperature) between two acoustic pulses propagated in opposite directions across a fixed path. The three velocity components of the wind are the longitudinal, lateral and vertical components denoted by  $u$ ,  $v$ , and  $w$  respectively along axes  $X$ ,  $Y$  and  $Z$  (Figure 1). The  $w$  component is obtained directly from the vertical axis, but  $u$  and  $v$  have to be computed from the velocity components  $U_A$  and  $V_B$  measured along the horizontal sonic paths  $A$  and  $B$  which are 120 degrees apart.

### B. COMPONENT PARTS OF THE SONIC ANEMOMETER/THERMOMETER

#### 1. Power Supply/Indicator Unit (PR-1)

The power supply/indicator unit and its component breakdown is pictured in Figures 2, 3, 4. The instrument operates on 100/115 volts with  $\pm$  10% variation at 50 to 60 Hz. Total power required is 100 watts. All switches and controls are located in this unit. Calibration and adjustment procedures (discussed later) are performed at

---

<sup>1</sup>Model PAT-313-1 manufactured by the Kaijo Denki Company Limited of Tokyo, Japan.



this unit. Visual meter output (analog form) is available for wind measurement on three range scales of 1) 0 to  $\pm 1$  m/sec, 2) 0 to  $\pm 3$  m/sec and 3) 0 to  $\pm 10$  m/sec (Figure 3). Temperature meter output is  $\pm 10^\circ\text{C}$  from mean air temperature which is dialed in on  $\bar{\theta}$  dial (Figure 4). Two BNC output jacks are available for tape recording or signal monitoring purposes on both wind and temperature units.

## 2. Probe (TR-31)

The probe has to be employed within the wind direction limits indicated in Figure 5. The wind velocity would be less than actual if the probe were positioned so that the wind was parallel to the path travelled by the sound pulses or if the supporting structure of the probe interrupted the wind flow.

The probe heads are ceramic type transducers from which sound waves are transmitted at a frequency of 100KHz. The transducers have high directivity and damping to minimize interference with other channels and are small physically in order to avoid blocking the air flow (Figure 6). The transducers screw into special holders designed to minimize acoustic coupling through the array. All probe heads are interchangeable with only minor adjustments required in the wind/temperature units affected by the change.

The probe heads, holders and entire array structure have been designed to reduce interference to the wind flow. All wiring and connections have been inserted inside the



**A,B**— axes along sonic paths.

**X,Y**— axes of symmetry for the array.

**x,y**— horizontal vector-mean axes of the wind.

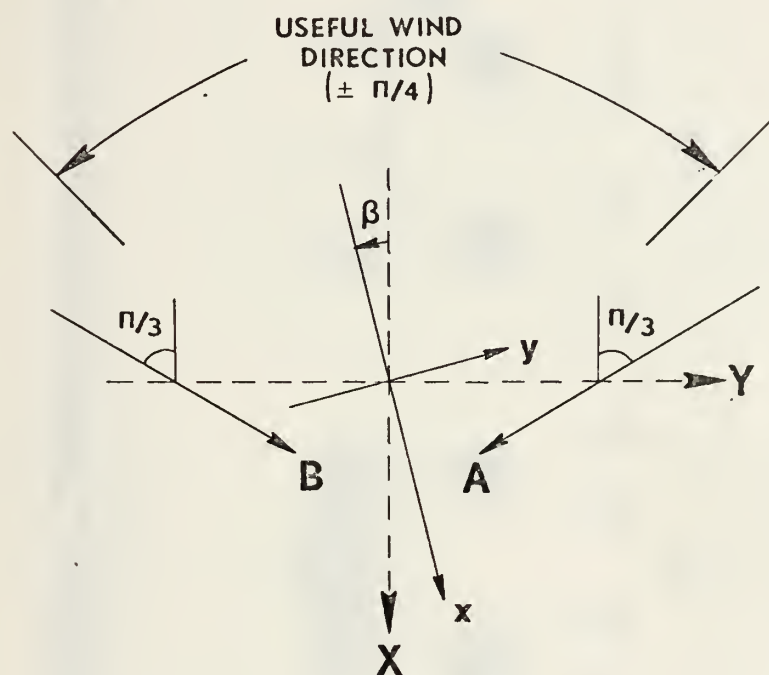


Figure 1. Wind and Sonic Axes.





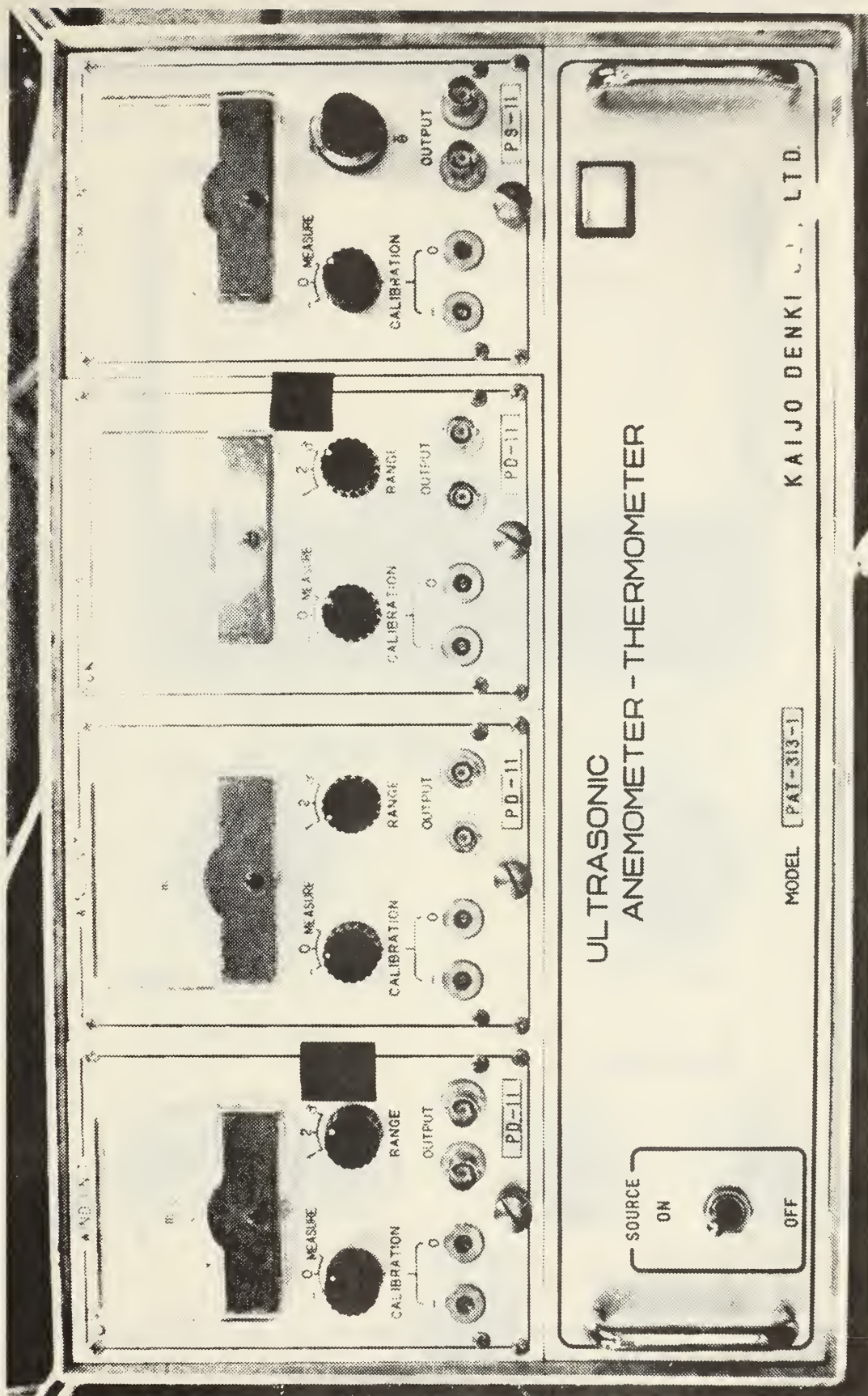


Figure 2. Power Supply/Indicator Unit (PR-1).



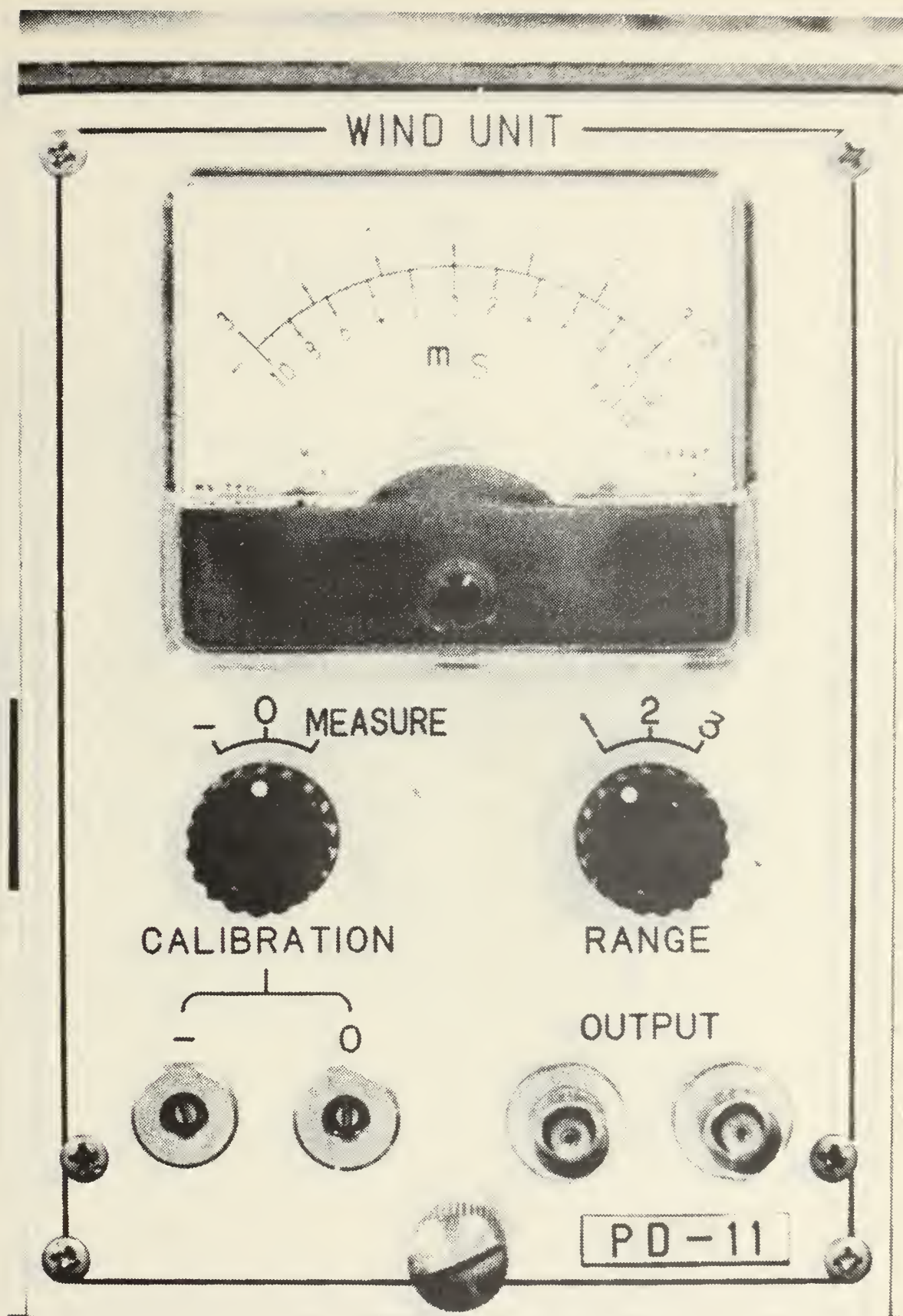


Figure 3. Wind Unit (PD-11).





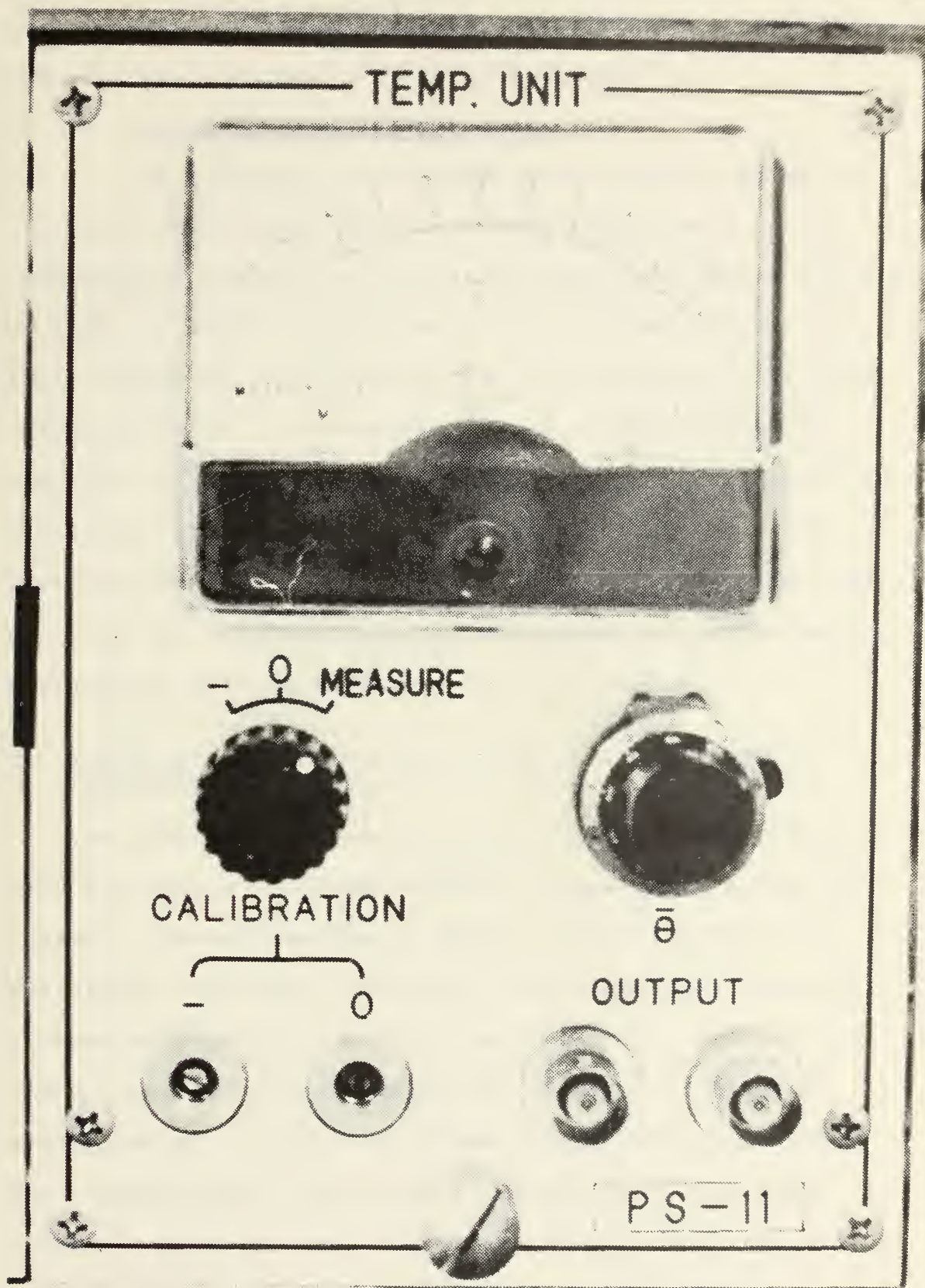


Figure 4. Temperature Unit (PS-11).



probe tubing for protection from the elements as well as for reducing air flow interference (Figure 7).

### 3. Junction Box (OA-33H)

The junction box contains three sets of pulse oscillators (which generate the 100KHz signal sent to the transducers) and six sets of head amplifiers (which amplify by 1000 the 100KHz signal sent to the transducers). The junction box is a watertight unit with connectors at both ends (Figure 8). One hundred meters of cable link the junction box and supply/indicator unit and three meters of cable link the junction box and probe (Figure 9). The junction box must be connected to the probe and power supply prior to turning the sonic anemometer on or the output transformer will be shorted.

### C. ADVANTAGES/DISADVANTAGES OF THE SONIC ANEMOMETER/THERMOMETER

The sonic anemometer/thermometer has many advantages over previously developed wind and temperature measuring systems. Recent results by McBean (1972) revealed the advantages the sonic anemometer has over a Gill propeller anemometer especially with respect to sensor response and angle of attack (cosine response) in eddy correlation measurements. A report by Kaimal et al (1971), in which they compared the pulse and continuous-wave type sonic anemometers, lists many advantages of the sonic anemometer system over other velocity measuring systems.





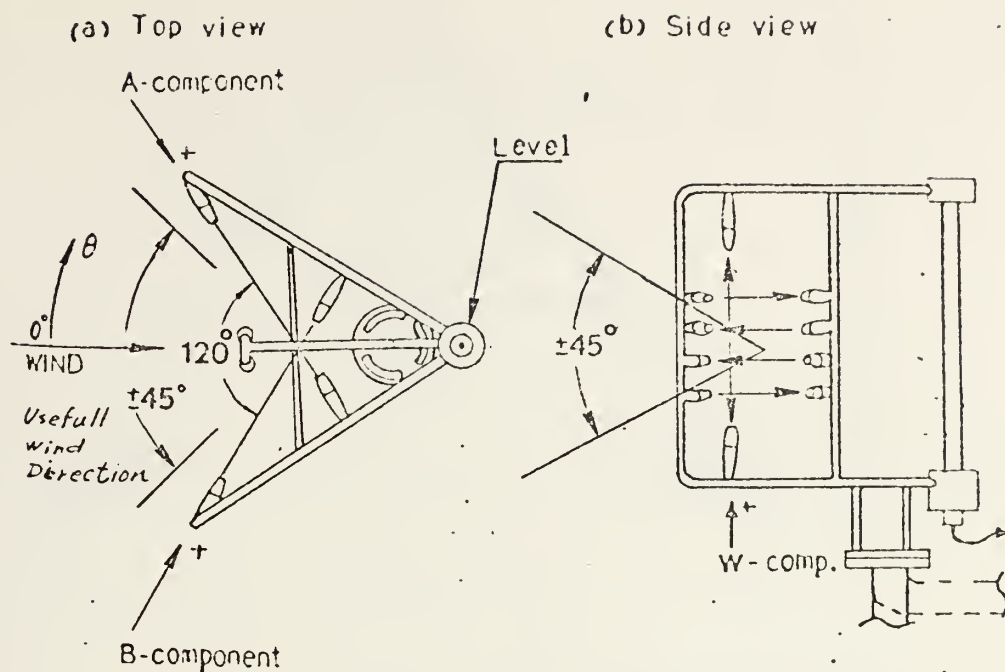


Figure 5. Wind Direction Limits of Probe Type TR-31.  
Kaijo Denki (1969)

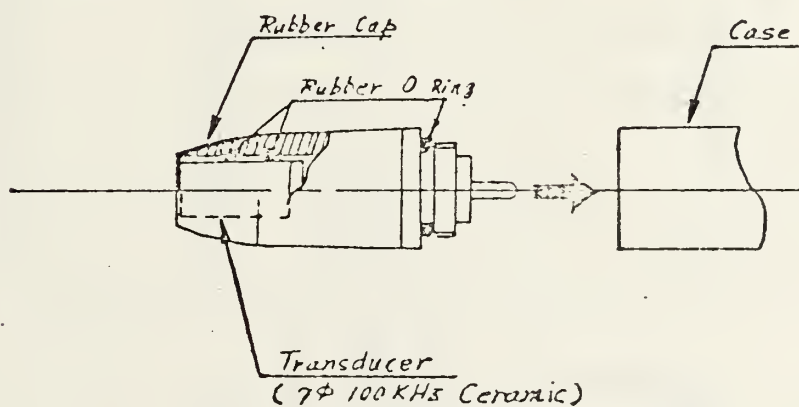


Figure 6. Probe Head. Kaijo Denki (1969)



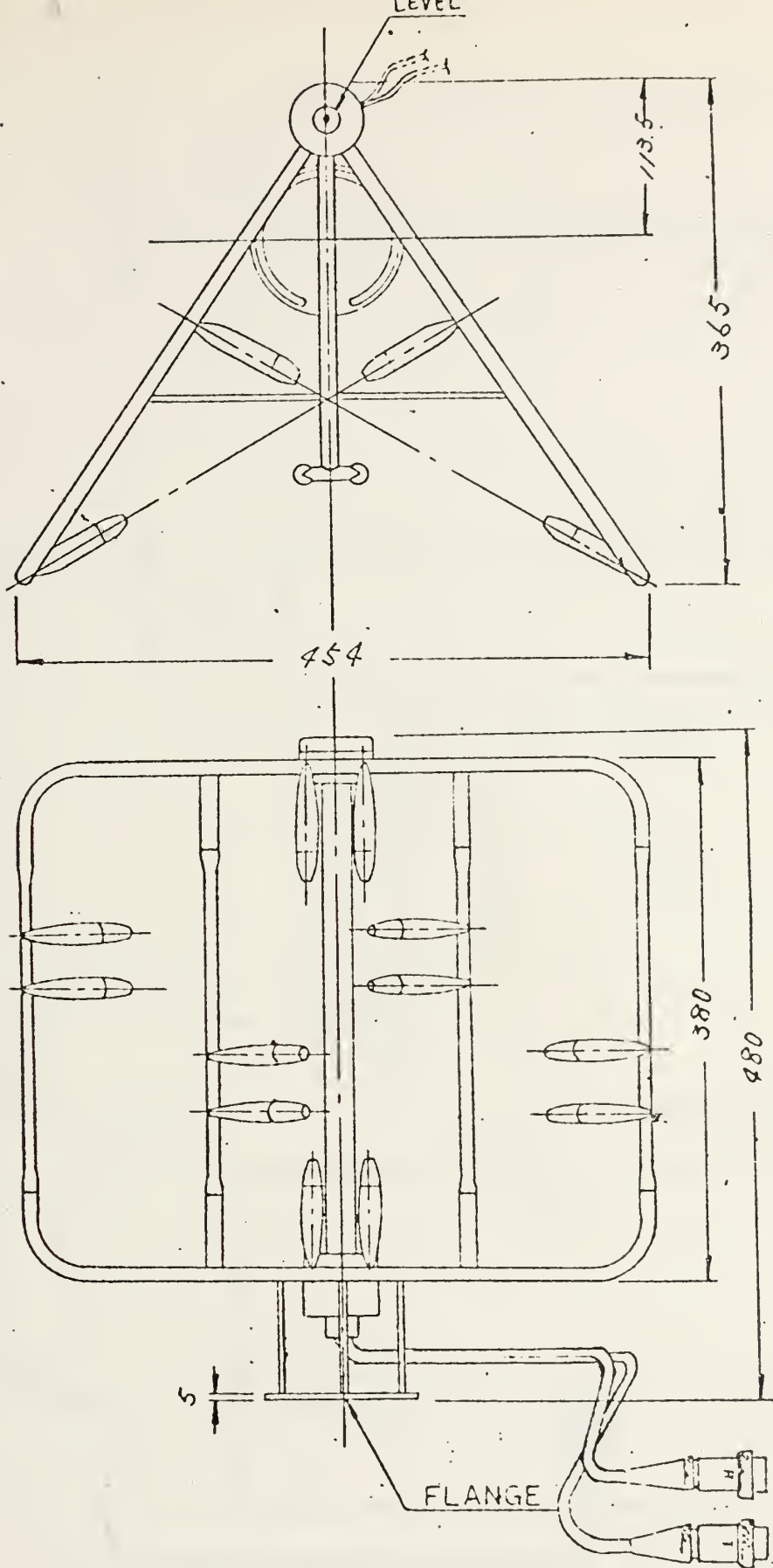


Figure 7. Probe Type TR-31. Kaijo Denki (1969)



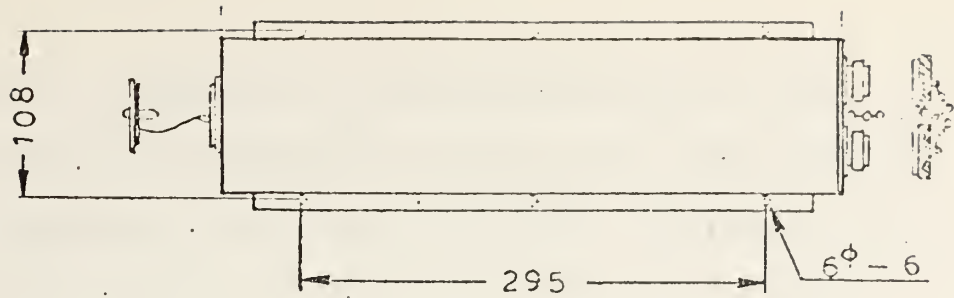
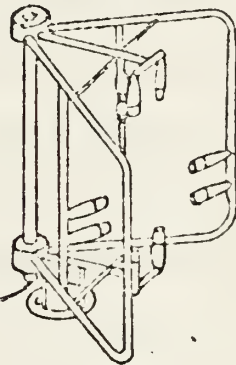
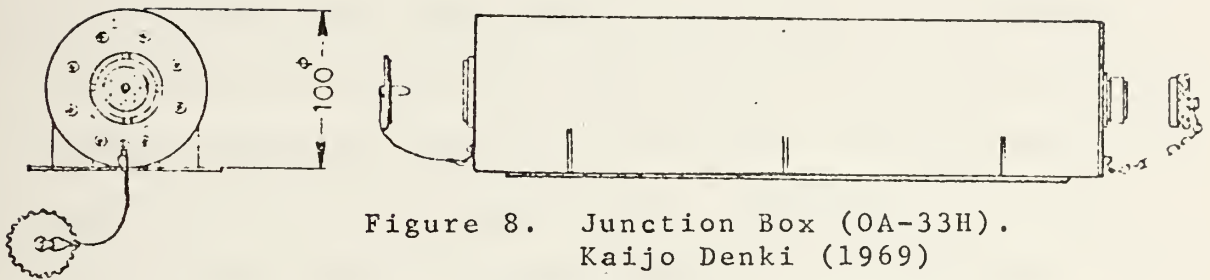


Figure 8. Junction Box (OA-33H).  
Kaijo Denki (1969)

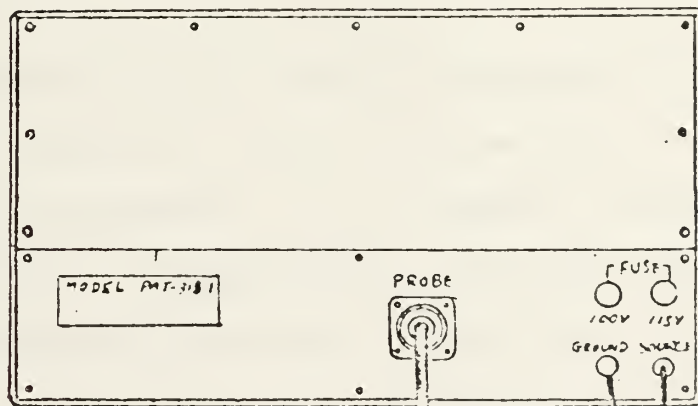


TR-31  
PROBE



OA-33H  
JUNCTION  
BOX

PAT-313 Equipment  
(back view)



Cable

AC 100/115

Figure 9. Wiring Diagram of PAT-313-1 System.  
Kaijo Denki (1969)



The PAT-313-1 system has no mechanical parts which eliminates lag due to mechanical inertia and thus allows the sonic to measure very light and sudden changes of the wind. The sonic also has high sensitivity and a broad range in all three wind components and in the temperature component.

The resolution of the sonic anemometer is  $\pm 2$  cm/sec in a span of 0-10 m/sec and the resolution of the sonic thermometer is  $\pm 0.1^{\circ}\text{C}$  in a span of  $\pm 10^{\circ}\text{C}$  centered around a mean temperature range of  $-10^{\circ}\text{C}$  to  $40^{\circ}\text{C}$ . The response is linear and so is its sensitivity. (Therefore, the response is the same at 5 cm/sec as it is at 10 cm/sec.)

The sonic anemometer has a time response in the millisecond range as it detects changes in pulse time between two sets of transducers. It takes measurements 440 times/sec for the wind components and 220 times/sec for the temperature component which allows it to detect changes of approximately 100 Hz at an accuracy of three percent (Kiajo Denki, 1969).

The sonic anemometer is not affected by exposure to the direct rays of the sun or to the rain as would a thermometer or a hot wire anemometer. It is, however, affected by immersion in water. A high moisture, high heat environment affects measurement procedures. These have to be corrected in order to get true readings because the measuring circuits are set for an atmosphere of zero percent relative humidity at a temperature of  $20^{\circ}\text{C}$ . The probe,





junction box and connecting cables are waterproofed allowing for all weather operation of this system. There are no easily broken, sensitive elements (such as a hot wire) exposed to the weather. It is a rugged system that can accept some rough handling. Cable connection points, especially where they enter the probe, are sensitive areas. Too much twisting of the cables can result in broken wires in the connectors. Care must be exercised so as not to bend the probe thus changing the length of transmission of the acoustic path and causing misalignment of the probe heads. Both problems would create serious errors in velocity and temperature measurement.<sup>2</sup> Each of the probe heads has a rubber cap over it to protect the ceramic transducer element but abrasive handling will rip it.

The probe has a small bubble level in the top plate which is used to insure that it is properly leveled when installed. Errors are introduced if the probe is not horizontal.<sup>3</sup> The probe should be mounted in such a way that it is free of vibrations. It measures relative speed of the environment with respect to the probe so any movement of the probe will introduce errors into the signals. Any object placed within two meters of the probe will reflect erroneous signals into the transducers. These are recognizable as noise spikes.

---

<sup>2</sup>Kaimal et al (1971) has an excellent discussion of these errors.

<sup>3</sup>Kaimal et al (1971) discusses this error.



## D. MEASUREMENT PROCESS

### 1. Wind Measurement

As described previously, the sonic anemometer measures wind velocity by detecting the transit time difference between two acoustic pulses propagated in opposite directions across a fixed path. The nomenclature used to describe the measuring process for a typical pair of transducers is shown in Figure 10.

The propagation times ( $t_1$ ,  $t_2$ ) for the pulses from  $TR_1$  to  $R_1$  and  $TR_2$  to  $R_2$  are

$$t_1 = \frac{\ell}{C \cos \alpha + V_d} \quad (1)$$

and

$$t_2 = \frac{\ell}{C \cos \alpha - V_d} \quad (2)$$

The travel time ( $t_1$ ) of the sound with the wind is less than the travel time ( $t_2$ ) with the sound against the wind. The difference  $\Delta t = t_2 - t_1$  is given by

$$\Delta t = \frac{2\ell V_d}{(C \cos \alpha)^2 - V_d^2} \quad (3)$$

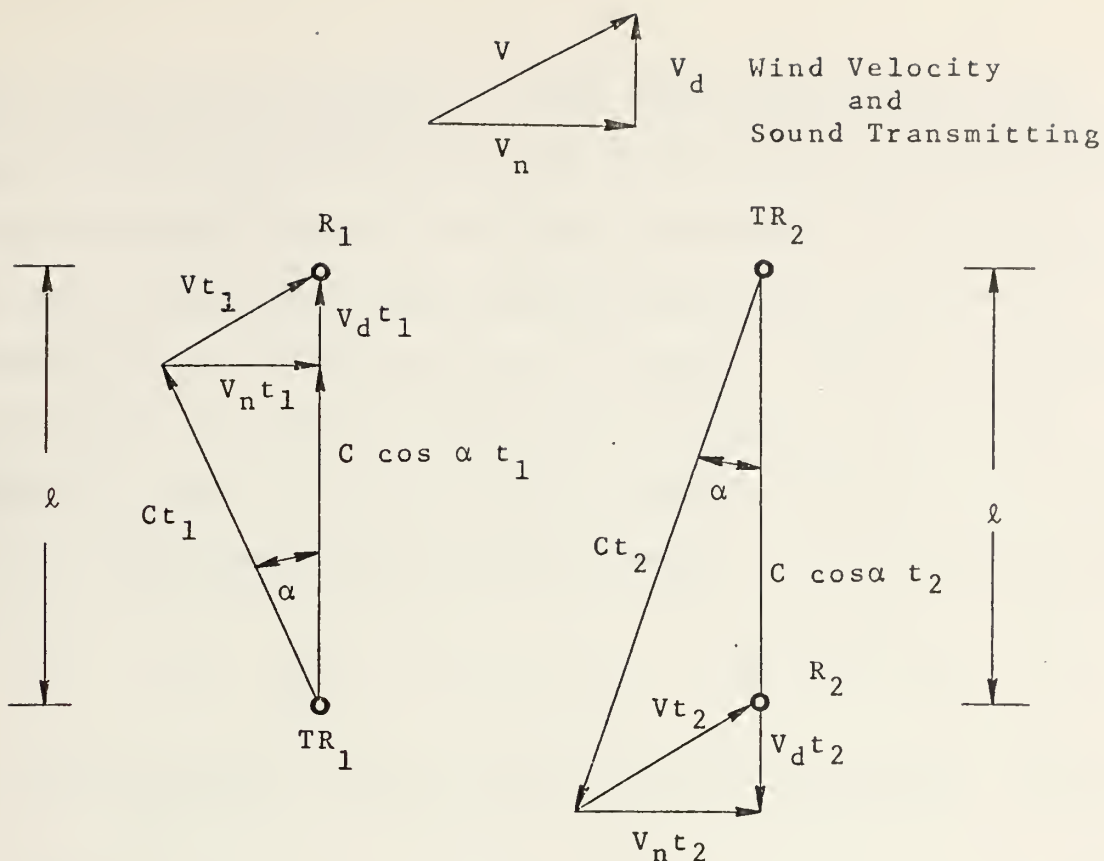
Angle  $\alpha$  is assumed to be small; therefore,  $\cos \alpha \sim 1$ . One further assumes that  $C^2 \gg V^2$  and therefore,  $C^2 \gg V_d^2$ . These approximations result in

$$\Delta t = \frac{2\ell}{C^2} V_d \quad (4)$$

which, when solved for  $V_d$  gives

$$V_d = \frac{C^2 \Delta t}{2\ell} \quad (5)$$





- KEY:
- $l$  = distance between transmitter and receiver
  - $C$  = sound velocity
  - $V$  = wind velocity
  - $V_n$  = component of wind velocity perpendicular to sound transmitting path
  - $V_d$  = component of wind velocity parallel to sound transmitting path
  - $t_1$  = time for sound to travel from  $T_1$  to  $R_1$  (with wind)
  - $t_2$  = time for sound to travel from  $T_2$  to  $R_2$  (against wind)
  - $TR_1, TR_2$  = transmitting transducers
  - $R_1, R_2$  = receiving transducers
  - $\alpha$  = angle between transmitting path and distressed sound path

Figure 10. Schematic of Typical Measuring Process and Nomenclature.



The wind velocity parallel to the sound transmitting path ( $V_d$ ) is therefore determined and is the quantity indicated on the metered output of the sonic anemometer as  $U_A$  or  $V_B$ . The values of  $u$  and  $v$  (the longitudinal and lateral wind components of the X and Y axes of Figure 1) have to be computed from the velocity components  $U_A$  and  $V_B$ . The  $w$  component is taken directly from the output.

The equations for  $u$  and  $v$  are:

$$u = (\cos \beta - \frac{1}{\sqrt{3}} \sin \beta) U_A + (\cos \beta + \frac{1}{\sqrt{3}} \sin \beta) V_B \quad (6)$$

$$v = -(\frac{1}{\sqrt{3}} \cos \beta + \sin \beta) U_A + (\frac{1}{\sqrt{3}} \cos \beta - \sin \beta) V_B \quad (7)$$

where

$$\beta = \tan^{-1} \frac{\bar{V}_B - \bar{U}_A}{\sqrt{3} (\bar{V}_B + \bar{U}_A)}$$

Overbar denotes time average over a suitably long period of time Kaimal et al (1971).

## 2. Temperature Measurement

Temperature is measured in a manner similar to the wind measurement except that the propagation times ( $t_1, t_2$ ) are added instead of subtracted. The  $w$  component transducers provide the data used for this measurement. The defining expression for temperature is

$$t = t_1 + t_2 = \frac{2\ell(C^2 - v_n^2)^{1/2}}{C^2 - v_d^2} \quad (8)$$





Again assuming  $C^2 \gg v_d^2$  and  $C^2 \gg v_n^2$  equation (8) reduces to:

$$t = \frac{2\ell}{C} \quad (9)$$

The speed of sound in air is expressed as:

$$C = 20.06 \cdot [T + (1 + 0.32 \frac{e}{p})]^{1/2} \quad (10)$$

where  $T$  is in degrees absolute (K),  $e$  is the vapor pressure in atmospheres and  $p$  is the atmospheric pressure in atmospheres. From (9) and (10)

$$T = \frac{(\frac{2\ell}{t})^2}{402.68(1 + 0.32 \frac{e}{p})} \quad (11)$$

Furthermore, set  $T_{SV} = T(1 + 0.32 \frac{e}{p})$  where  $T_{SV}$  is sound virtual temperature (taken as the true temperature in degrees K) measured by the sonic thermometer. Equation (11) is rewritten as:

$$T_{SV} = (\frac{2\ell}{20.067t})^{1/2} \quad (12)$$

$T_{SV}$  is the parameter obtained by measuring  $t$  from the sonic thermometer. Being a virtual temperature, this measurement is subject to humidity effects.

### 3. Discussion of Possible Errors in Wind Velocity and Temperature Measurements

Errors are introduced by humidity, temperature and atmospheric pressure which require correcting the readings from the sonic anemometer/thermometer. Detailed discussion of errors resulting from misalignment of the array, line-averaging, finite spatial resolution of the array and noise in the detector has been described by Kaimal et al (1971).



As seen in equation (5) and equation (10), the wind velocity measured will be a function of temperature, humidity and atmospheric pressure. From equation (12), however, the measured temperature will depend on humidity and atmospheric pressure only. For hot humid days the effect on velocity cannot be ignored. Humidity significantly effects the absolute temperature but is negligible as far as fluctuations in temperature are concerned provided the fluctuations in humidity are small.

The ratio K, between the wind velocity  $V_{20}$  (at the temperature  $T_{20} + 293K$  or  $20C$  and  $e/p = 0$ )<sup>4</sup> and the wind velocity  $V_{TSV}$  (at the temperature  $T_{SV}$ ) is

$$K = \frac{V_{TSV}}{V_{20}} = \frac{T_{SV}}{T_{20}} = \frac{293 + \theta_{SV}}{293} \quad (13)$$

where  $\theta_{SV}$  = sound virtual temperature measured by the sonic thermometer in degrees C. Any wind velocity or temperature measured by the sonic anemometer/thermometer in an atmosphere other than  $20C$  and zero percent relative humidity must be corrected by a factor K (Figure 11A, 11B).

The error introduced by the assumption of  $C^2 \gg V^2$  is

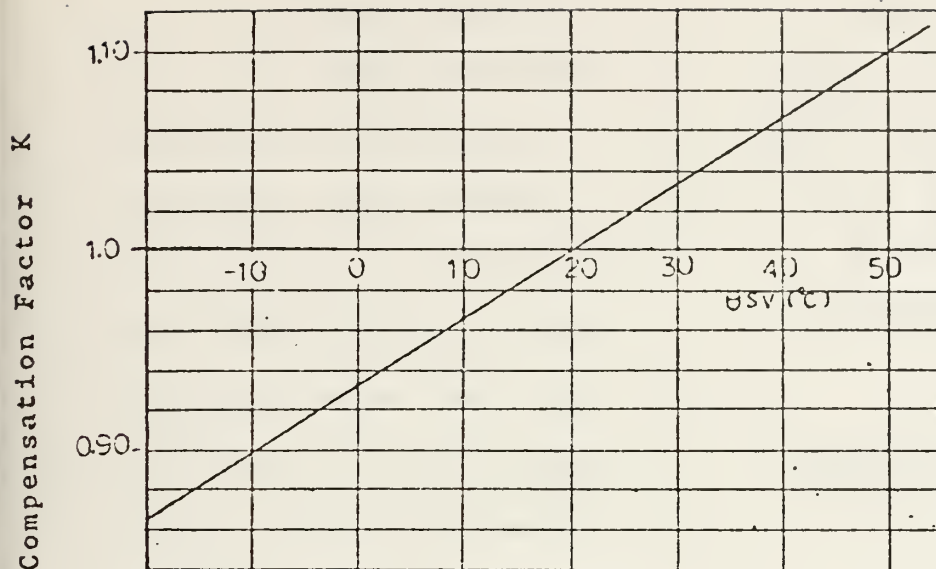
$$\Sigma w = \frac{V^2}{C^2} \quad (14)$$

and is such that for wind speeds of less than 10 m/sec it is zero (Figure 12).

---

<sup>4</sup> Sonic anemometer/thermometer circuitry is set for a base temperature of  $20C$  and zero percent relative humidity.





$$V_{\theta_{SV}} = K \cdot V_{20}$$

$$dT_{SV} = K \cdot dT_{20}$$

$V_{20}$  = Wind Unit Indicated Reading

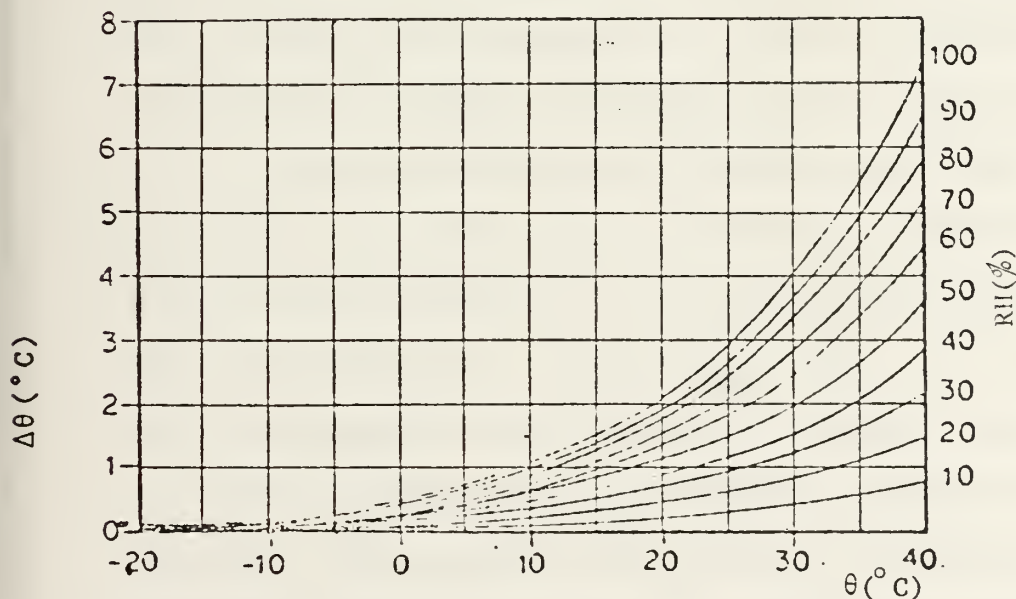
$V_{\theta_{SV}}$  = Wind velocity at the temp.  $\theta_{SV}$

$dT_{20}$  = Thermometer sensitivity at 20 degrees C.

$dT_{SV}$  = Temperature sensitivity at temp.  $T_{SV}$

Figure 11A. Temperature Compensating Constant..

Note: The  $\theta$  dial and the meter scale of the TEMP UNIT calibrated in  $\theta_{SV}$ .



$$\theta = \theta_{SV} - \Delta\theta$$

$\theta$  = Temperature

$\theta_{SV}$  = Sound virtual temperature

(The temperature measured by ultrasonic thermometer)

RH = Relative humidity

Figure 11B. Humidity Compensation Graph.  
Kaijo Denki (1969)



#### 4. Timing Sequence

A more detailed analysis by Soumie and Businger (1958) showed that velocity and temperature fluctuations, within certain limits, were proportional to the fluctuations in the difference and the sum of the time in-

tervals respectively. A discussion of the method of obtaining these time intervals is of use in order to understand the setting up and calibration of the sonic anemometer/thermometer. Only the vertical transmitter-receiver array (that used to measure the vertical velocity component and temperature) needs to be considered in order to understand the triggering and pulse measuring system used in the instrument.

Pulses are emitted simultaneously from  $TR_{W1}$  and  $TR_{W2}$  at time  $T$ , and reach their respective receivers  $R_{W1}$  and  $R_{W2}$  after time intervals of  $t_{w1}$  and  $t_{w2}$  seconds (Figure 13). The time difference  $\Delta t_w = t_{w2} - t_{w1}$  is converted by a wind analog card (within the  $w$  unit) and changed into a voltage representing the vertical component of the wind velocity. The output of  $R_{W1}$  drives the delay card  $D_1$  which generates the delay time  $t_{D1}$ . This output synchronizes the generation of the next pulse or oscillation at time  $T'$  which

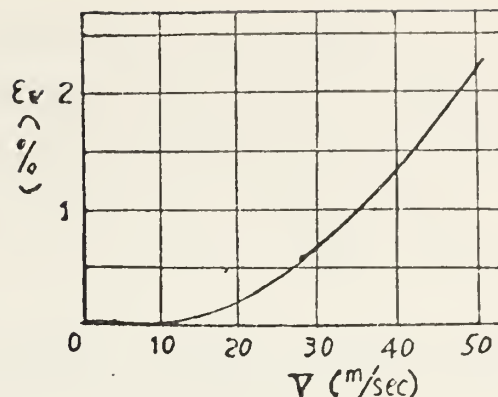


Figure 12. Error by Wind Velocity. Kaijo Denki (1969)





reach their receivers after time intervals  $t'_{w1}$  and  $t'_{w2}$  seconds. Therefore, the pulse spacing is  $t_{w1}$  and  $t_{D1}$  and the total time from the emitting of the first pulse,  $T$ , to the receiving of the second pulse,  $T'$ , by  $R_{w2}$  is  $t_{w1} + t_{D1} + t'_{w2}$ .

In terms of the speed of sound in still air,  $C$ , and the separation,  $\ell$ , of the transmitter and receiver,

$$t_{w1} + t_{D1} + t'_{w2} = \frac{2\ell}{C} + t_{D1} \quad (15)$$

As previously discussed, the temperature measurement is sampled at half the rate of the wind measurement (220 times/sec as compared with 440 times/sec). Therefore, the time,  $t = t_{w1} + t'_{w2}$  is related to temperature. Since  $\Delta t_{\theta}$  changes very slowly with temperature, a time  $t_{D2}$  generated by another time delay circuit is subtracted from  $t + t_{D1}$ . The time difference,  $\Delta t_{\theta} = t + t_{D1} - t_{D2}$ , is then supplied to a temperature analog card which changes it into a  $\overline{\Delta t_{\theta}}$  (the mean temperature found on the  $\overline{\theta}$  dial of the temperature unit. The dial is operated manually). The time difference is also changed into  $\Delta t'_{\theta}$ , the fluctuating component, which is changed into a voltage that appears on the  $\theta_{SV}$  meter (Figure 14).

The time delay  $t_{D2}$  is adjustable (longer at lower temperatures) since it is preferable to keep  $\Delta t_{\theta}$  small. If  $\Delta t_{\theta}$  is made too small, however, a sluggish limiting of the temperature signal will occur--the effect showing as a rounding to flattening of the high temperature peaks.



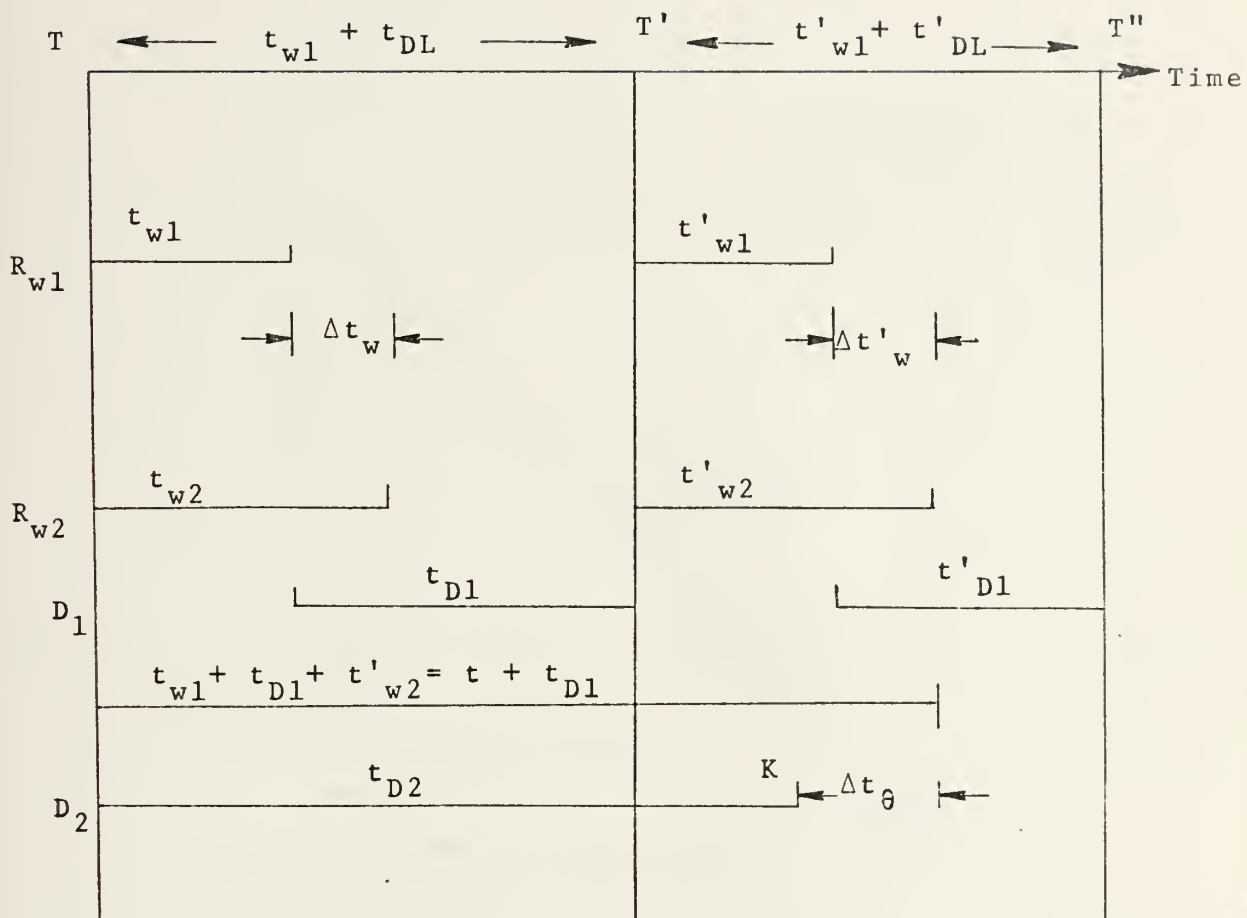


Figure 13. Timing Sequence Schematic. Kaijo Denki (1969)



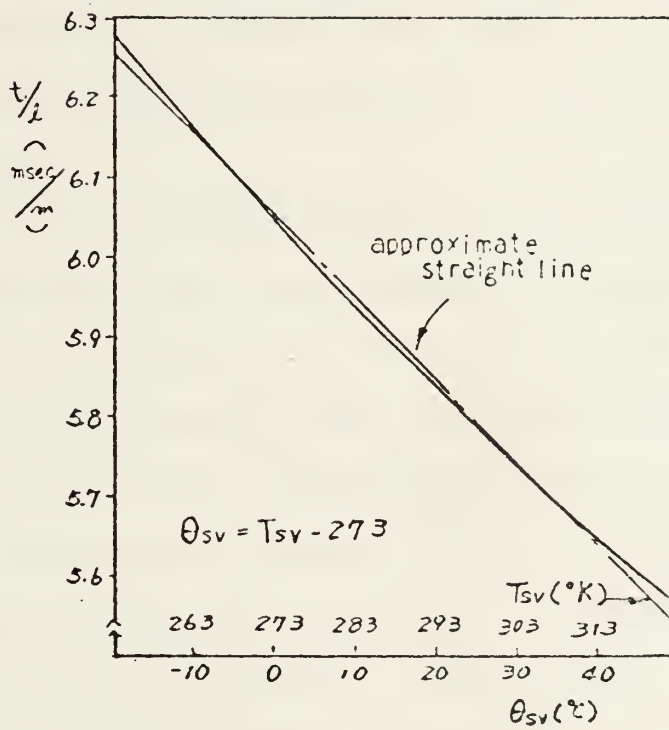


Figure 14. Temperature and Time Relationship.  
Kaijo Denki (1969)



### III. DATA ANALYSIS

#### A. GENERAL

Turbulent processes appear as erratic changes in temperature and in direction and speed of the wind. A knowledge of the nature of turbulent processes in the atmosphere (fluctuations of such parameters as wind velocity, temperature and moisture for example) can lead to a better understanding of heat, energy and momentum transfers which occur over the ocean.

The mechanics of turbulence are so complex that it is almost traditional now to use statistical methods through which an understanding of the mean characteristics can be obtained if not in detail. One statistical method which has been used with some considerable success is spectral analysis. From spectral analysis the distribution of energy of a fluctuating, turbulent process (e.g. wind velocity, temperature) can be plotted as a function of frequency.

Analog measurements were recorded of wind velocity and temperature fluctuations from the sonic anemometer/thermometer, hot wire anemometer and a one mil thermocouple then digitized and then spectral analyzed by a Fast Fourier Transform method. A general discussion of procedures used in the analog-to-digital conversion and spectral analysis will be given in the next sections. More detailed discussion of procedures and theory appear in McKendrick (1971) Jones (1971) and Wilson et al (1969).





## B. KOLMOGOROV'S HYPOTHESIS

### 1. General

An important consideration in turbulence theory is whether the turbulence is anisotropic or isotropic. Anisotropy exists for large scale eddies and isotropy is thought to exist for small scale eddies. Isotropy was described by Lumley and Panofsky (1964) as follows:

"An isotropic field is one in which there is no preferred direction. Thus all average functions describing the statistics of such a field must remain unchanged regardless of a rotation (or reflection) of coordinate system. For example, the spectrum of a function,  $\phi(k)$ , homogeneous in three spatial directions, which is also isotropic, cannot be a function of the separate components of the wave number vector, for a rotation to a new coordinate system would change those. It can be a function only of the length of the vector, for that is the only quantity characterizing 'k' which does remain unchanged under a rotation."

Kolmogorov postulated that at high wave numbers turbulence should be isotropic even though it is generated from and embedded in anisotropic eddies of low wave number. If the Reynolds number (ratio of inertial forces to viscous forces in the flow) is high enough, turbulence will adjust until a statistically steady state, independent of initial conditions, is attained. Turbulence is adjusted through inertial transfer (forces due to fluctuating velocity gradients) and viscous dissipation. This steady state consists of energy transfer by inertial forces into the high wave number range that is equal to energy lost through viscous dissipation. This predicted behavior of velocity spectra



was utilized in interpretation and comparison of the sonic anemometer, hot wire anemometer and one mil thermocouple data. Prediction by Kolmogorov's hypotheses are discussed in more detail in the following paragraphs.

## 2. Kolmogorov's First Hypothesis: Equilibrium Range

At high Reynolds numbers "small scale" eddies are isotropic and in universal statistical equilibrium. Their properties depend on dissipation ( $\epsilon$ ) and on kinematic viscosity ( $\nu$ ) and not directly on time. Motion associated with the equilibrium range is uniquely determined by  $\epsilon$  and  $\nu$ .

Kolmogorov concluded that the energy spectrum  $[E(k)]$ , in units of energy per unit wave number, is

$$\frac{E(k)}{(\epsilon \nu^5)^{1/4}} = f\left(\frac{k}{k_S}\right)$$

where  $f\left(\frac{k}{k_S}\right)$  = undesignated function

$$\frac{1}{k_S} = \left(\frac{\nu^3}{\epsilon}\right)^{1/4}$$

$k_S$  = characteristic wave number

## 3. Kolmogorov's Second Hypothesis: Inertial Subrange

If the Reynolds number is large enough, the energy containing eddy wave number region and the "dissipation" wave number region should be well separated in wave number space. There should exist a range of wave numbers (eddy sizes) on the low "k" side of the dissipation range (but at higher wave number than energy containing wave numbers) in which the universal statistical steady state holds



$[\frac{\partial}{\partial t} E(k) = 0]$  but where there is negligible dissipation of energy, [Figure 15 from Lumley and Panofsky (1964)]. This range of wave numbers where the dominant feature is energy flux by inertial forces is called the inertial subrange.

Since viscosity is not important in this wave number range, statistical properties are determined only by dissipation rate ( $\epsilon$ ) and wave number ( $k$ ). Kolmogorov stated that energy spectrum should have the following functional relation

$$E(k) = C \epsilon^{2/3} k^{-5/3}$$

$\epsilon$  = dissipation of turbulent  
kinetic energy

$k$  = wave number

$C$  = constant of proportionality

Since frequency is directly proportional to wave number, a log-log plot (base 10) of energy spectra versus frequency would yield a curve with a  $-5/3$  slope if the spectral estimates are within the frequency band of the inertial subrange.

## C. ANALOG TO DIGITAL PROCEDURES

### 1. General

Analog data recorded in the field were digitized through use of a Hybrid computer system.<sup>5</sup> The Hybrid system consists of an analog computer, COMCOR Ci-5000, electronically connected to a digital computer, XDS-9300. A program

---

<sup>5</sup> This system is located in Spanagel Hall, Naval Postgraduate School, Monterey, California.



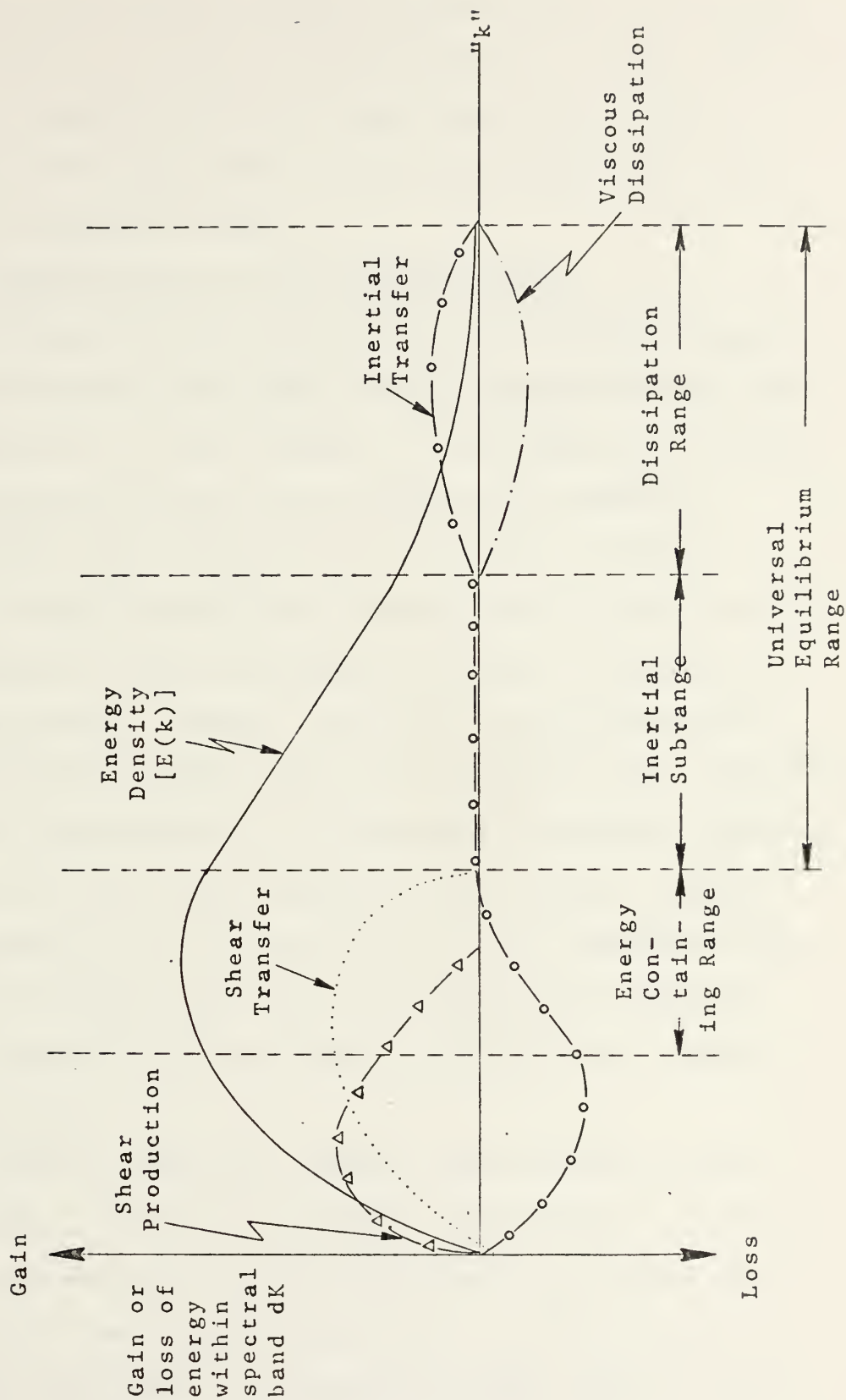


Figure 15. Schematic Drawing of Spectral Energy Transfer in Free Convection. Lumley and Panofsky (1964)





exists for digitizing, using the XDS-9300 and the Ci-5000 analog computer. An analog patchboard and a logic board, which are plugged into the Ci-5000 were also available. Digitization was performed in the octal number base onto seven track magnetic tapes.

## 2. Considerations Prior to Digitization

Considerations taken into account prior to digitization were noise, D.C. level, analog signal strength and total analog data record length, T (corresponding to time). All of these were functions of collection technique.

Noise that contaminates the desired signal is usually of high frequency and normally can be low pass filtered during the data recording procedures. This is the preferred method. However, filtering can be done in the Hybrid computer facility just prior to digitizing. In this study, the analog data were filtered at the Hybrid computer. Data from the four sonic anemometer/thermometer channels were filtered at 31.25 Hz and the hot wire anemometer data and one mil thermocouple data were filtered at 100.0 Hz. (Filter frequencies should equal one-half of the digital sampling rate.)

The D.C. level was removed from all data during digitization. If it were necessary that the D.C. level be removed from the data during data recording, a band pass filter with a low frequency cut off of less than one hertz could have been used. This would preserve some of the low



frequencies while eliminating the high frequency noise and the D.C. level.

All analog signals were amplified in order to take full advantage of the range of the Hybrid computer system. The Hybrid system is able to digitize signals of  $\pm 100$  volts. Channels A and B of the sonic anemometer/thermometer and the hot wire anemometer were amplified by 50; Channels W and T of the sonic anemometer/thermometer and the thermocouple were amplified by 100. Amplification factors were taken into account, in this study, in the Fast Fourier Transform program.

Consideration had to be given to obtaining an optimum analog data record length, T, during the field experiments. In optimizing this total record length for the frequencies of interest, the relationship between T and the shape of the convolved wave forms (Fourier Transform) must be considered. Jones (1971) described fully the effects of record lengths on the shape of the convolved wave forms. In general there is some optimum record length where the difference between the convolved spectrum and true spectrum is very small. Although Jones (1971) did not find an optimum record length, he found that increasing a record from 140 seconds to 360 seconds had no significant effect on spectral shape between 10 Hz and 1000 Hz. Data collected in this study had a record length of 30 minutes.

Low frequency resolution is also tied directly to the length of the analog record. According to Rayleigh's



Criterion, it is hard to distinguish low frequencies ( $f$ ) in the interval  $0 \leq f \leq 1/2T$  (where  $T$  = analog record length in seconds). When dealing with a finite record the original signal is truncated. A long record narrows the frequency resolution. Record lengths of 30 minutes gave a low frequency resolution of approximately 0.0003 Hz although statistical reliability would not be expected until 0.003 Hz.

Another factor which had to be considered prior to digitizing was that of aliasing. Aliasing is dependent on the folding (Nyquist) frequency which is  $1/2$  the sampling frequency. In order to prevent the "folding back" of energy from higher frequencies into the lower frequencies of interest, a sampling rate greater than twice the highest frequency desired must be chosen. The folded back energy will be centered around the Nyquist frequency. Sonic anemometer/thermometer data from Experiment I was run at two different sampling rates. Sampling rates of 390.5 Hz and 62.5 Hz gave aliasing frequencies of 195.25 Hz and 31.25 Hz respectively. The hot wire anemometer data and the thermocouple data from Experiment II were sampled at 200.0 Hz which gave an aliasing frequency of 100.0 Hz. Experiment II sonic anemometer/thermometer data were sampled at 62.5 Hz only.

#### D. CONVERSION OF SEVEN TRACK TO NINE TRACK

Digitization of analog data on the above system produced a seven track tape in the octal number case. To utilize this data in the IBM-360/67 computer system, digitized data



had to be converted to a nine track tape in the hexadecimal number base. This conversion process was done using an available program, CONVERT. Complete listings and Job Control Language (JCL) card setups for the CONVERT program can be found in theses by McKendrick (1971) and Jones (1971), and in a report by Raney (1971).

#### E. FOURIER COEFFICIENT COMPUTATIONS

Fourier coefficients were obtained by using the FTOR program, one of two UBC time series programs currently on file in the IBM-360/67 subroutine library at the Naval Postgraduate School.

Transformation of digitized signal data from the time domain into the frequency domain was done using a finite form of the Fourier Transform. Data were read off the converted nine track tape, a record at a time. The Fourier coefficients were computed and were then stored on a separate tape.

The longer the record, the closer together in frequency will be the spectral estimates because the value of the frequency is given by  $(n/T)$ . That is, the discrete frequency bandwidth is inversely proportional to the record length.

Due to the prohibitive amount of computer time used to compute coefficients, the direct finite Fourier Transform of a series of data points was not used. The Fast Fourier Transform of Cooley and Tukey (1965) was used and it is a variation of the direct method. The Fast Fourier Transform





is incorporated into the FTOR program resulting in considerably less computer time for Fourier coefficient computation. This method yields an improvement in excess of five orders of magnitude in computational time (McKendrick 1971) over the direct method.

The FTOR program transforms a maximum of  $2^{13}$  (8192) data points. This maximum is set by dimension limitations in the program. Turbulence data normally includes many more data points than this so the data points are read in as records consisting of integral powers of two (up to a maximum of  $2^{13}$ ) and these records are transformed consecutively.

#### F. UBCSCOR PROGRAM

Once the Fourier coefficients have been computed, the second UBC program, SCOR, converts them to power spectral densities.

Spectral values  $E_{jk}(n)$  are computed from the complex Fourier coefficients by forming the product of the complex coefficient  $[A_j(n) = a_j(n) - i b_j(n)]$  with a conjugate  $[A_k^*(n) = a_k(n) + i b_k(n)]$  where  $j$  and  $k$  could be the same or different.

Spectral values were obtained by the following computations

Spectrum density:  $j = k$ ,

$$E_{jj}(n) = \frac{A_j(n) \cdot A_j^*(n)}{2\Delta n} = (a_n^2 + b_n^2) \frac{T}{2}$$

$$\text{where } \Delta n = \frac{1}{T}$$



Cross spectrum:  $j \neq k$ ,

$$E_{jk}(n) = \frac{A_j(n) \cdot A_k^*(n)}{2\Delta n}$$

$$= \frac{T}{2}[(a_n c_n + b_n d_n) - i(b_n c_n - a_n d_n)]$$

The real and imaginary parts of the cross spectrum are the cospectrum and quadrature spectrum respectively and were denoted as; Cospectrum:

$$E_{jk}(n) = (a_n c_n + b_n d_n) \frac{T}{2}$$

Quadrature spectrum:

$$E_{jk}(n) = (b_n c_n - a_n d_n) \frac{T}{2}$$

The spectra and cospectra are computed for each frequency in successive records and then these records are averaged consecutively. The program also divides the spectral densities into 32 bandwidths and averages them across the bandwidths as well as along the records to obtain a mean and a variance of the quantities.

In the SCOR program one can specify the number of channels to be analyzed, the number of records in a file, the start point for analysis, selection of spectra and/or cospectra, bandwidth desired (logarithmic or linear), the type of graphic plot desired and for this study, machine-set coordinates for the graphic output. Programmer-set-coordinates also can be used. The program computes, the spectra and/or cospectra for each record in sequence until all records requested have been analyzed or the "end-of-file" mark is reached on the tape.



#### IV. FIELD EXPERIMENTS

##### A. PRELIMINARIES

The sonic anemometer/thermometer used in the field experiments had been in storage for a period of two years. The first consideration was to thoroughly check the sonic anemometer/thermometer electronically. It was checked out in accordance with manufacturer's instructions [Kaijo Denki (1969), Appendix D and E which included voltage and wave form checks at certain critical points]. A large number of transistors in both the power supply and junction box had to be replaced.

Once the sonic anemometer/thermometer was checked electronically, wind tunnel tests were performed. Simple, operational tests in a controlled environment were made to insure that the sonic anemometer/thermometer was measuring wind speed and temperature correctly. Once satisfactory wind tunnel measurements were made, field experiments were conducted.

##### B. OBJECTIVE OF EXPERIMENTS

The objective of the field experiments was to gather comparative turbulence data from the sonic anemometer/thermometer, the hot wire anemometer and a one mil thermocouple. All three sets of data were then similarly spectrally analyzed.



## C. EXPERIMENTS

### 1. Installation of Instruments

The procedures described in this section applies to both experiments. All equipment was installed at the Naval Postgraduate School beach lab, indicated in Figure 16 and Figure 17. The sonic probe, hot wire probe and one mil thermocouple were mounted on a pole at a height of three meters (Figure 18) and positioned so that all sensors were facing directly into the wind flow which was blowing off the water. During the experiments, all probes were kept into the wind such that the velocity measured on channels A and B were equal. A hand held wind vane was used to check on the wind direction in order to maintain proper probe orientation.

All recording devices, power supplies and amplifiers were installed inside the beach lab (Figure 19). Analog data were recorded on a SANGAMO FM tape recorder model 3562 at a speed of 1-7/8 inches per second. This recorder uses one inch magnetic tape and has 14 tracks available for data and two edge tracks available for voice recording.

The hot wire anemometer used for velocity comparisons was a TSI model 1050. A copper constantan, unsheathed, fine gauge Omega Engineering Company (SSTSSP-020E-6) thermocouple was used for temperature measurements.

### 2. Experiment I - 14 December 1972

Wind speed and temperature measurements were made during the late afternoon on 14 December 1972. Visibility was unlimited. Winds were from the west to northwest, off





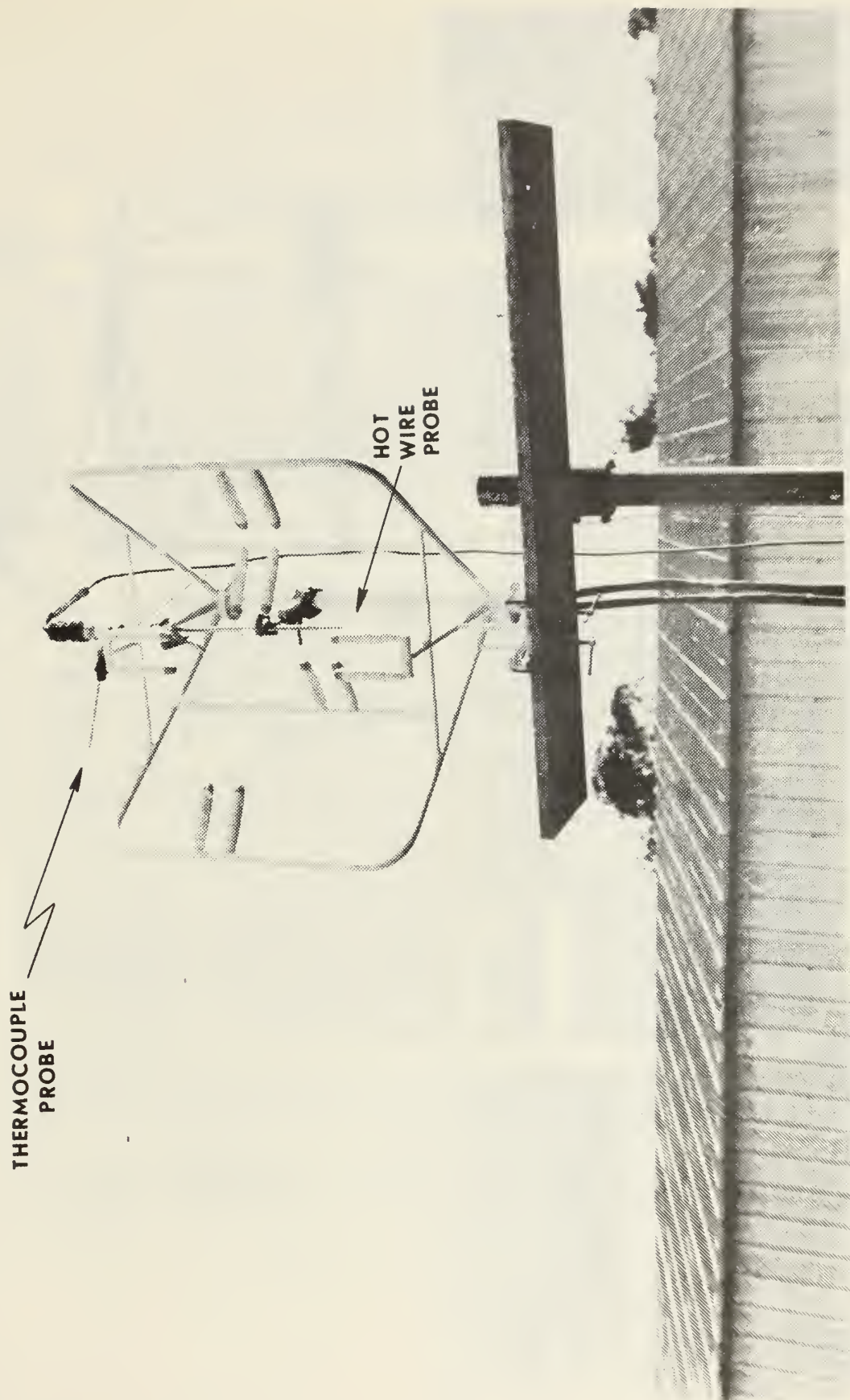


Figure 16. Arrangement of Probes for Experiments I and II.



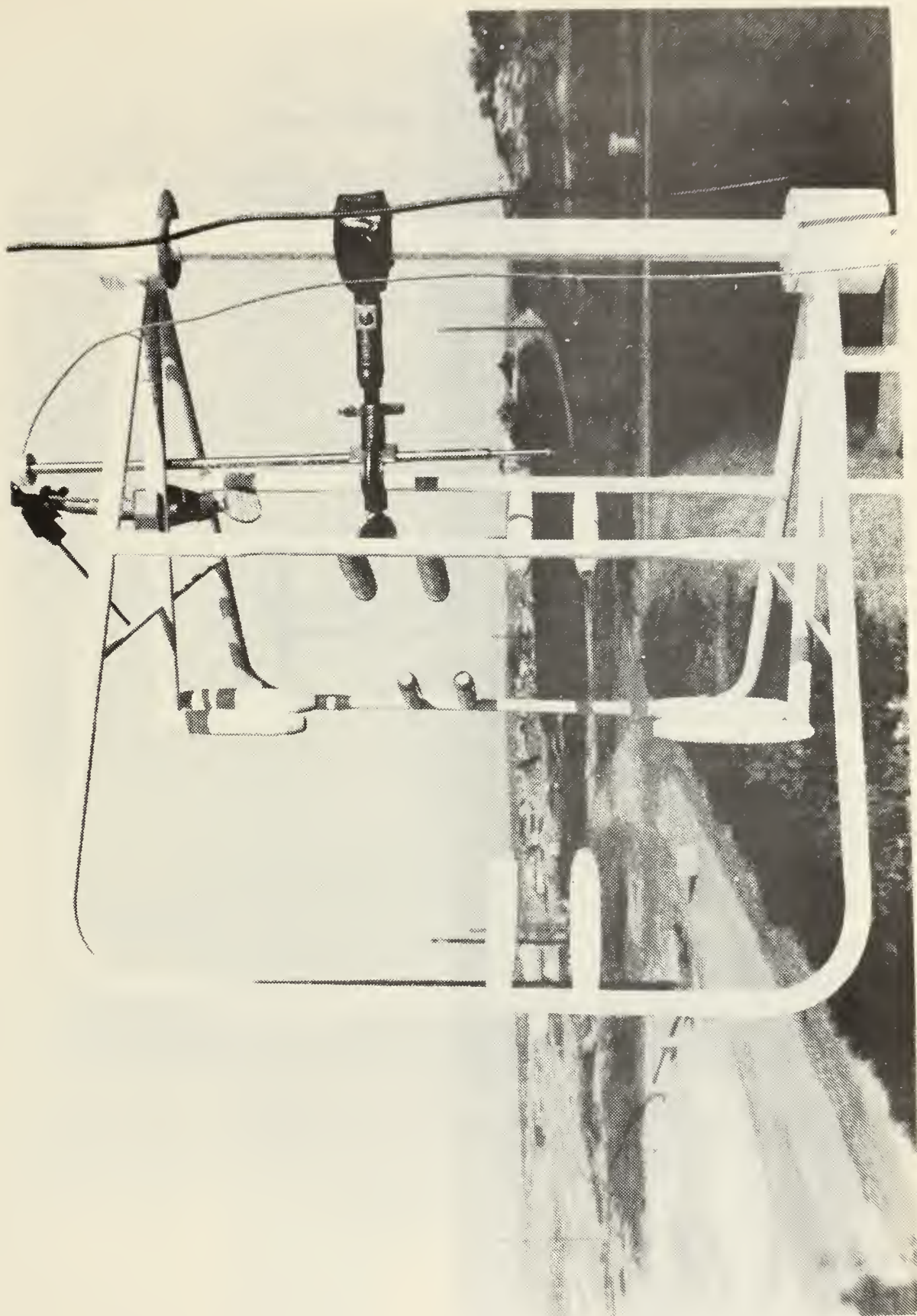


Figure 17. Closeup of Probe Arrangement.





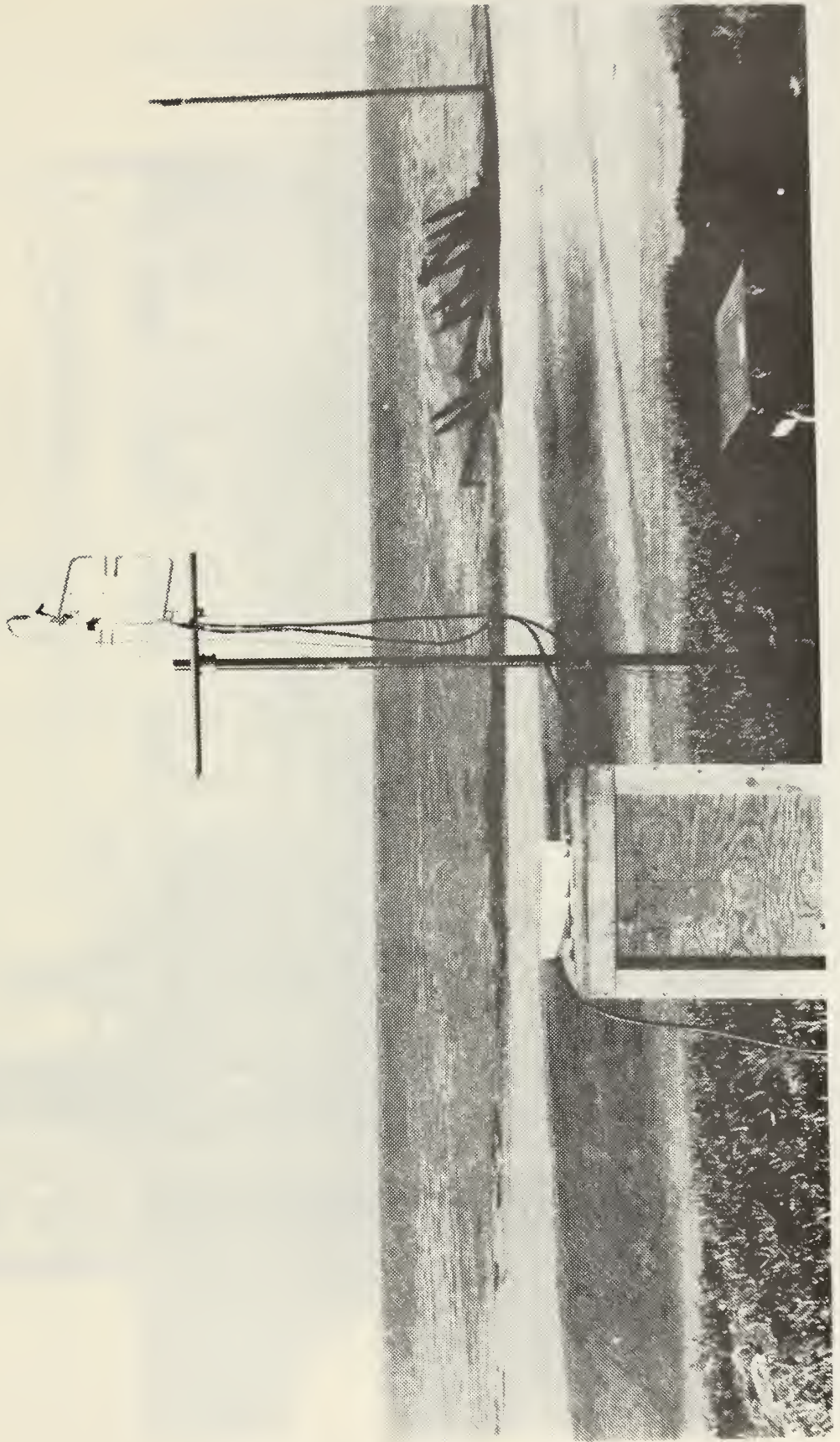


Figure 18. Probe Stand Orientation.





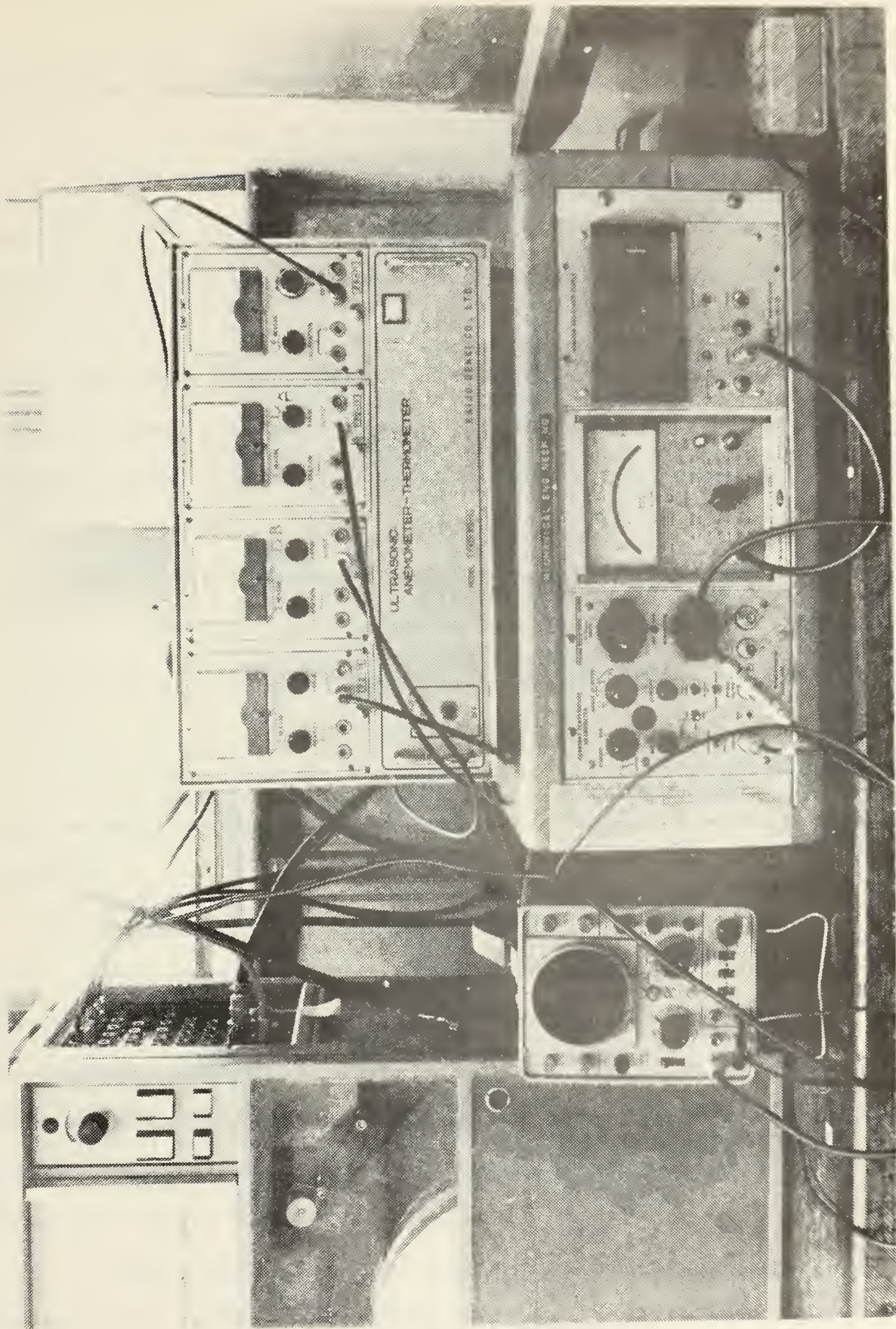


Figure 19. Inside Installation of Equipment.





the ocean, at an average speed of 2-4 m/sec. Mean air temperature for the period (1430-1700 PST) was 52°F.

Three separate 30 minute analog data records were recorded (1500 to 1530, 1546 to 1616 and 1620 to 1650 PST). Data on all channels were recorded without amplification. During the measurements, spikes were observed on all channels. The spikes were found, after this experiment, to have been caused by faulty transistors in the junction box. Examples of these spikes appear in the strip chart recording in Figure 20.

Hot wire anemometer and thermocouple data were not recorded because the record amplifier on the hot wire channel of the tape recorder failed and the thermocouple malfunctioned.

The three separate analog data records from the sonic anemometer/thermometer data were digitized and spectral analyzed.

### 3. Experiment II - 27 February 1973

This experiment was similar to experiment I except that hot wire anemometer data and thermocouple data were successfully recorded. Channel B of the sonic anemometer/thermometer was not operating because of a short in the connector cable on that channel. This malfunction did not affect the other channels.

Again, wind speed and temperature data were obtained during three separate 30 minute periods (1030 to 1100, 1345



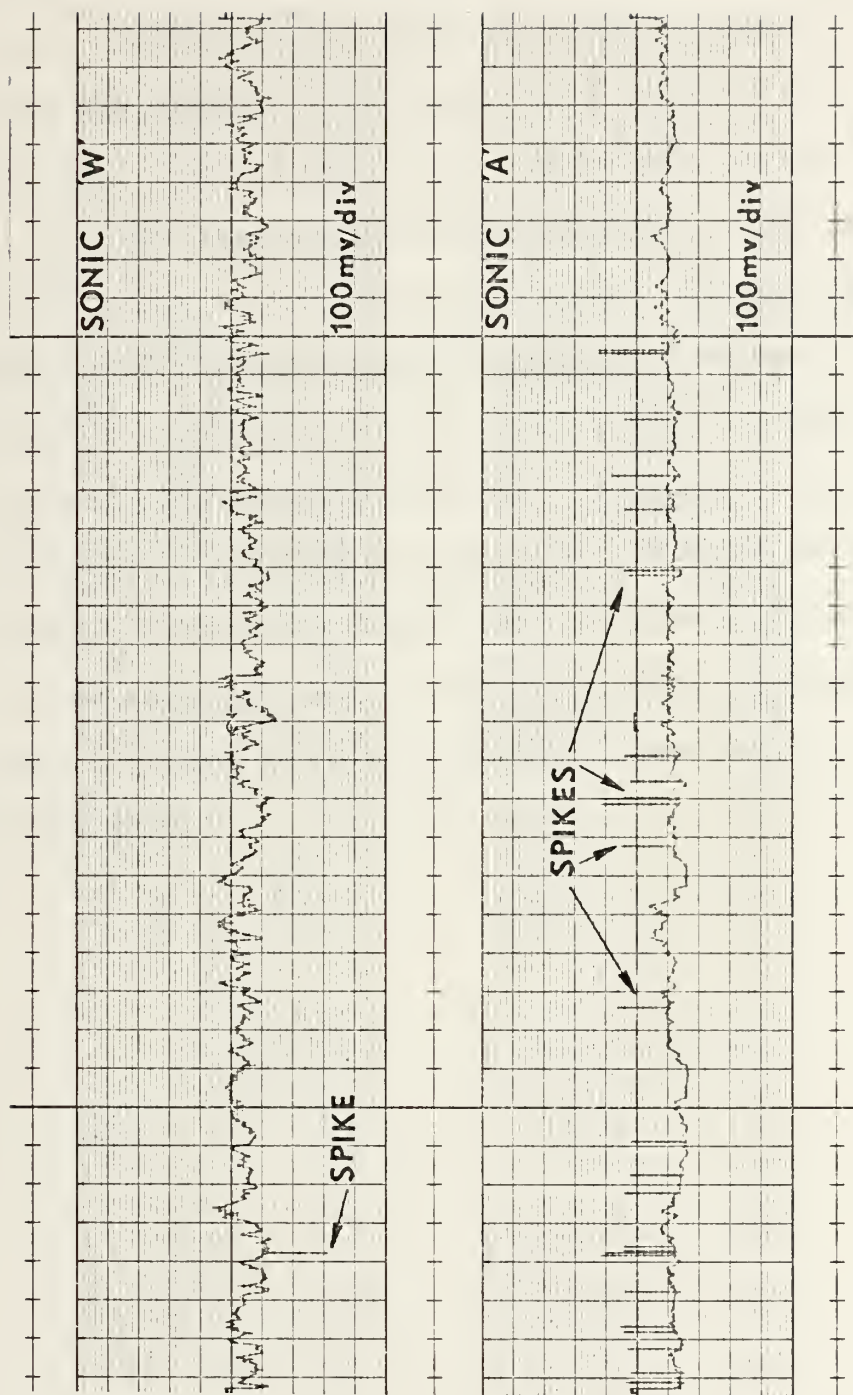


Figure 20. Strip Chart Recording of the Sonic A and W Channels Indicating Spikes.



to 1415 and 1530 to 1600 PST). It was an overcast sky. Visibility was approximately six miles. Winds were from the west, off the ocean, with an average speed of 4-8 m/sec. Mean air temperature ranged from 58°F in the late morning period to 60°F in the early afternoon period.

During the recording periods, all but one of the data channels were amplified using Preston 8300-XWB amplifiers. The amplification factors were two for the sonic W and T channels, one for the sonic A channel, twenty for the hot wire channel and one thousand for the thermocouple channel. The hot wire data were filtered before recording using a Krohn-Hite model 3750 bandpass filter low set at 0.2 Hz and high set at 200.0 Hz. The three separate 30 minute analog data records were digitized and spectrally analyzed.



## V. RESULTS AND CONCLUSIONS

### A. GENERAL PERFORMANCE OF SONIC ANEMOMETER/THERMOMETER

In general the sonic anemometer/thermometer satisfactorily measured the wind and temperature fluctuations during the field experiments, but it did not operate at its peak potential because of various electronic problems. For example, spiking occurred on all channels during both experiments I and II and a short occurred in channel B during experiment II. These could have been a result of the instrument being idle for two years.

Spiking proved to be a continuous problem during the field experiments even though numerous transistors in the system had been replaced.

### B. SPECTRA PLOTS

#### 1. General

Sonic anemometer/thermometer data recorded on 14 December 1972 (experiment I) were digitized at a sampling rate of 390.5 Hz (aliasing frequency 192.25 Hz) and also at 62.5 Hz (aliasing frequency 31.25 Hz).

No editing or filtering was performed on any of the channels during digitization at the higher sampling rate. The higher sampling rate (390.5 Hz) enabled the examination of a frequency band from 0 Hz to approximately 100 Hz.

The analog data tape was edited prior to digitizing at the lower sampling rate. This led to the elimination of





the first time period which had the heaviest spiking. The remaining two time periods were digitized at 62.5 Hz and filtered at 31.25 Hz. The lower sampling rate shifted the frequency band examined (approximately 0.5 Hz to 40 Hz) towards the lower end of the frequency spectrum. The spectral results indicate both the energy containing frequency band as well as the lower frequency end of the inertial sub-range.

Hot wire data were not taken during experiment I because of a recording amplifier failure. Two samples of hot wire data taken on a day that had similar synoptic characteristics (air temperature and wind) as the day of experiment I are included for comparison purposes. They are considered representative samples of data which would have been taken by a hot wire anemometer system on that day. These results represent a frequency band of from 0.01 Hz to approximately 100 Hz. The data for both of these results were digitized at a rate of 200.0 Hz (aliasing frequency 100.0 Hz) and filtered at 100.0 Hz.

On 28 February 1973 (experiment II), sonic anemometer/thermometer, hot wire anemometer and one mil thermocouple data were collected during the three 30 minute time periods. The sonic data were digitized at a sampling rate of 62.5 Hz and filtered at 32.25 Hz. The hot wire and thermocouple data were digitized at a sampling rate of 200.0 Hz and filtered at 100.0 Hz. Sonic channel B was inoperative.



2. Sonic Anemometer/Thermometer Data Sampled at  
390.5 Hz - 14 December 1972 (Experiment I)

Figure 21 to Figure 32 are for the three 30 minute periods from 1500 to 1700. A  $-5/3$  slope exists on the log-log plot in the frequency band from 1.0 Hz to 10.0 Hz for all channels. Spectra from channels A, B, W have  $-5/3$  slopes which continue beyond 10.0 Hz but the T spectra slopes drop off more rapidly than  $-5/3$  before 10.0 Hz.

3. Sonic Anemometer/Thermometer Data Sampled at  
62.5 Hz - 14 December 1972 (Experiment I)

Figure 33 to Figure 40 are from the two edited periods of data which were filtered and then sampled at the lower rate. Spectra from channels A and B in both periods have definite  $-5/3$  slopes within the 1.0 Hz to 10.0 Hz band with some departure around 8.0 Hz. For both periods, W channel spectra have  $-5/3$  slopes up to 6.0 Hz with rapid deterioration beyond. For the second period, the T spectrum has a drop off from a  $-5/3$  slope at approximately 4.0 Hz but for the third period, the T spectra has a definite  $-5/3$  slope throughout the 1.0 Hz to 10.0 Hz frequency band.

4. Hot Wire Anemometer Data Sampled at 200.0 Hz  
- 10 January 1973

Figure 41 and Figure 42 are from hot wire anemometer data taken on 10 January 1973. Two periods are discussed and each period was approximately 50 minutes in length. A distinct  $-5/3$  slope is found in the frequency band from 1.0 Hz to approximately 40.0 Hz for both periods of data.



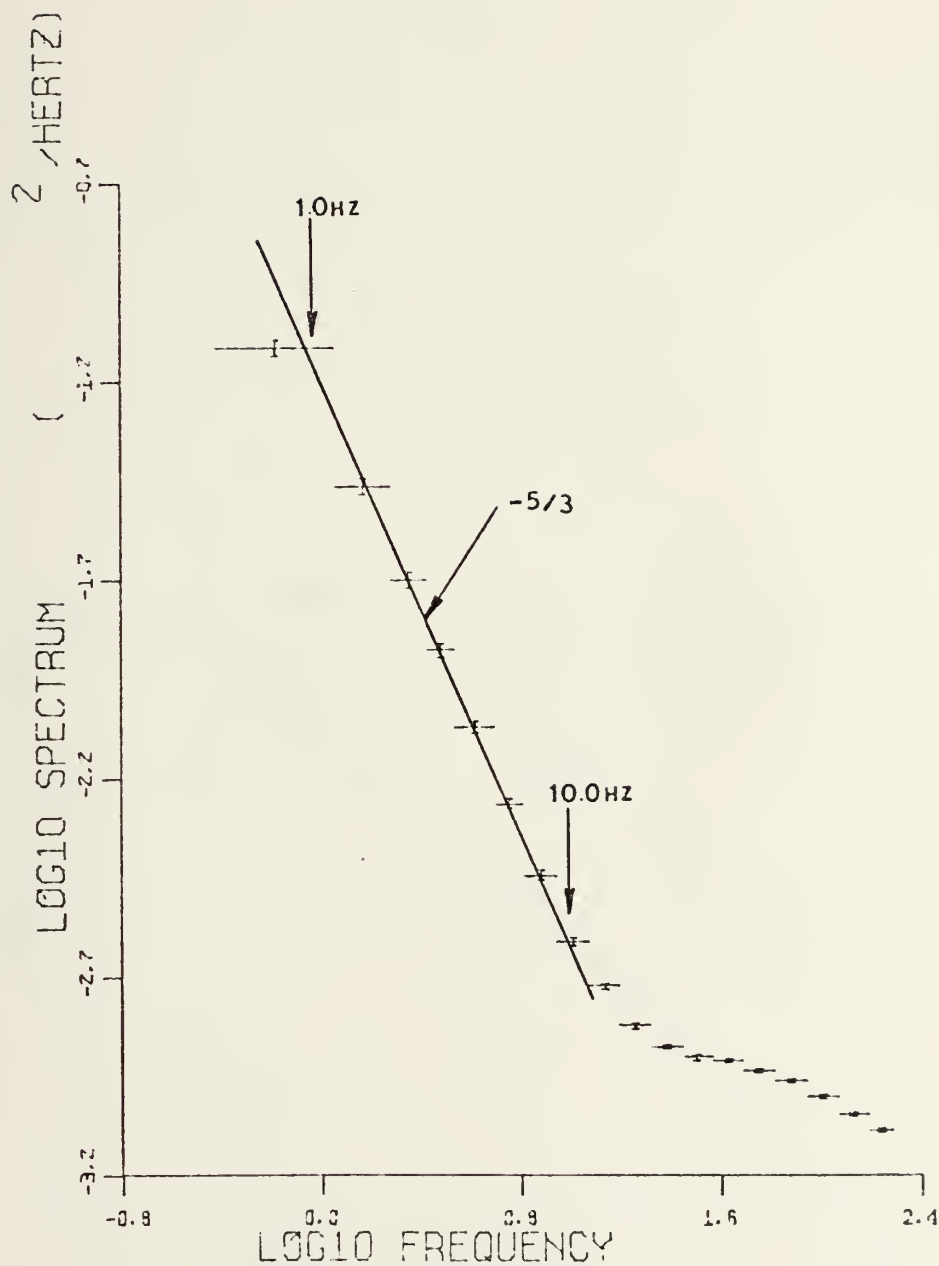


Figure 21. Sonic "A" Channel Data Observed 14 December 1972 1st Period (Experiment I) High Sample Rate.



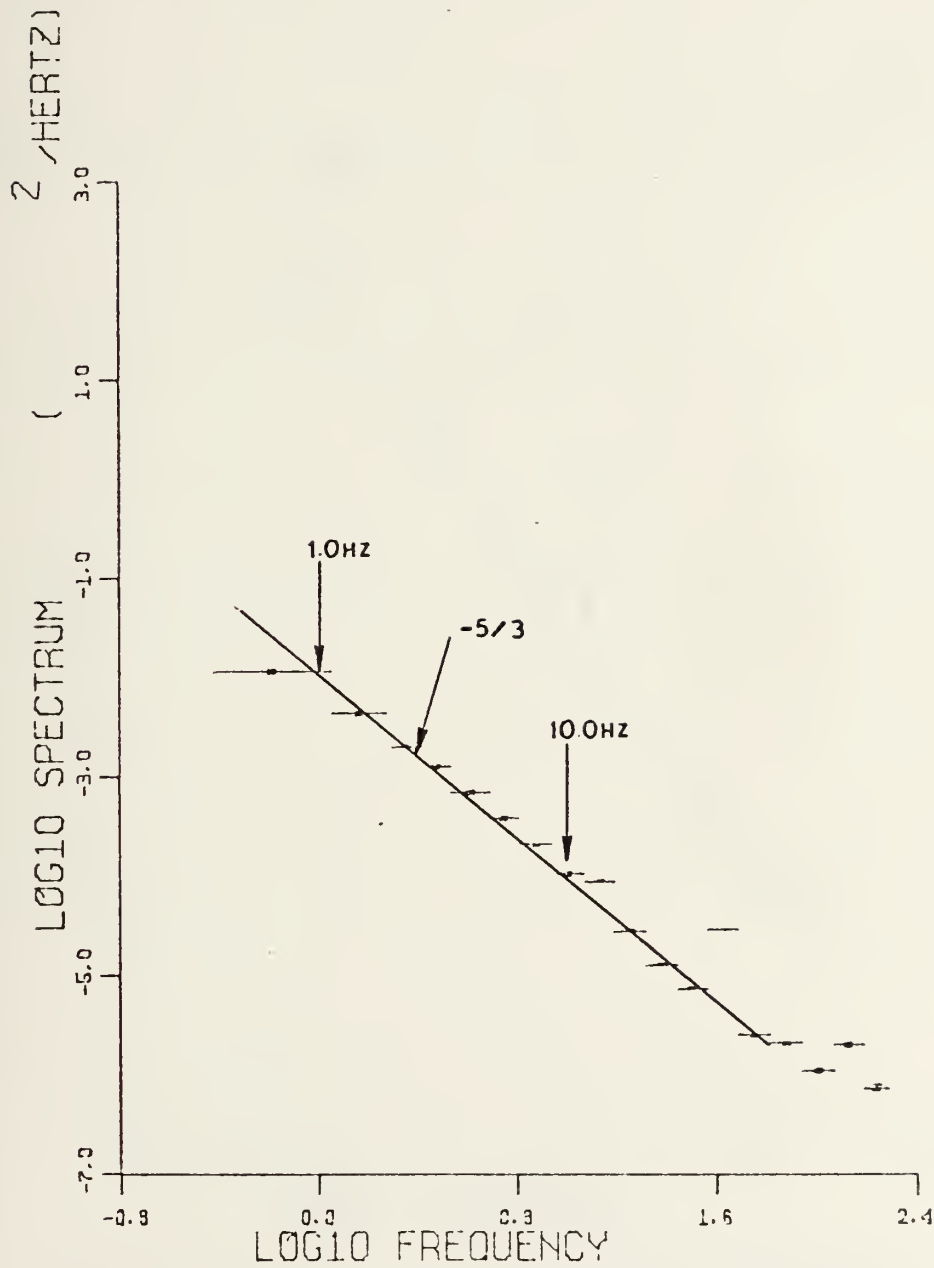


Figure 22. Sonic "B" Channel Data Observed 14 December 1972 1st Period (Experiment I) High Sample Rate.





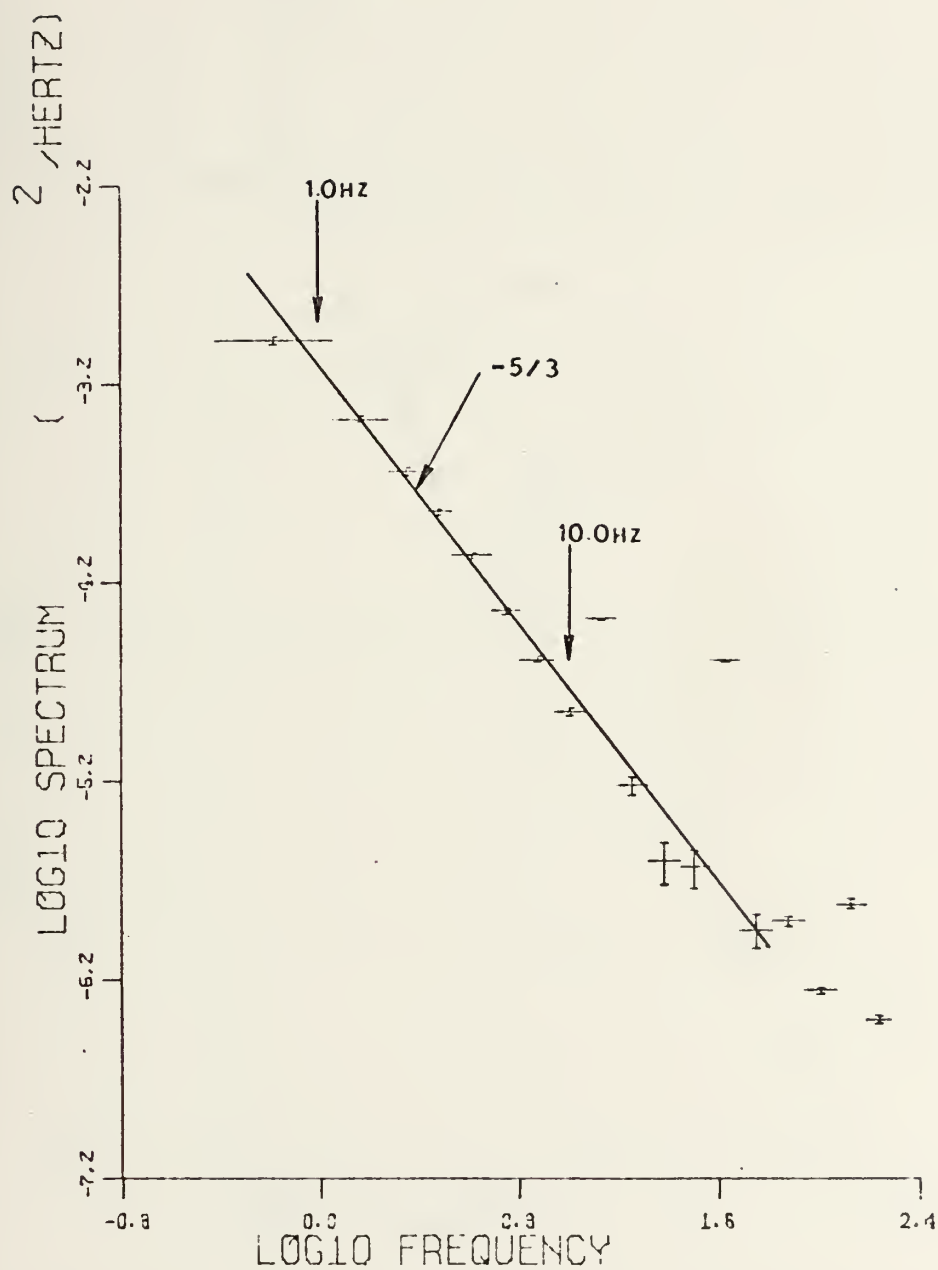


Figure 23. Sonic "W" Channel Data Observed 14 December 1972 1st Period (Experiment I) High Sample Rate.



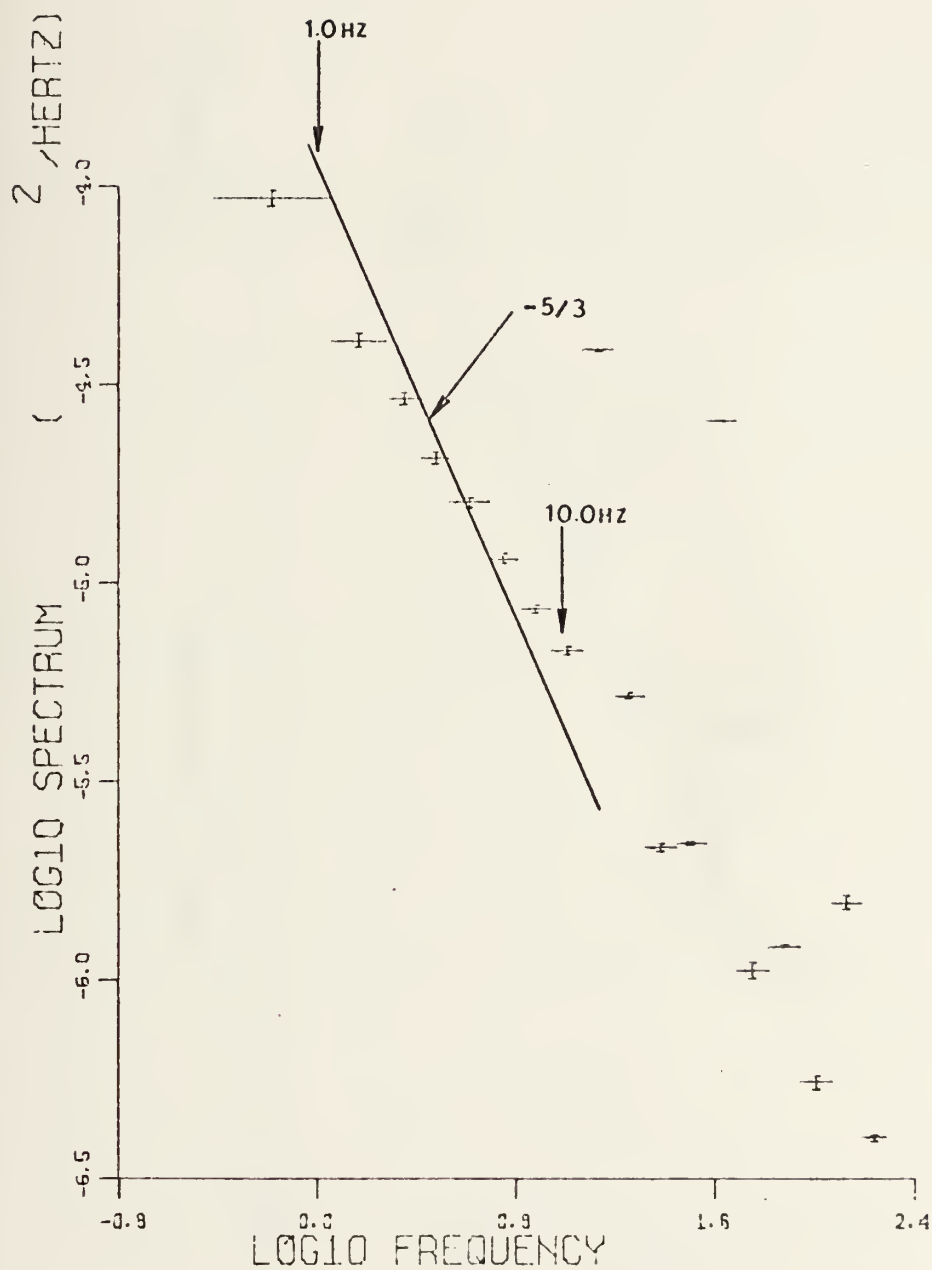


Figure 24. Sonic "T" Channel Data Observed 14 December 1972 1st Period (Experiment I) High Sample Rate.



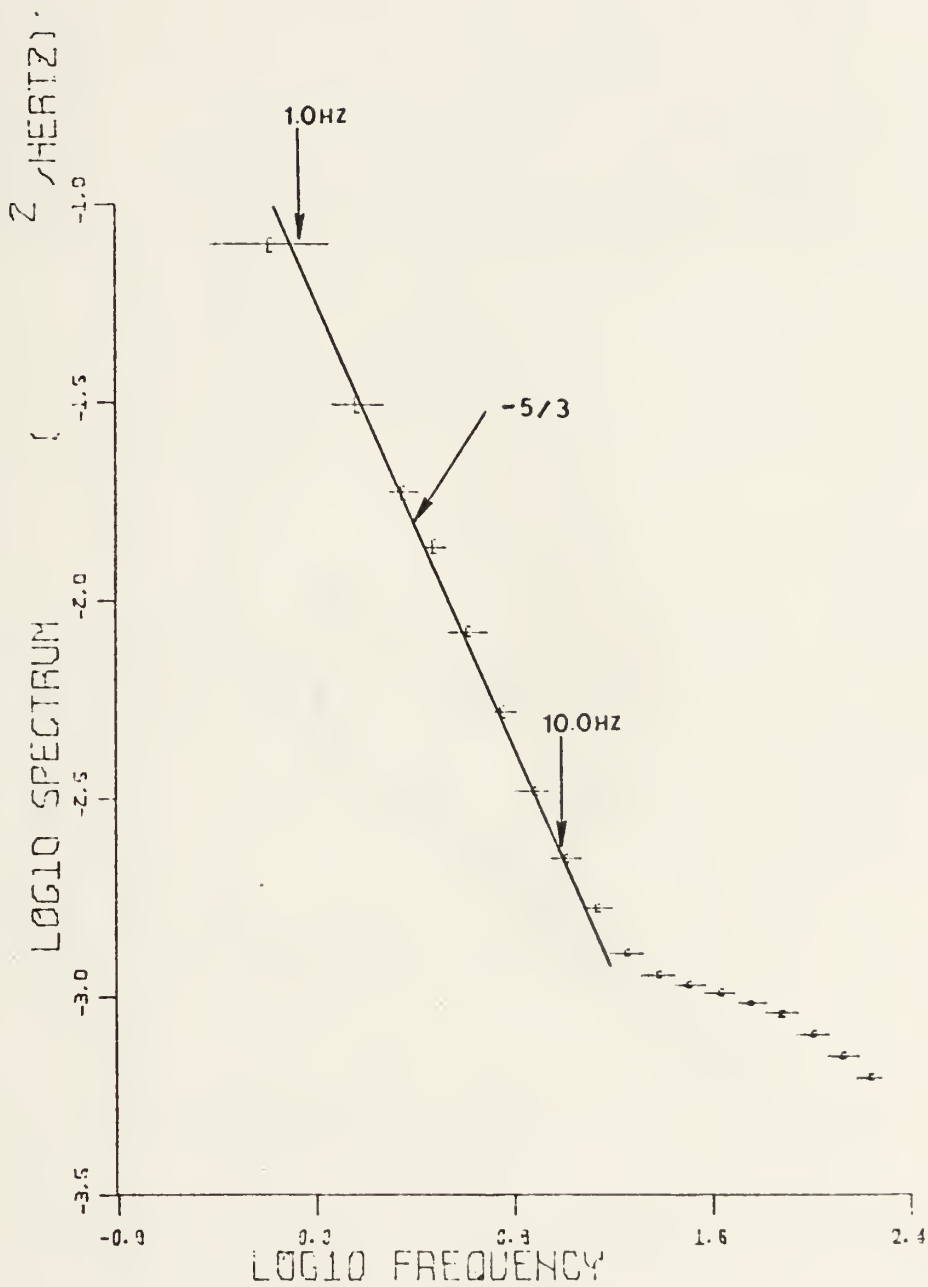


Figure 25. Sonic "A" Channel Data Observed 14 December 1972 2nd Period (Experiment I) High Sample Rate.



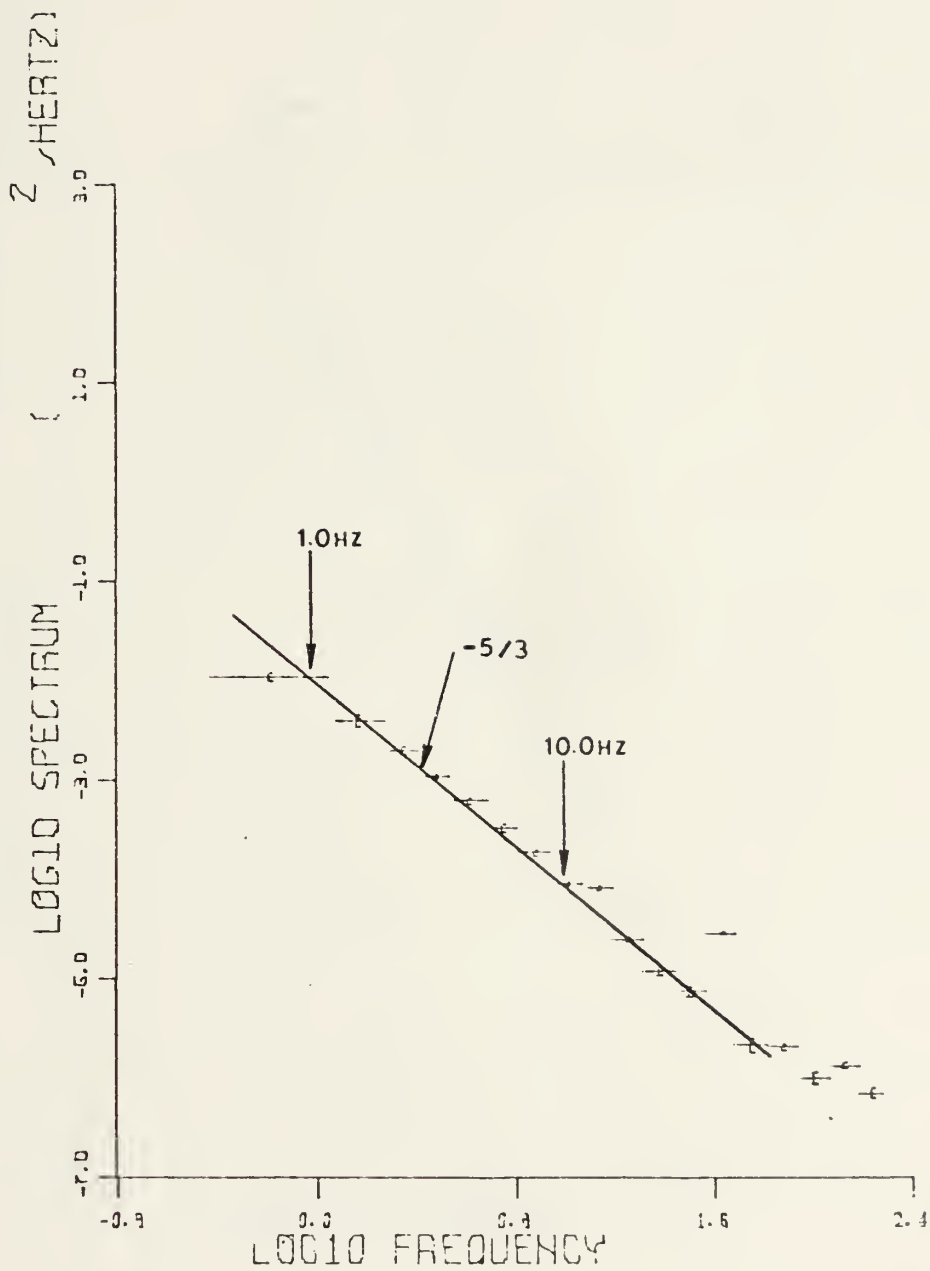


Figure 26. Sonic "B" Channel Data Observed 14 December 1972 2nd Period (Experiment I) High Sample Rate.





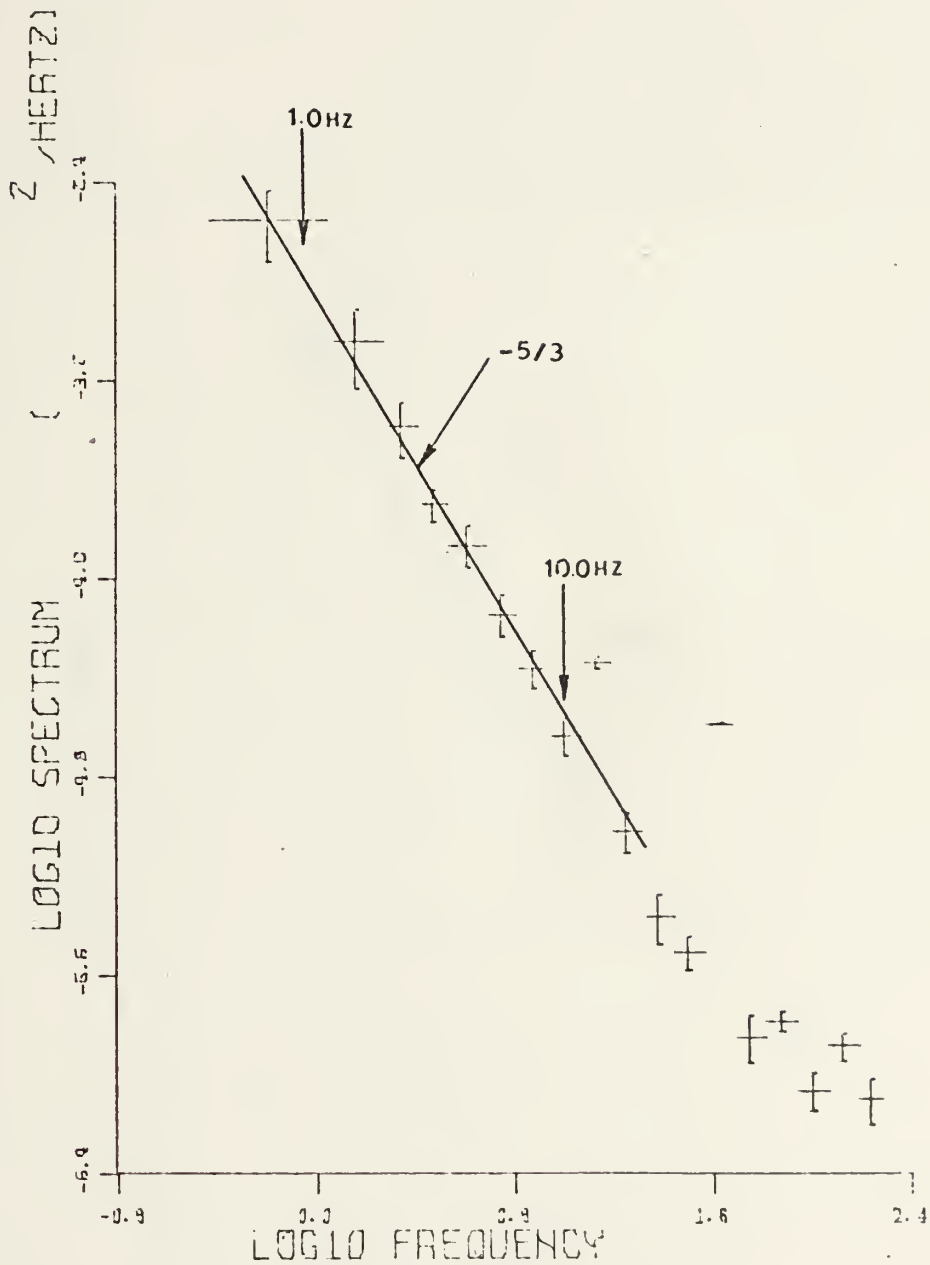


Figure 27. Sonic "W" Channel Data Observed 14 December 1972 2nd Period (Experiment I) High Sample Rate.



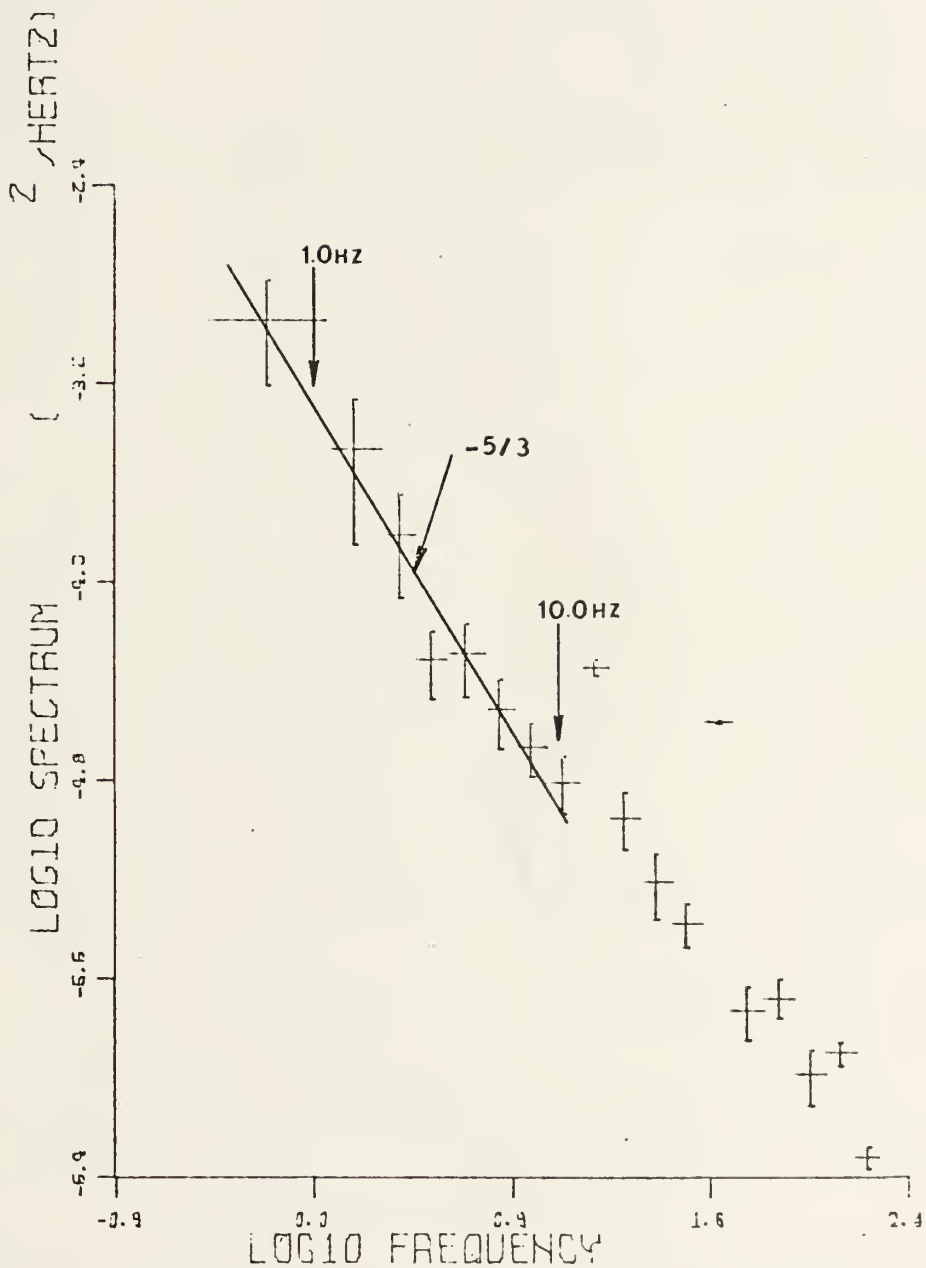


Figure 28. Sonic "T" Channel Data Observed 14 December 1972 2nd Period (Experiment I) High Sample Rate.



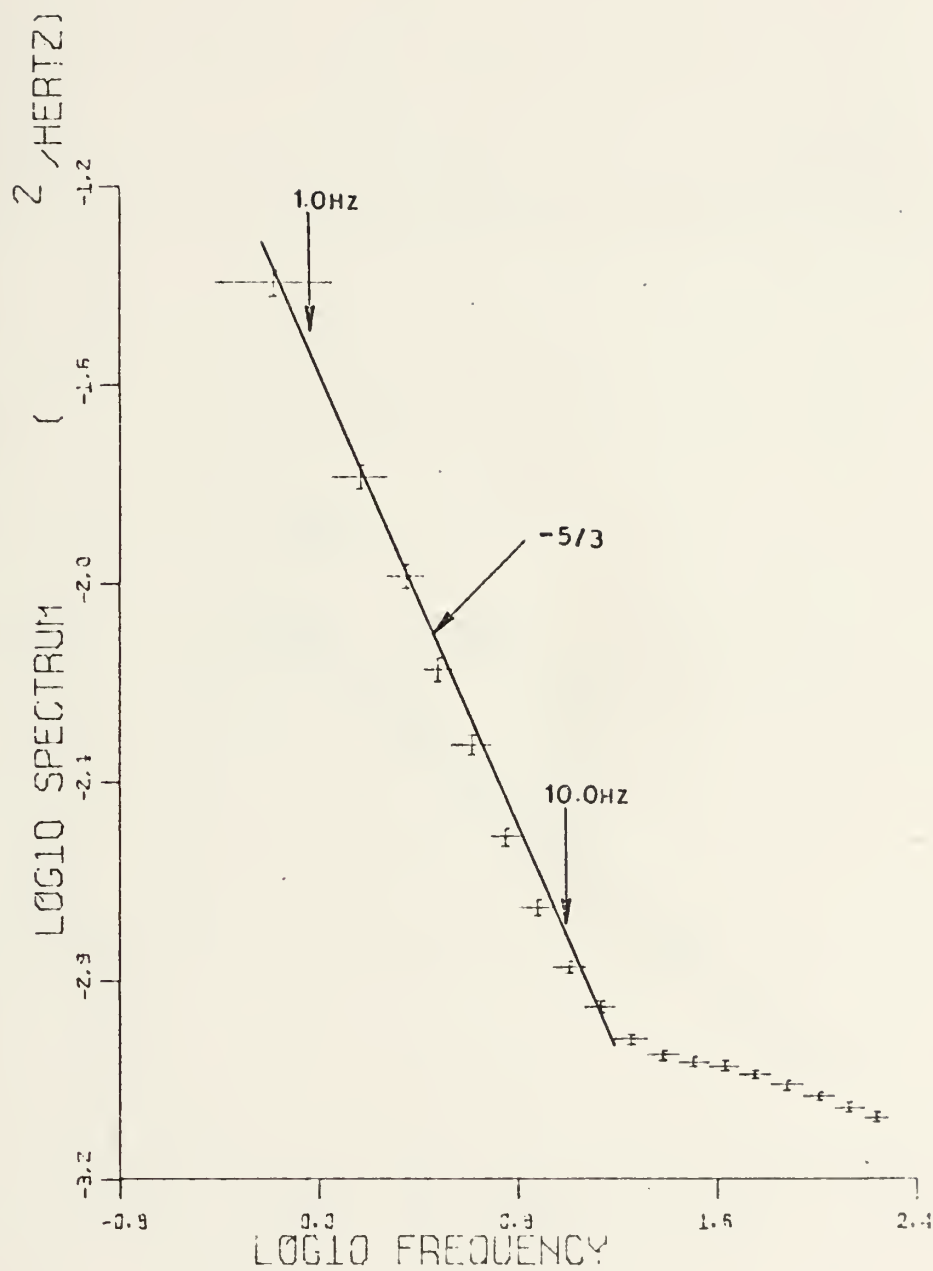


Figure 29. Sonic "A" Channel Data Observed 14 December 1972 3rd Period (Experiment I) High Sample Rate.



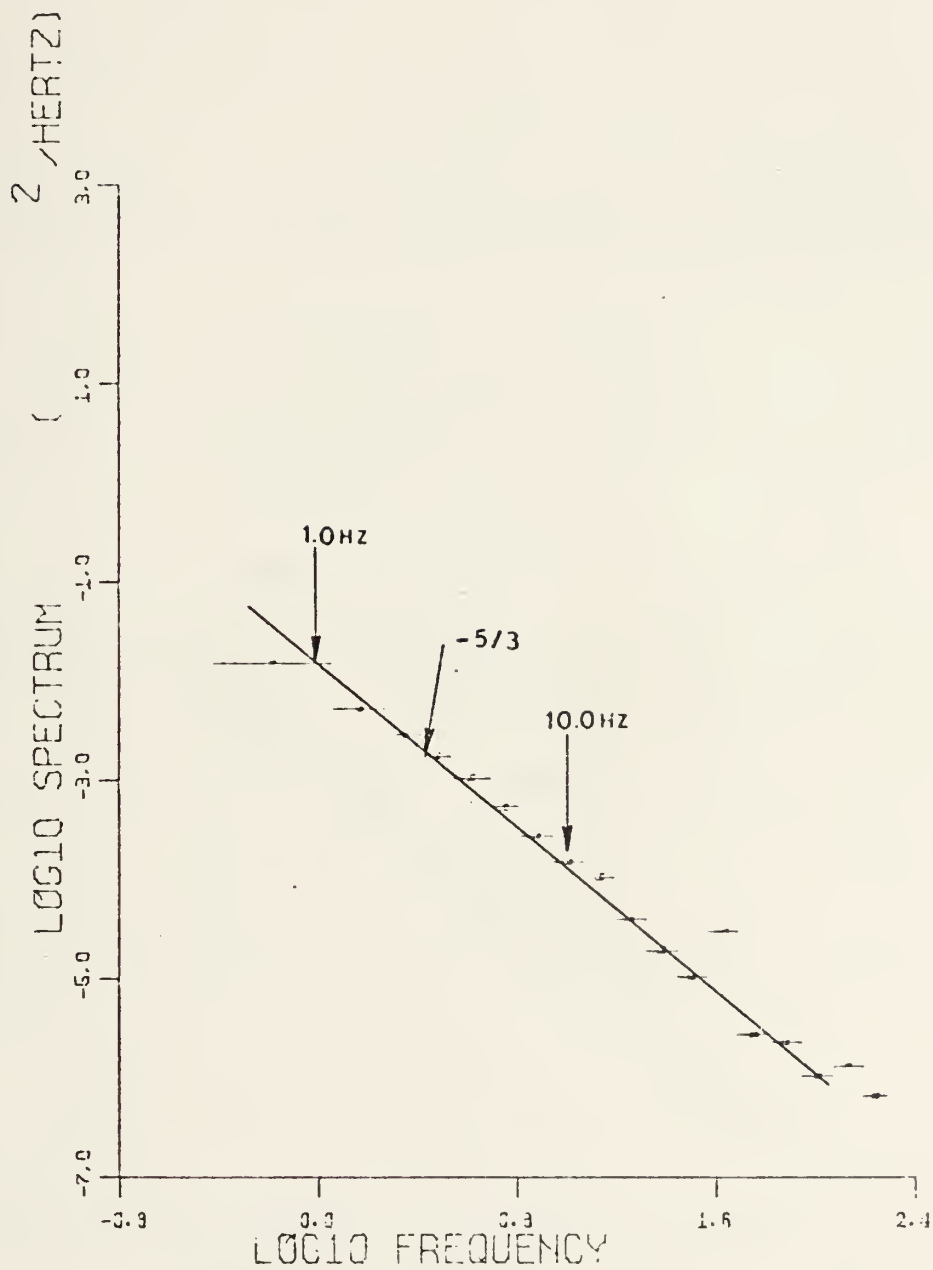


Figure 30. Sonic "B" Channel Data Observed 14 December 1972 3rd Period (Experiment I) High Sample Rate.





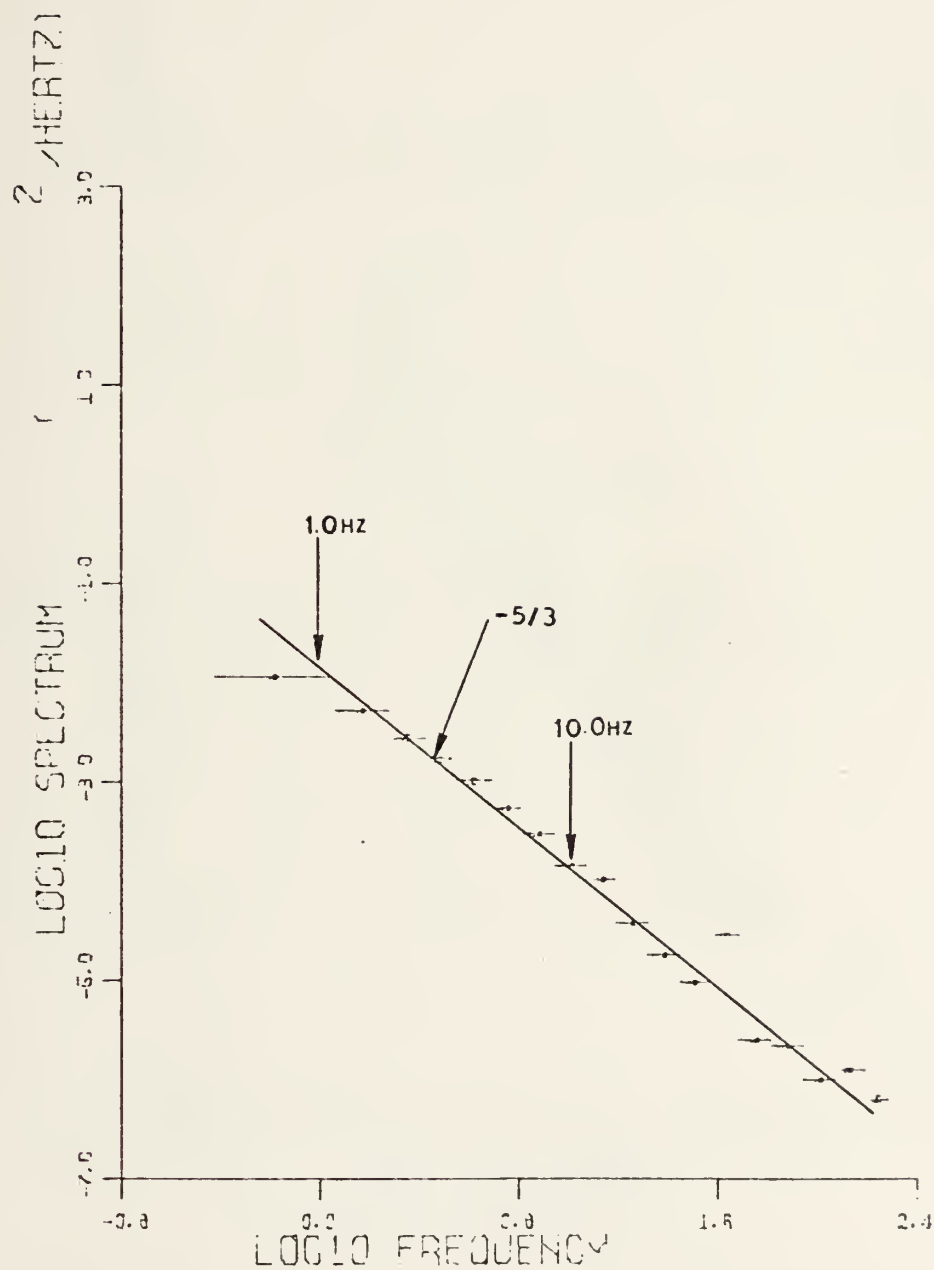


Figure 31. Sonic "W" Channel Data Observed 14 December 1972 3rd Period (Experiment I) High Sample Rate.



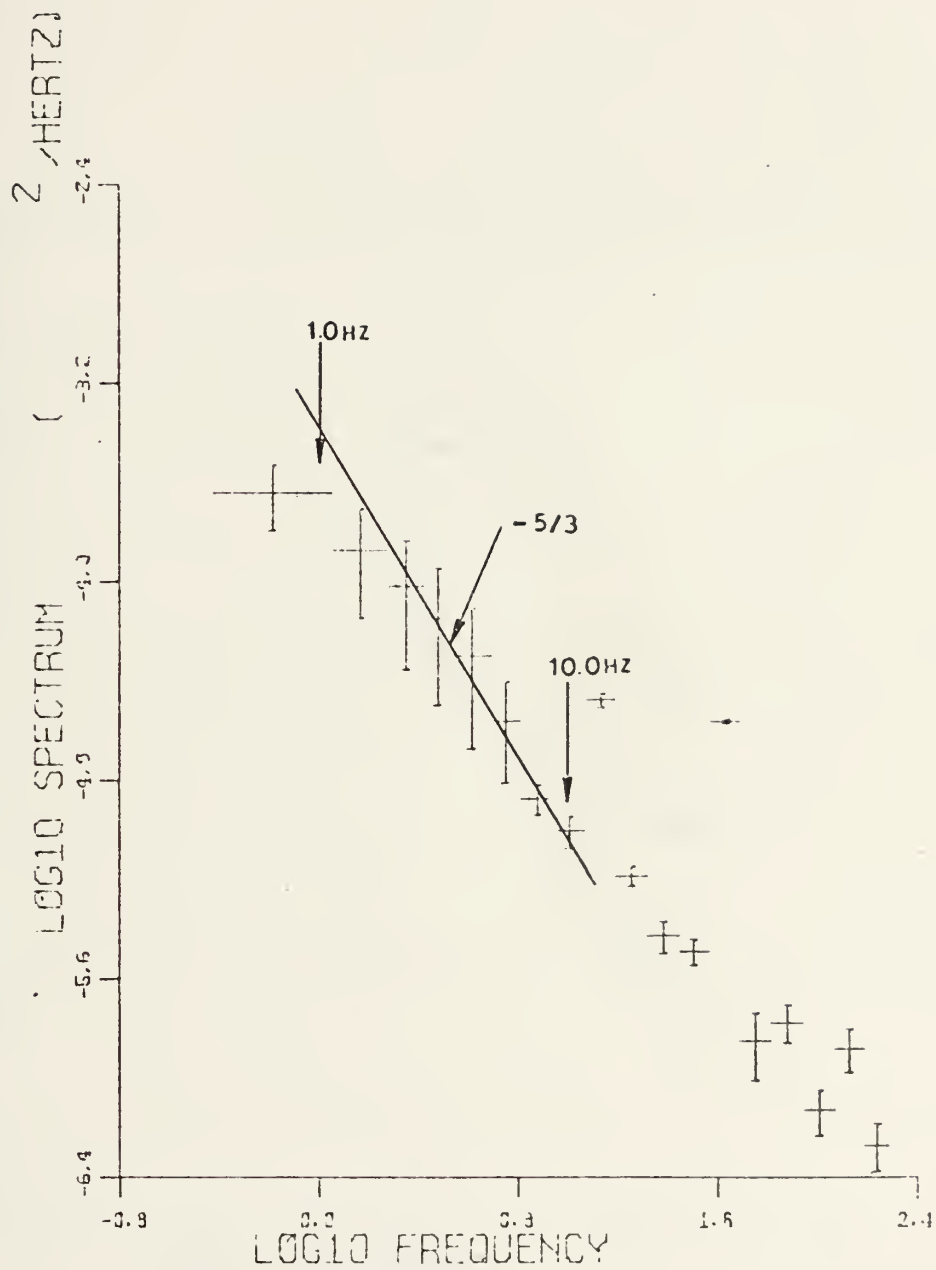


Figure 32. Sonic "T" Channel Data Observed 14 December 1972 3rd Period (Experiment I) High Sample Rate.



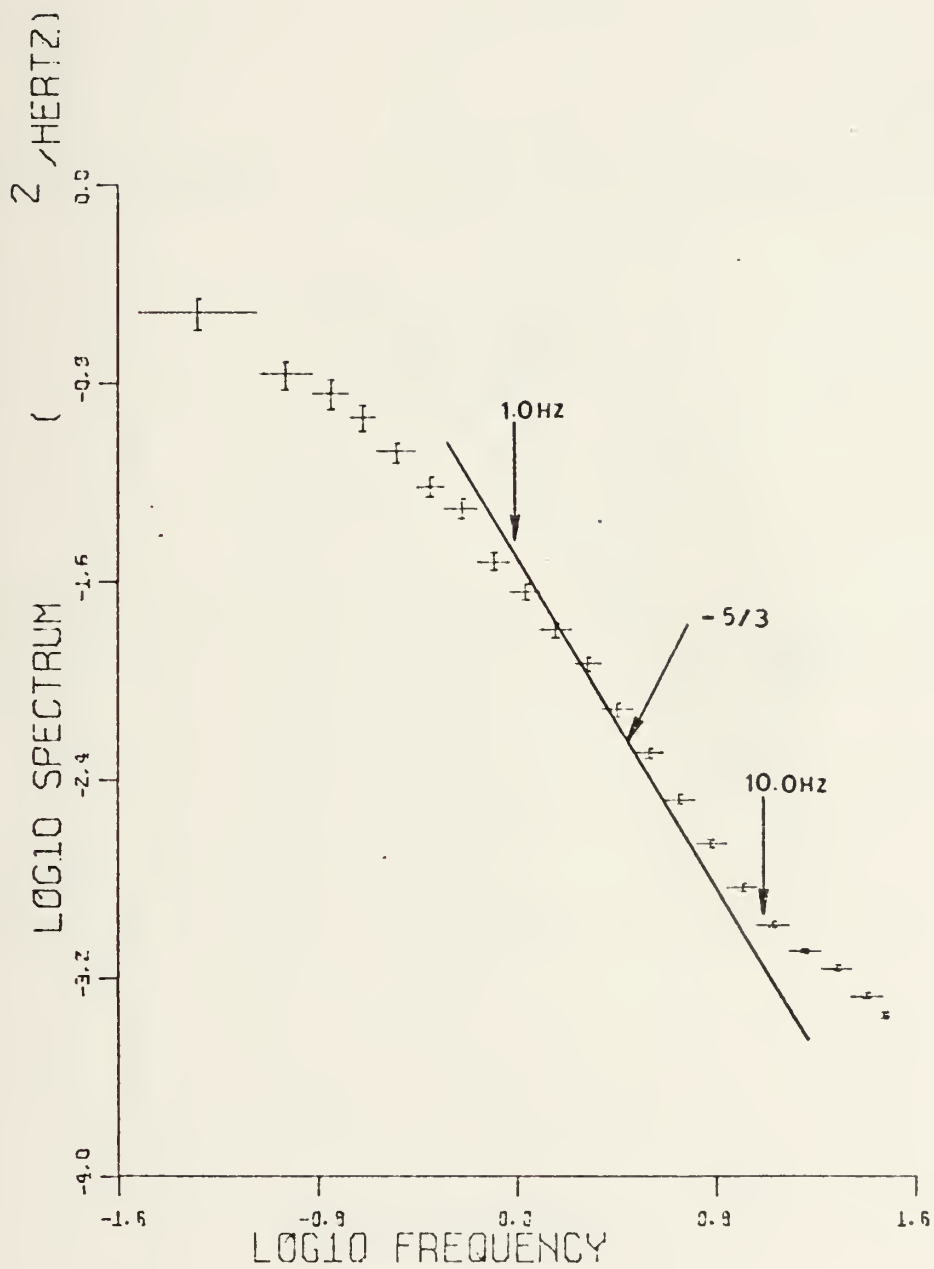


Figure 33. Sonic "A" Channel Data Observed 14 December 1972 2nd Period (Experiment I) Low Sample Rate.



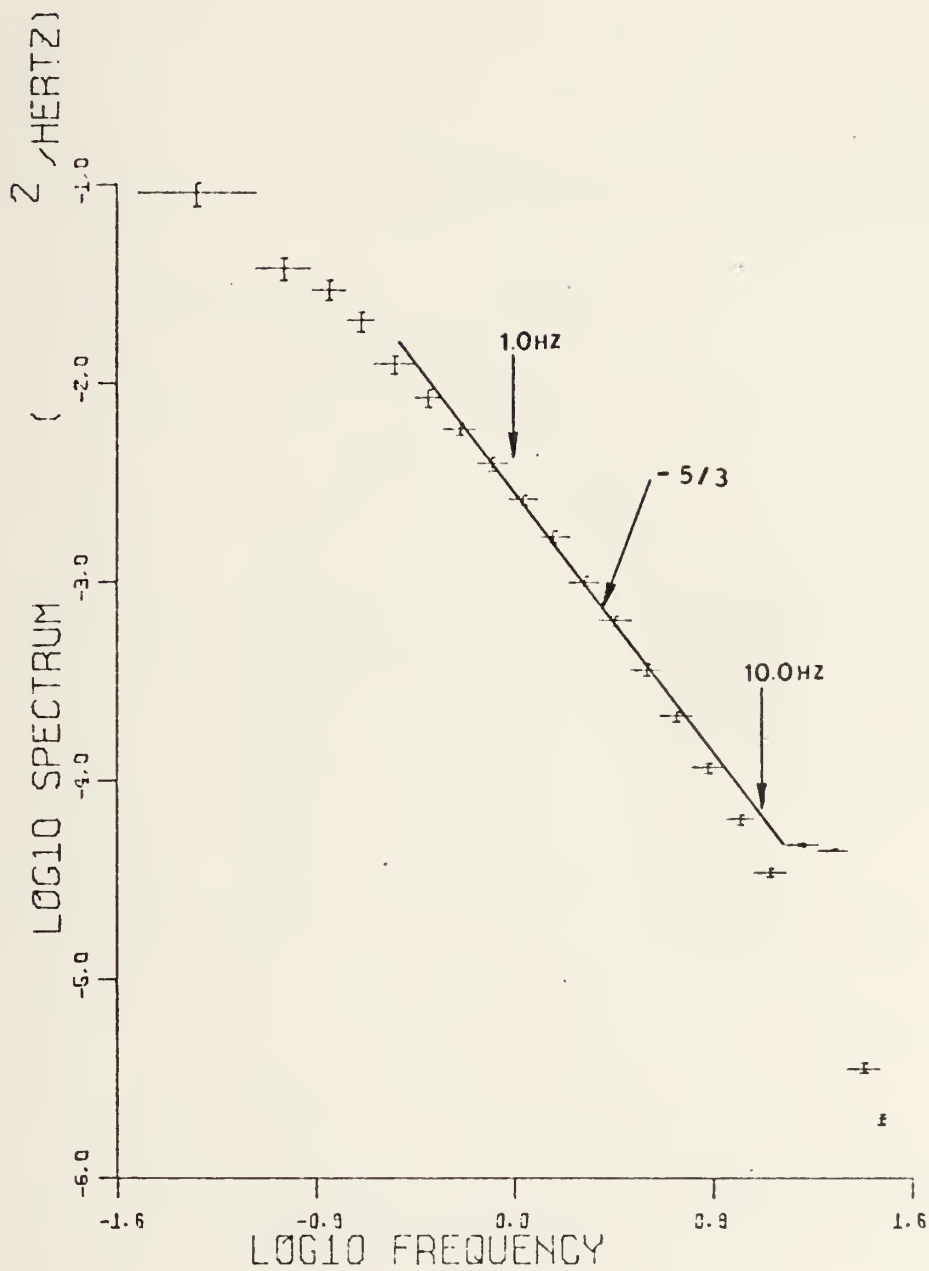


Figure 34. Sonic "B" Channel Data Observed 14 December 1972 2nd Period (Experiment I) Low Sample Rate.





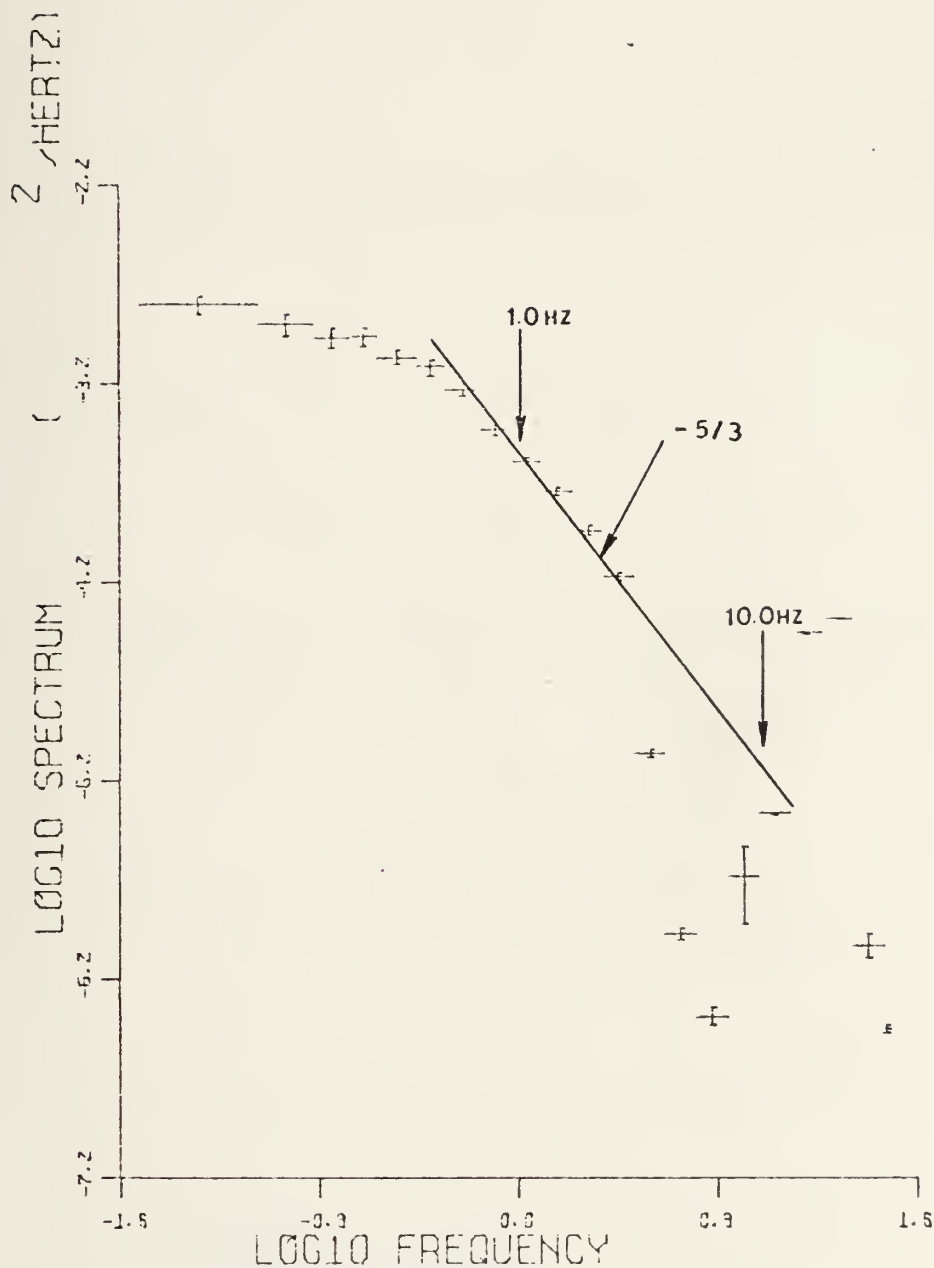


Figure 35. Sonic "W" Channel Data Observed 14 December 1972 2nd Period (Experiment I) Low Sample Rate.



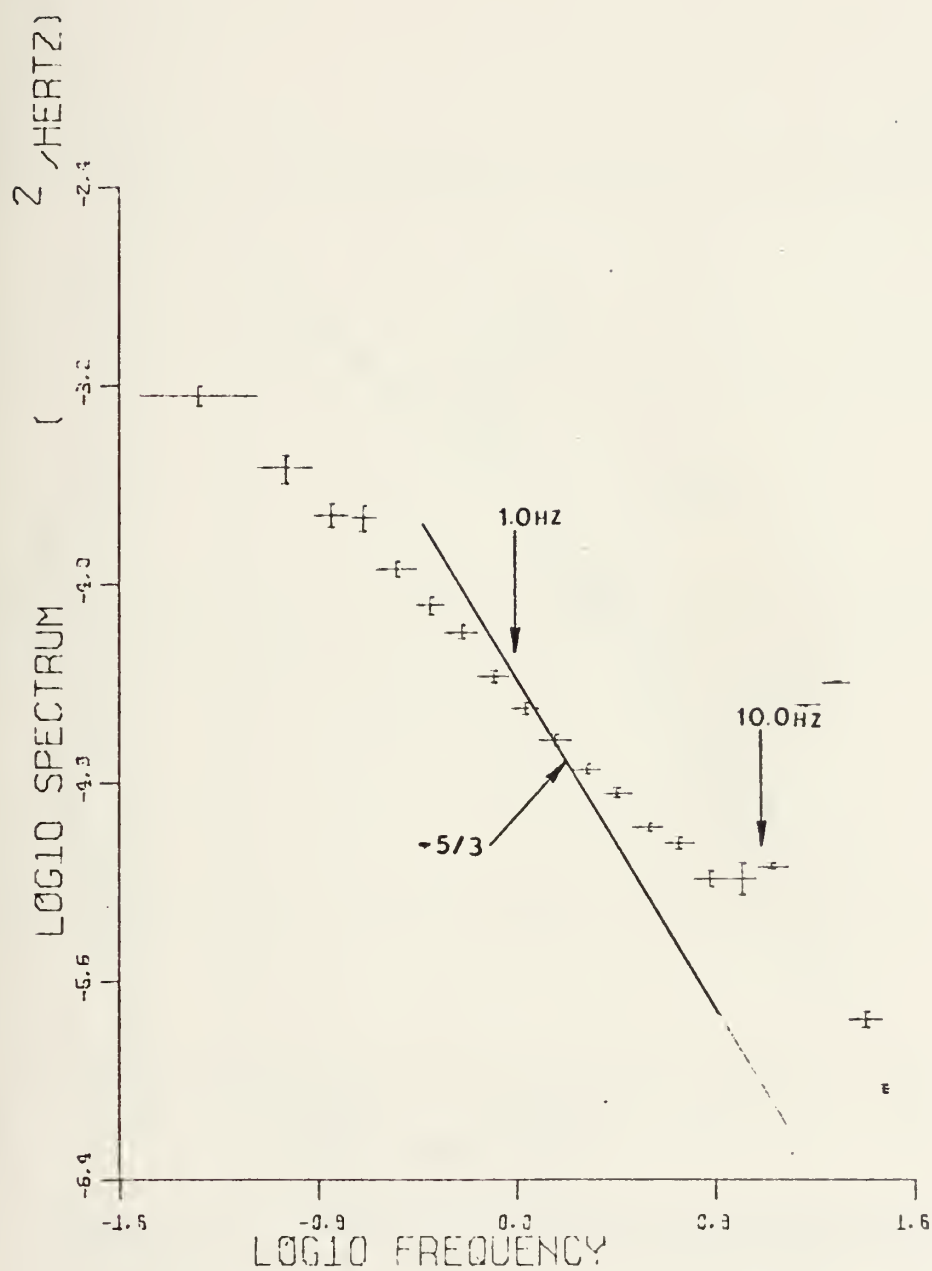


Figure 36. Sonic "T" Channel Data Observed 14 December 1972 2nd Period (Experiment I) Low Sample Rate.



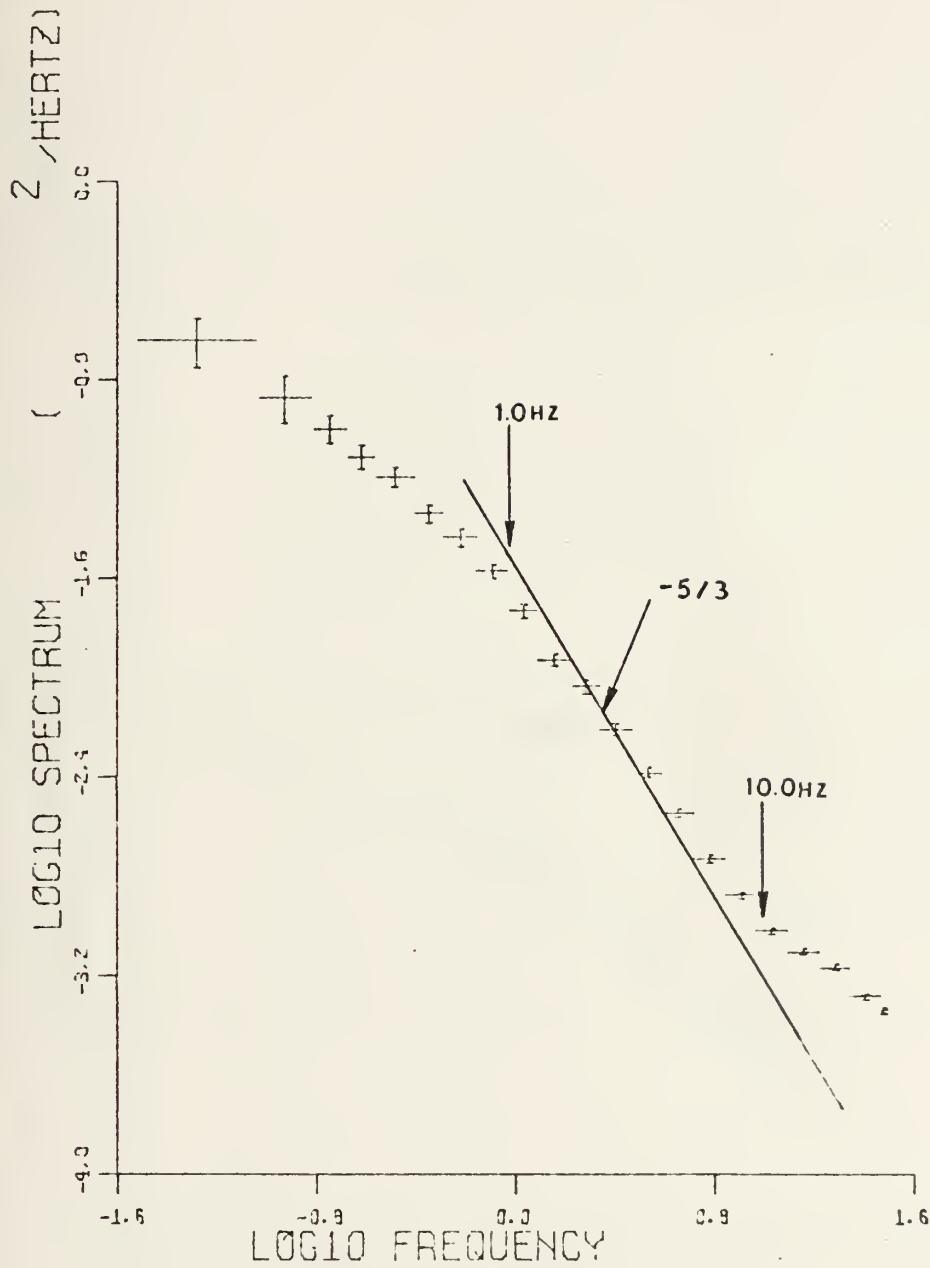


Figure 37. Sonic "A" Channel Data Observed 14 December 1972 3rd Period (Experiment I) Low Sample Rate.



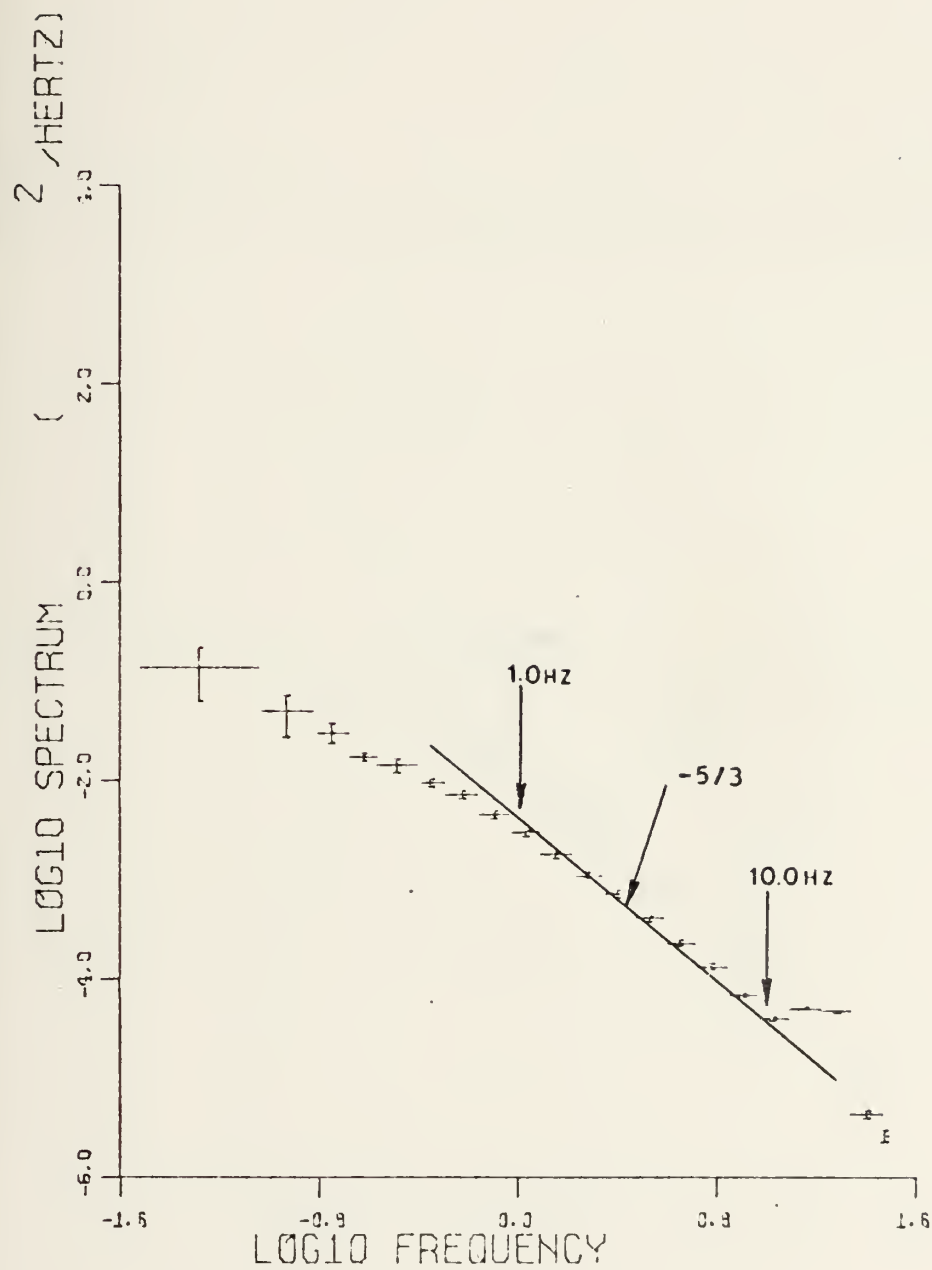


Figure 38. Sonic "B" Channel Data Observed 14 December 1972 3rd Period (Experiment I) Low Sample Rate.





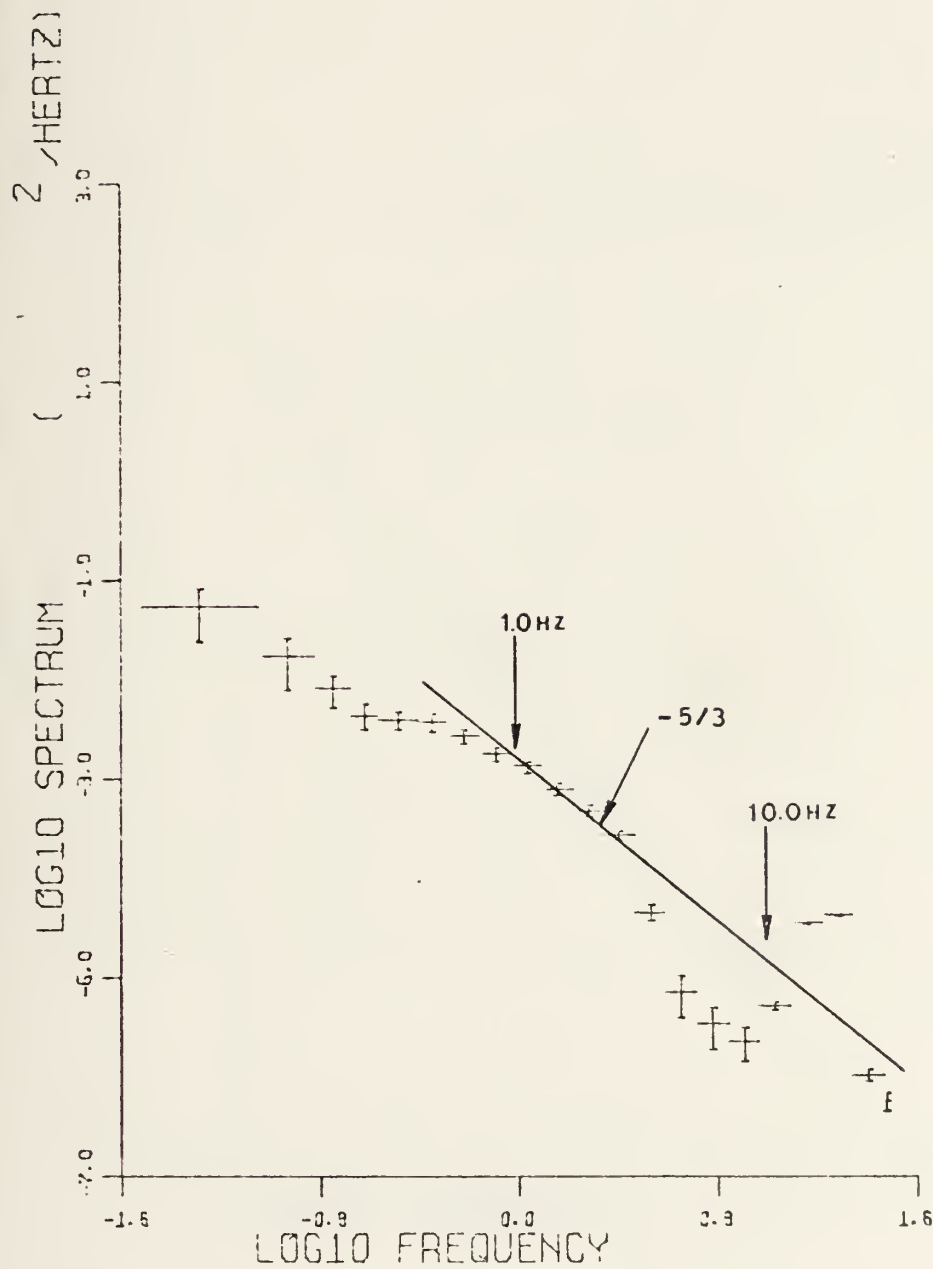


Figure 39. Sonic "W" Channel Data Observed 14 December 1972 3rd Period (Experiment I) Low Sample Rate.



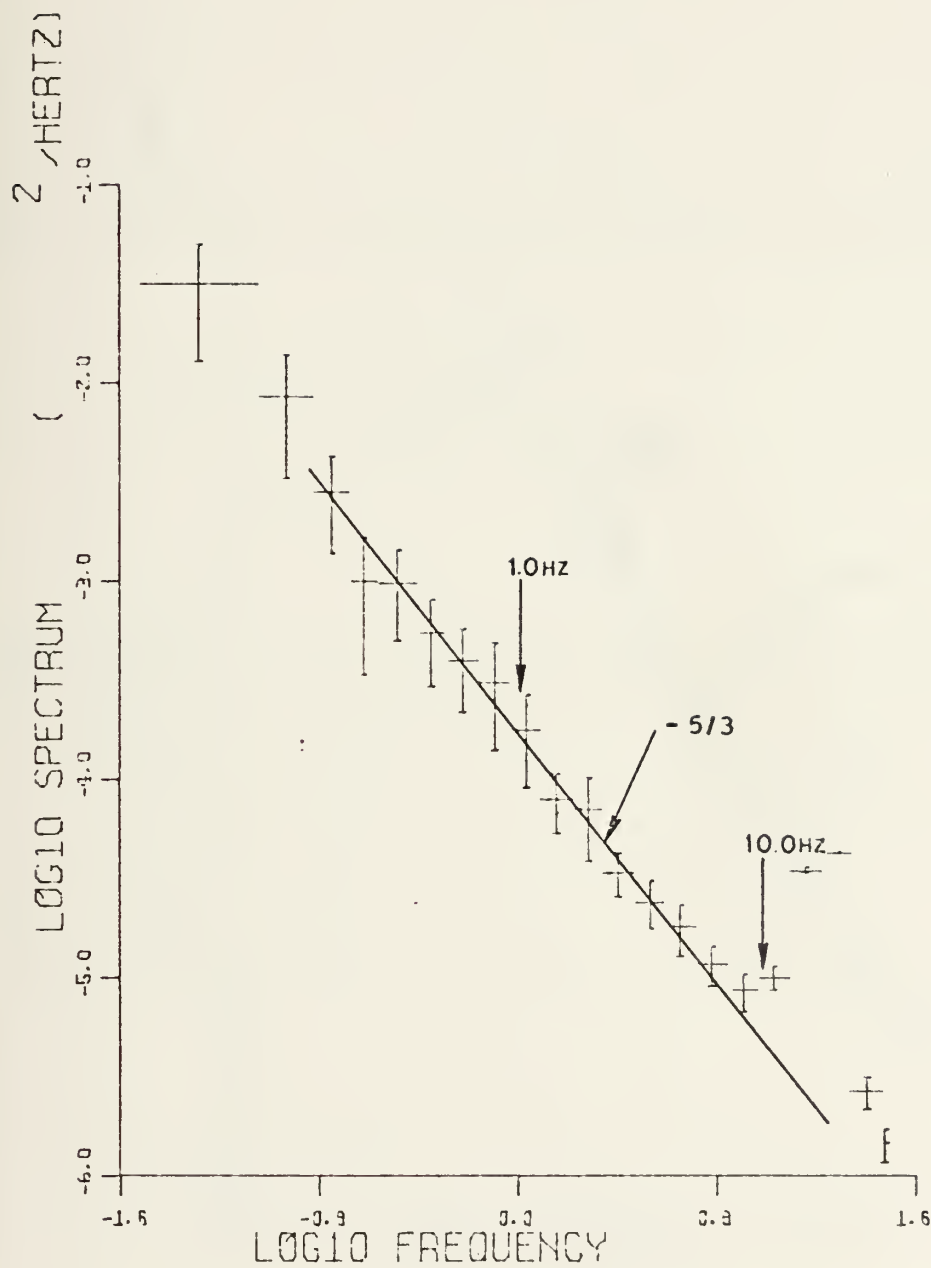


Figure 40. Sonic "T" Channel Data Observed 14 December 1972 3rd Period (Experiment I) Low Sample Rate.



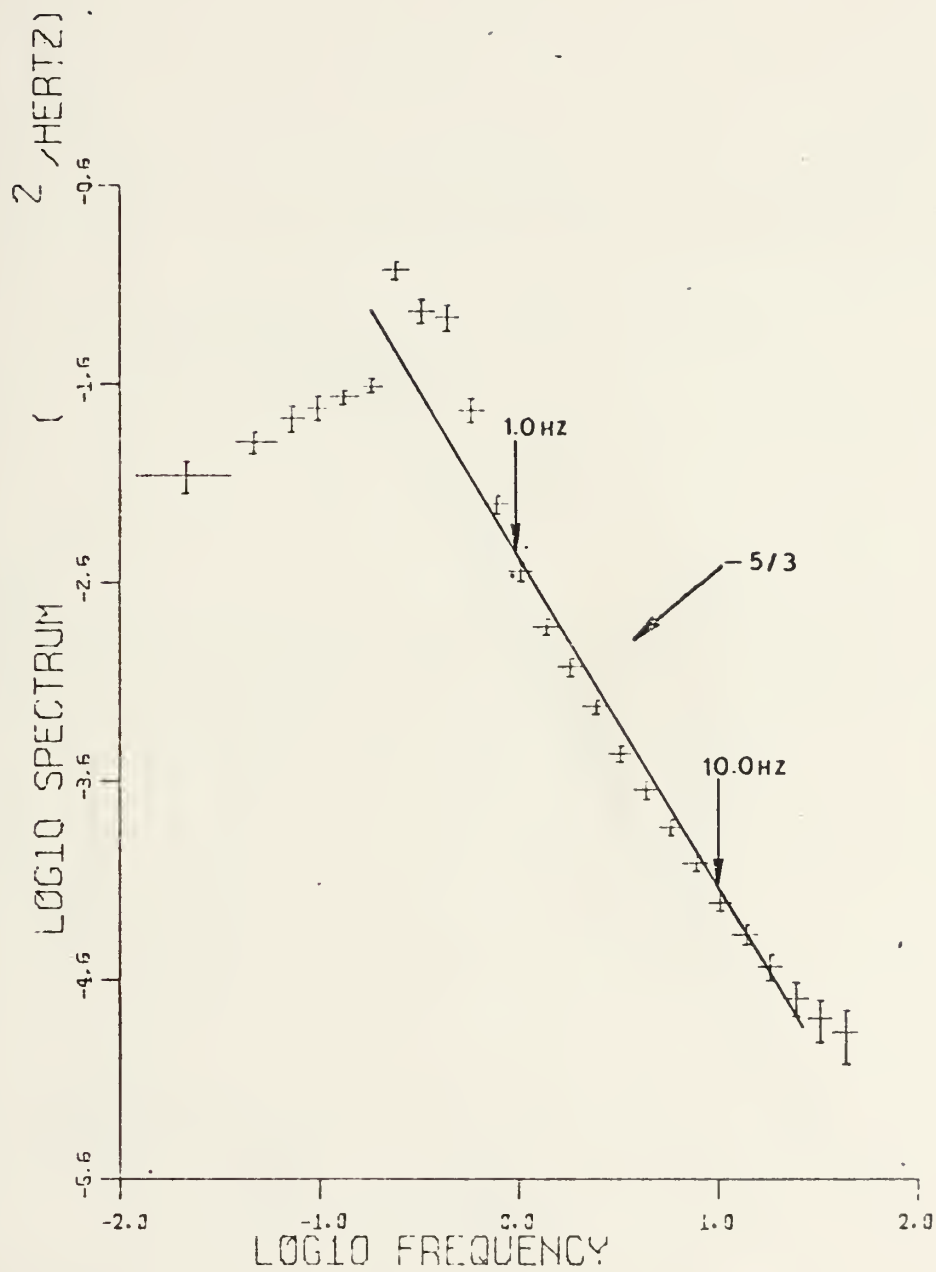


Figure 41. Hot Wire Data Observed 10 January 1973  
1st Period.



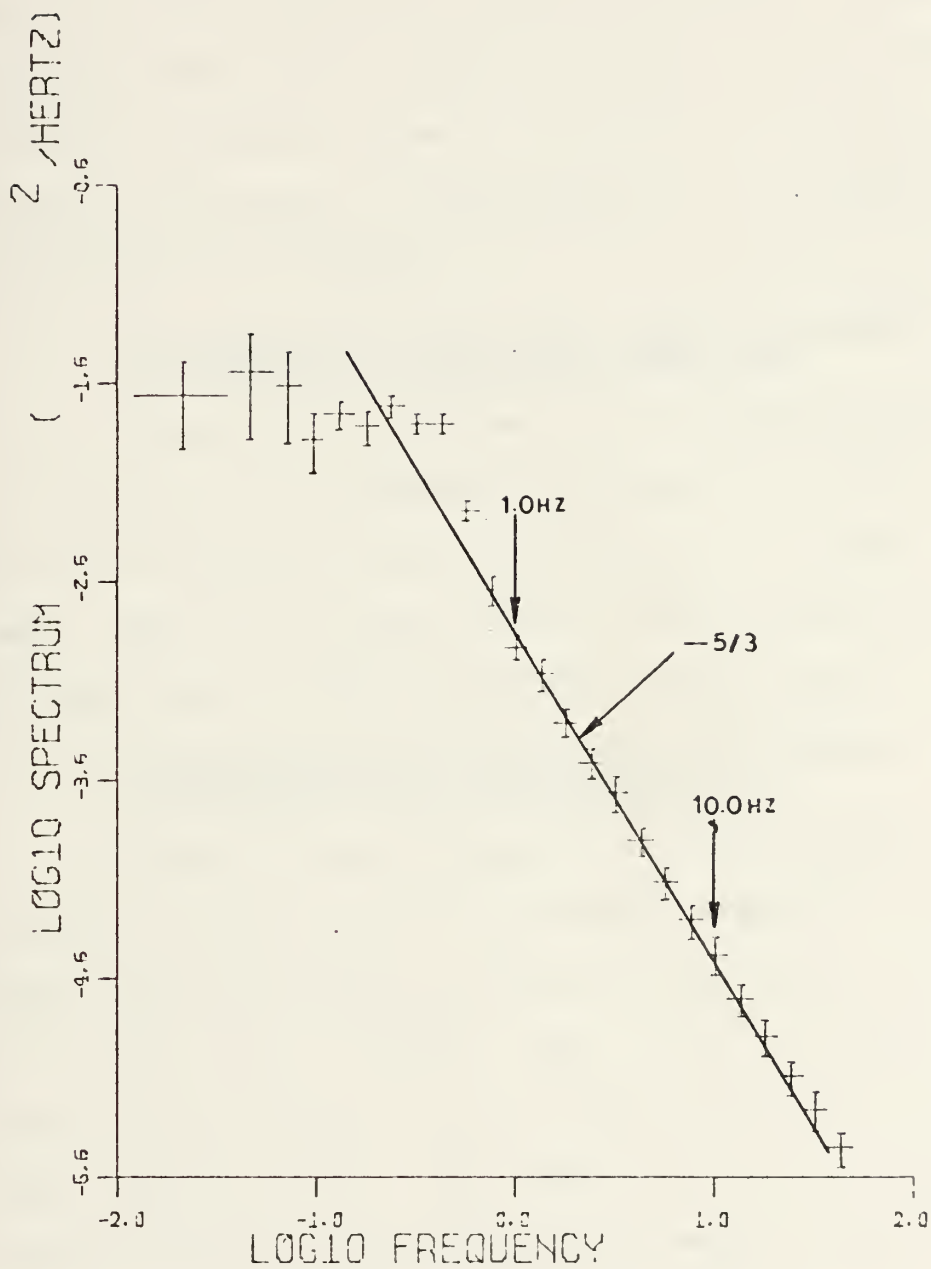


Figure 42. Hot Wire Data Observed 10 January 1973  
2nd Period.





5. Sonic Anemometer/Thermometer Data Sampled at  
62.5 Hz - 28 February 1973 (Experiment II)

Figure 43 to Figure 51 are spectra from the sonic anemometer/thermometer data recorded on 28 February 1973. Channel B was inoperative during the period. Spectra from channels A and W show a definite  $-5/3$  slope in the 1.0 Hz to 10.0 Hz frequency band. A  $-5/3$  slope in a very narrow band of frequencies of approximately 1.0 Hz to 4.0 Hz appears in the T spectra.

6. Hot Wire Anemometer Data Sampled at 200.0 Hz  
- 28 February 1973 (Experiment II)

Figure 52 and Figure 53 are hot wire spectra from the second and third periods recorded on 28 February 1973. The first period of data was lost due to a faulty magnetic tape. Spectra from both periods have definite  $-5/3$  slopes in the region 1.0 Hz to approximately 91.0 Hz.

7. Thermocouple Data Sampled at 200.0 Hz -  
28 February 1973 (Experiment II)

Figure 54 and Figure 55 are thermocouple spectra from the second and third periods recorded on 28 February 1973. The first period of data in this case was also lost due to the faulty magnetic tape. From the second period plot the  $-5/3$  slope starts at approximately 4.4 Hz and goes just beyond 10.0 Hz. From the third period plot, a definite  $-5/3$  slope exists in the range 1.0 Hz to 10.0 Hz.

## C. CONCLUSIONS

The sonic anemometer/thermometer system proved to be a reliable, rugged and easily installed instrument for the



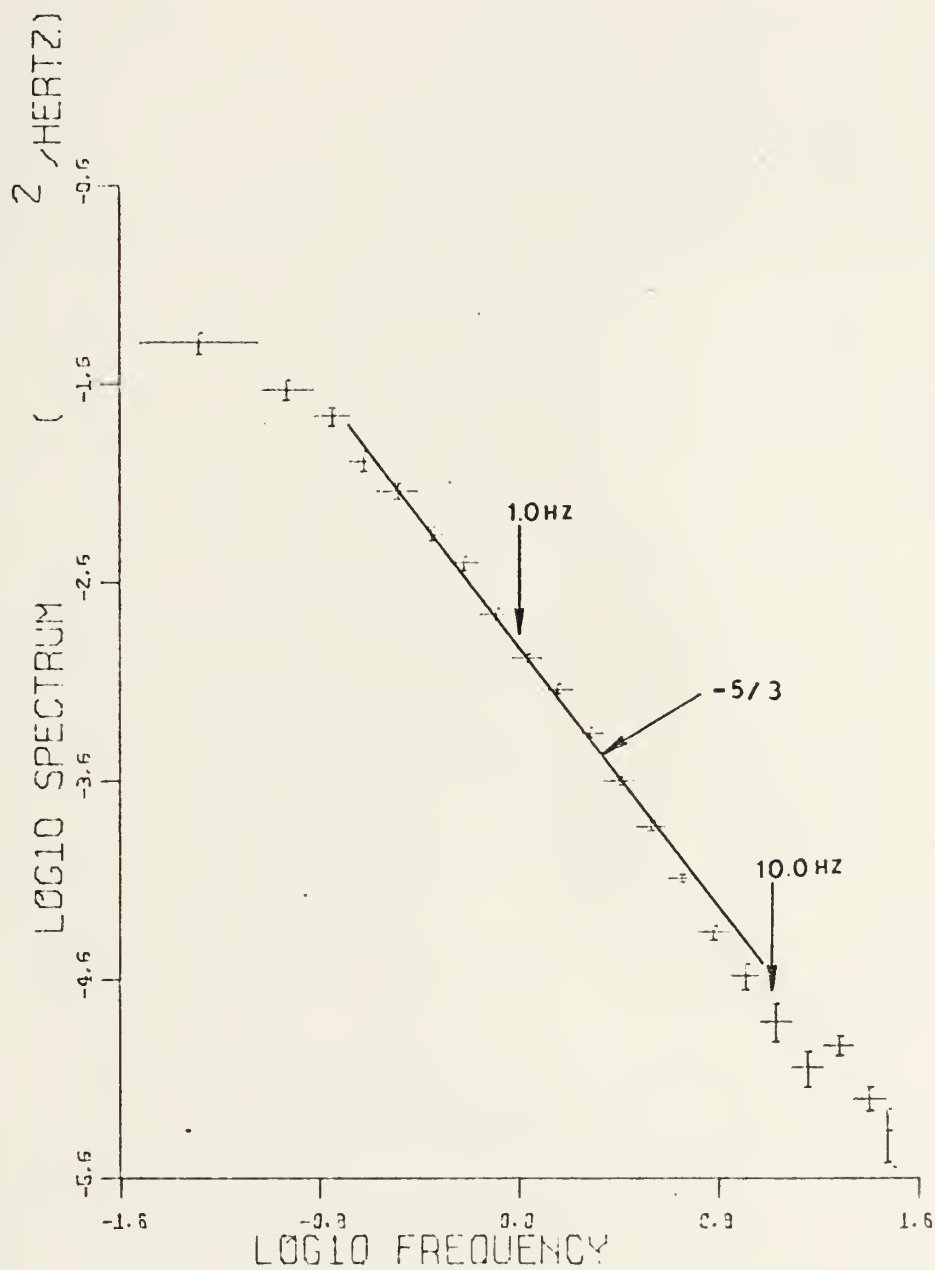


Figure 43. Sonic "A" Channel Data Observed 28 February 1973 1st Period (Experiment II).



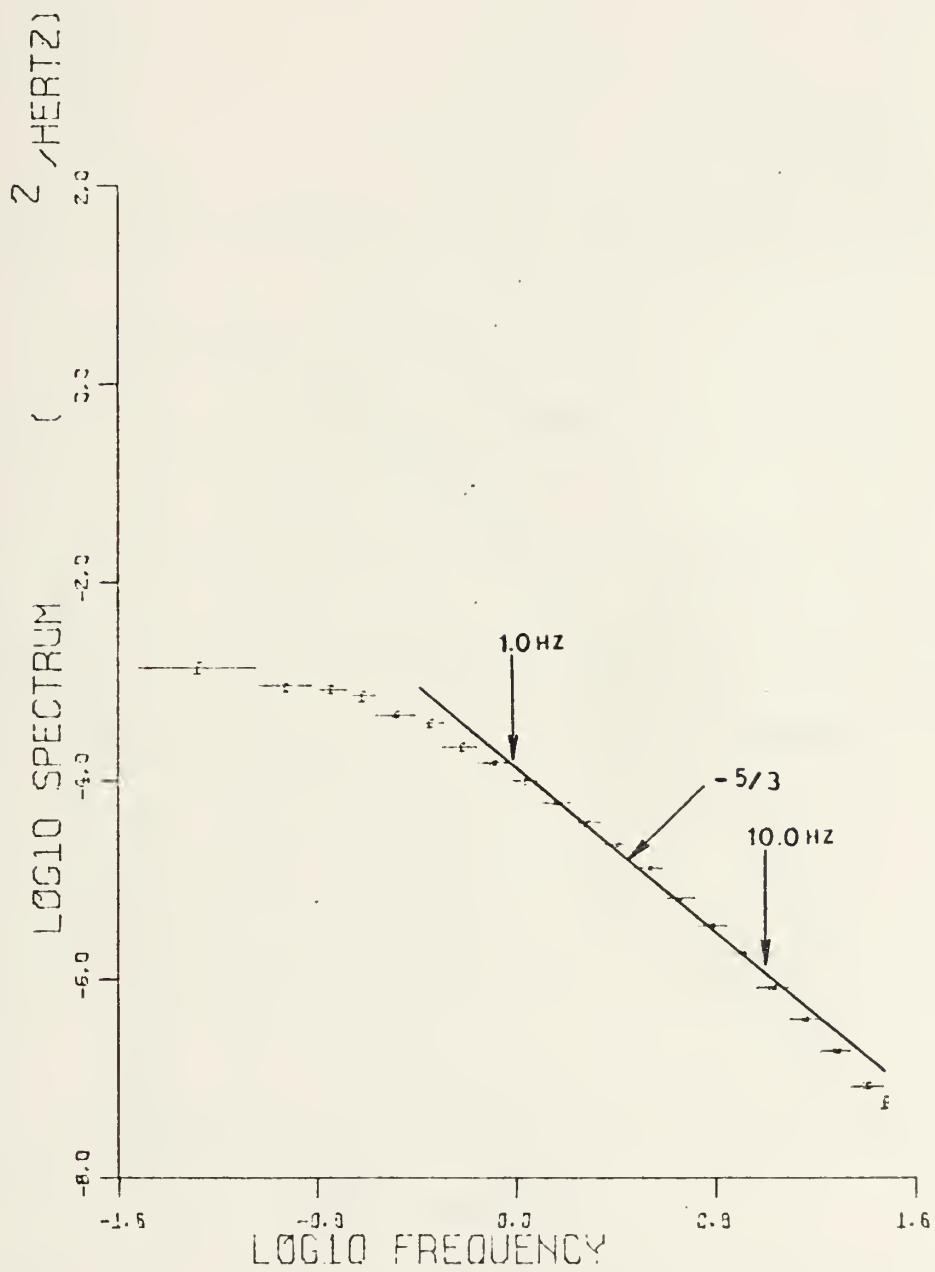


Figure 44. Sonic "W" Channel Data Observed 28 February 1973 1st Period (Experiment II).



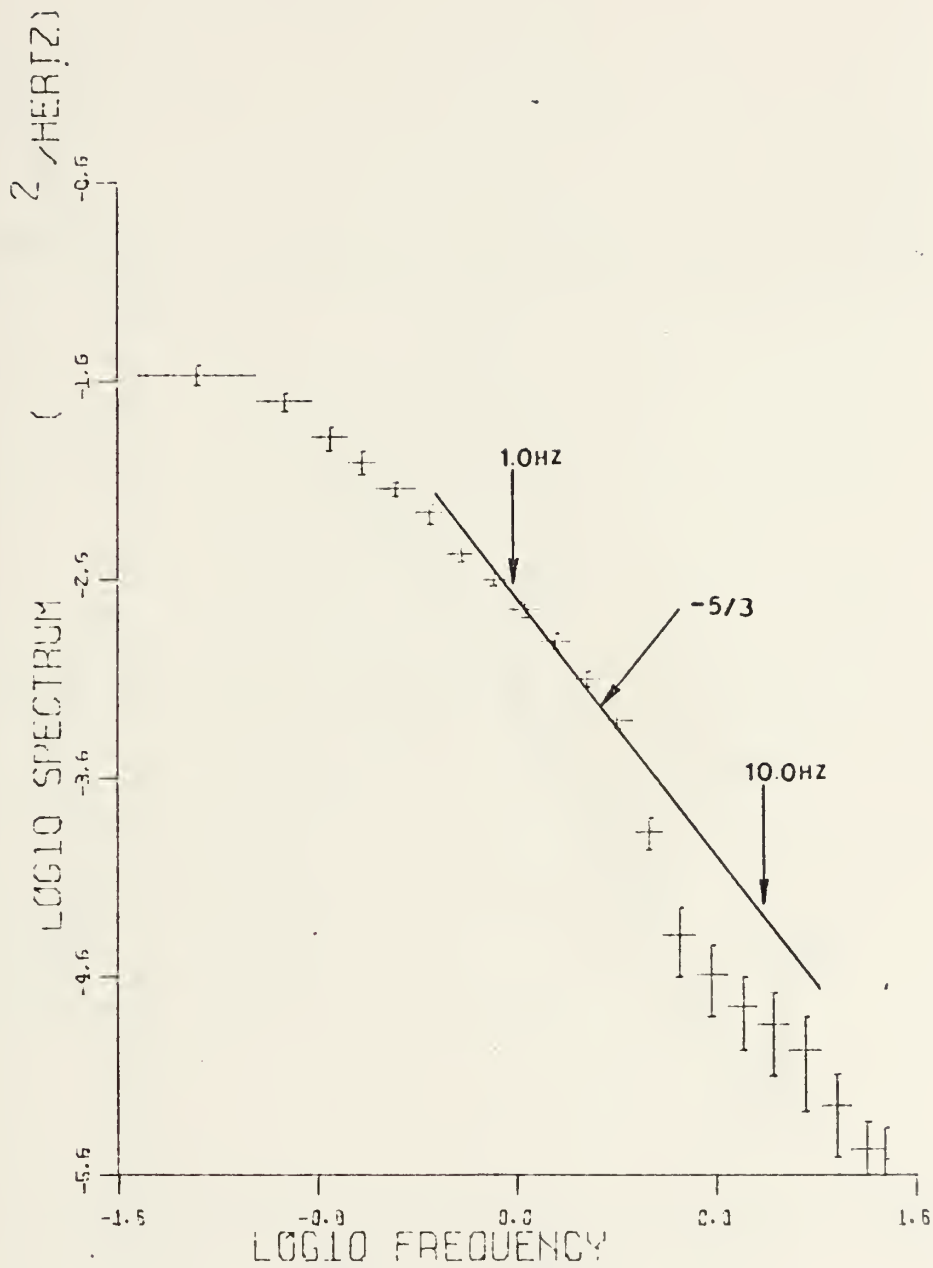


Figure 45. Sonic "T" Channel Data Observed 28 February 1973 1st Period (Experiment II).





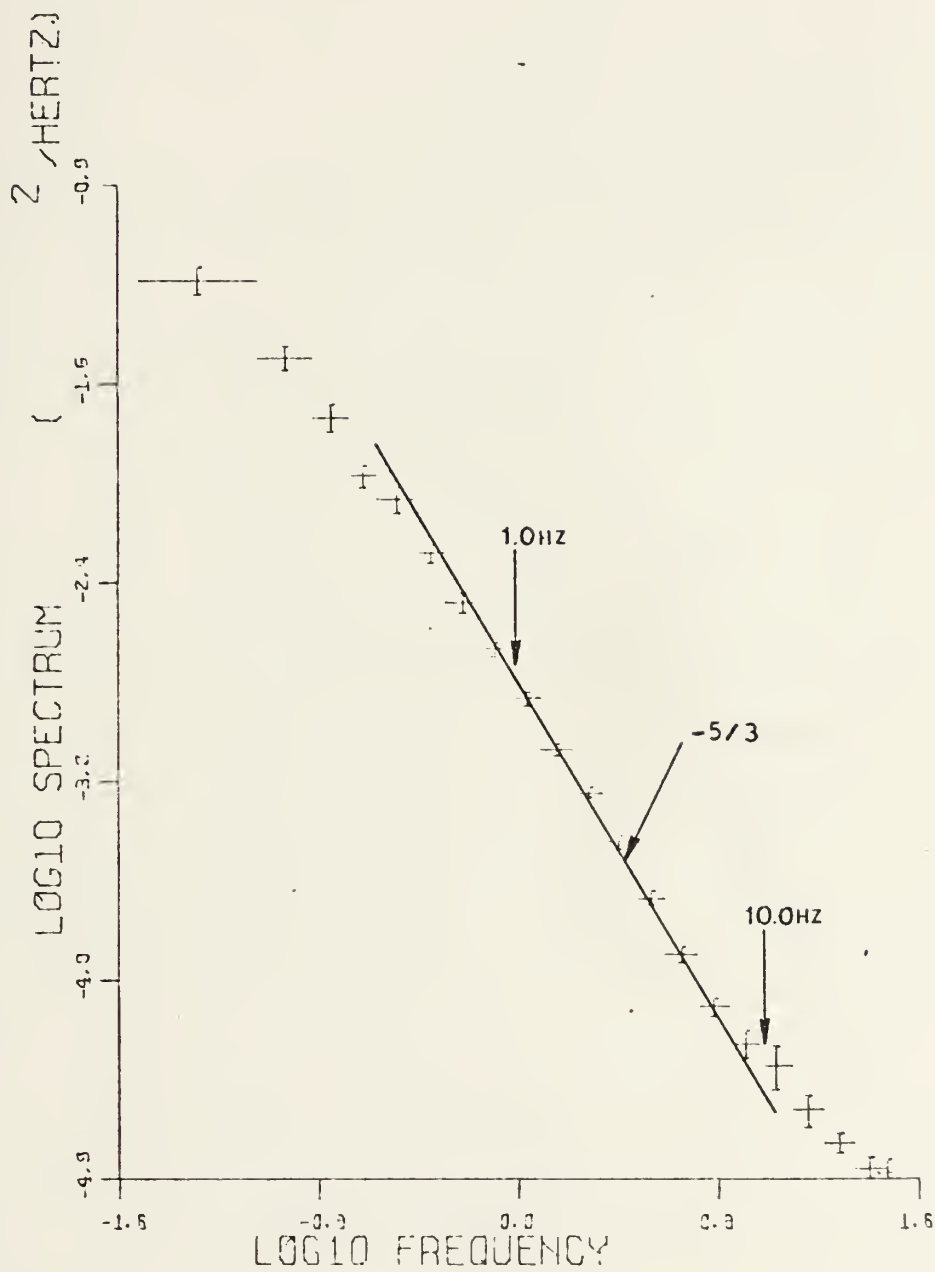


Figure 46. Sonic "A" Channel Data Observed 28 February 1973 2nd Period (Experiment II).



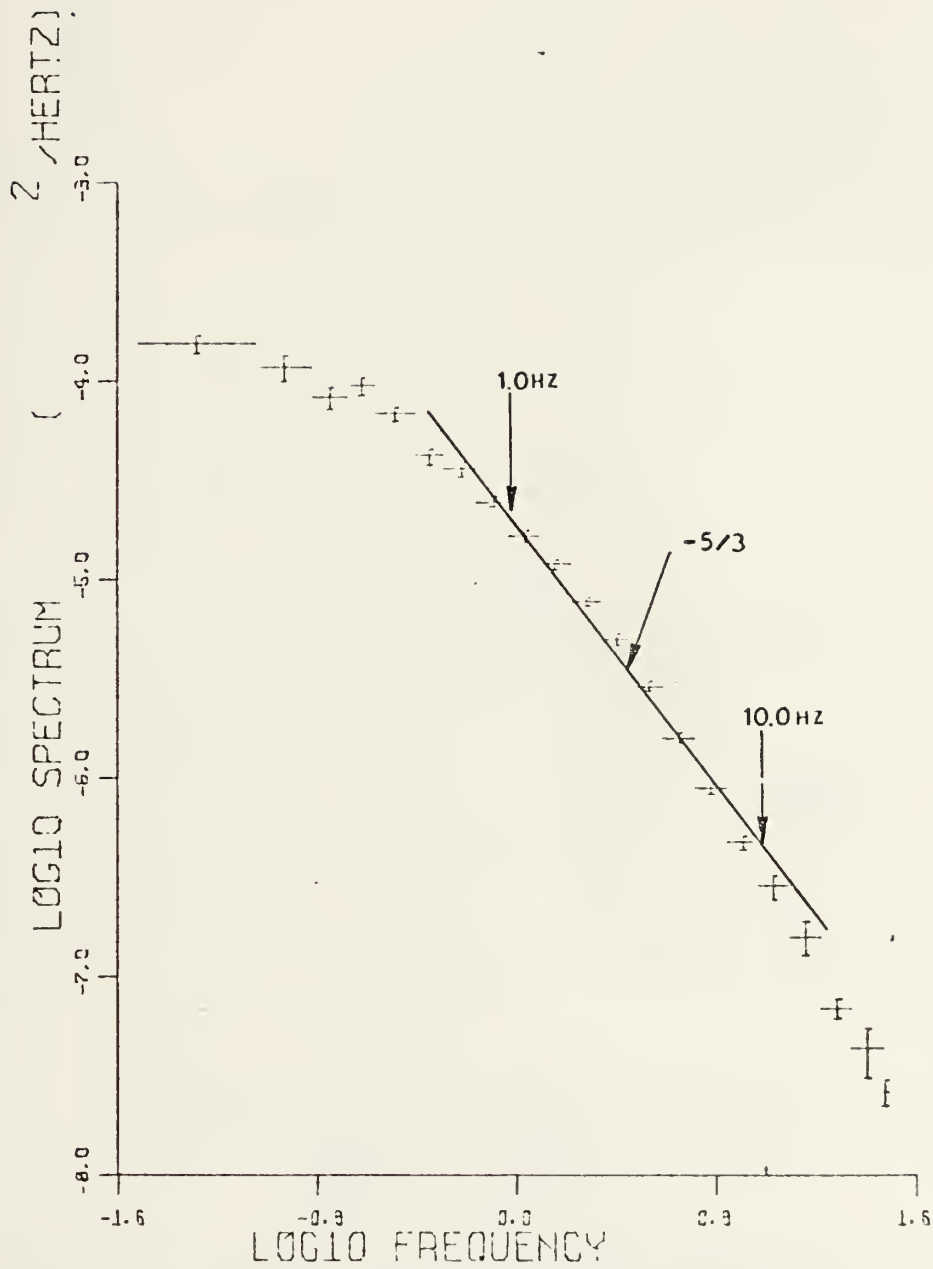


Figure 47. Sonic "W" Channel Data Observed 28 February 1973 2nd Period (Experiment II).



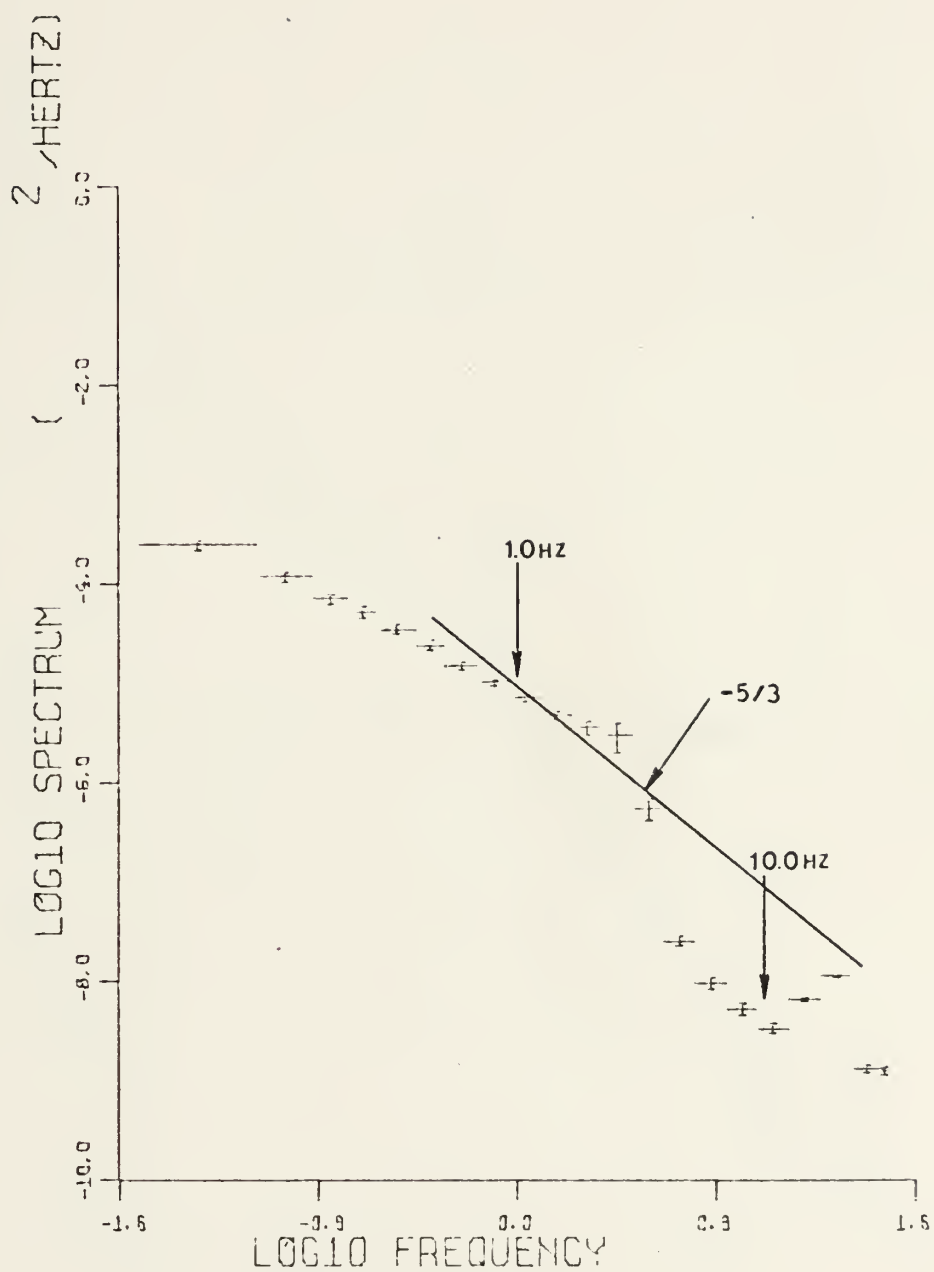


Figure 48. Sonic "T" Channel Data Observed 28 February 1973 2nd Period (Experiment II).



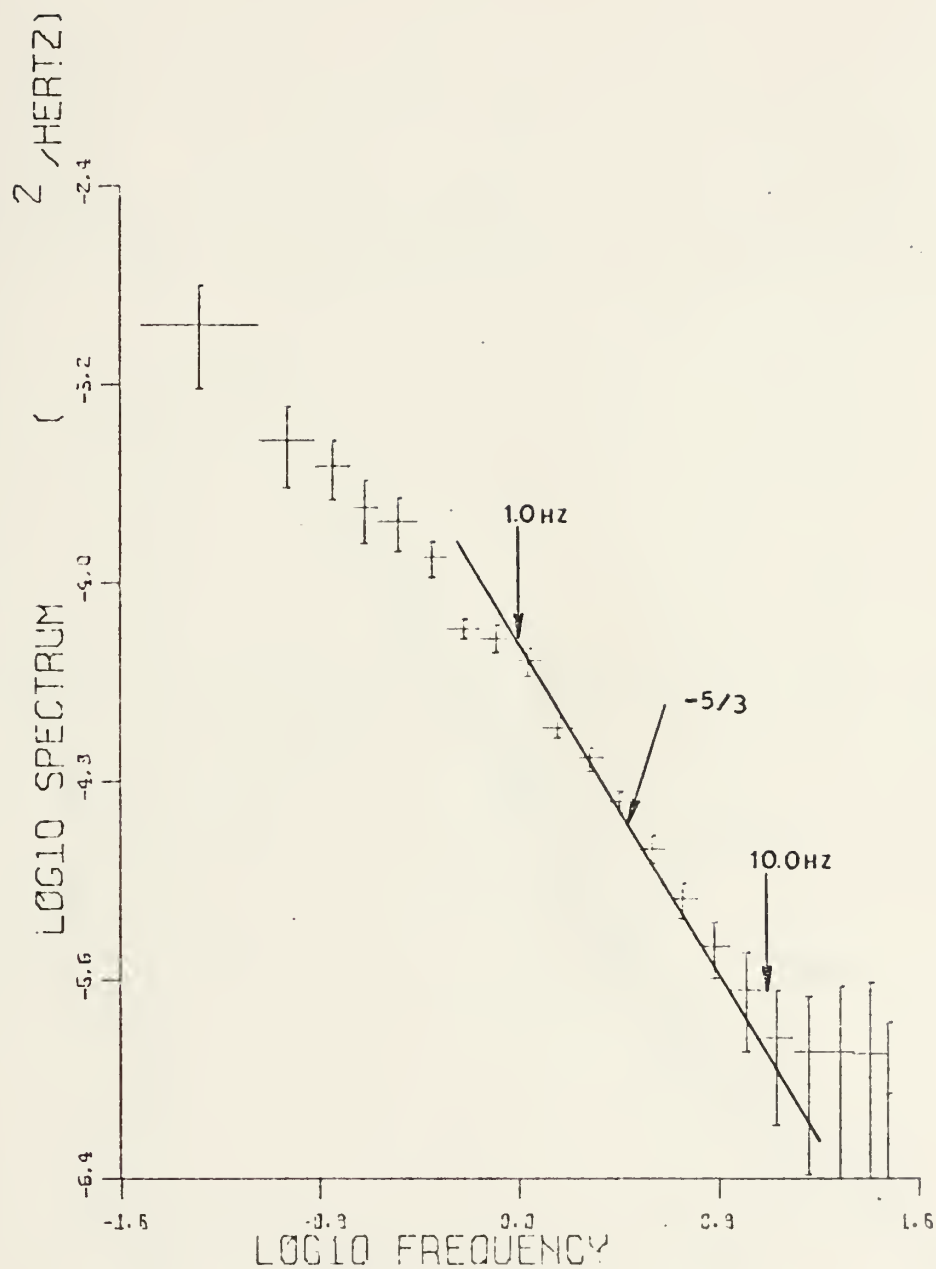


Figure 49. Sonic "A" Channel Data Observed 28 February 1973 3rd Period (Experiment II).





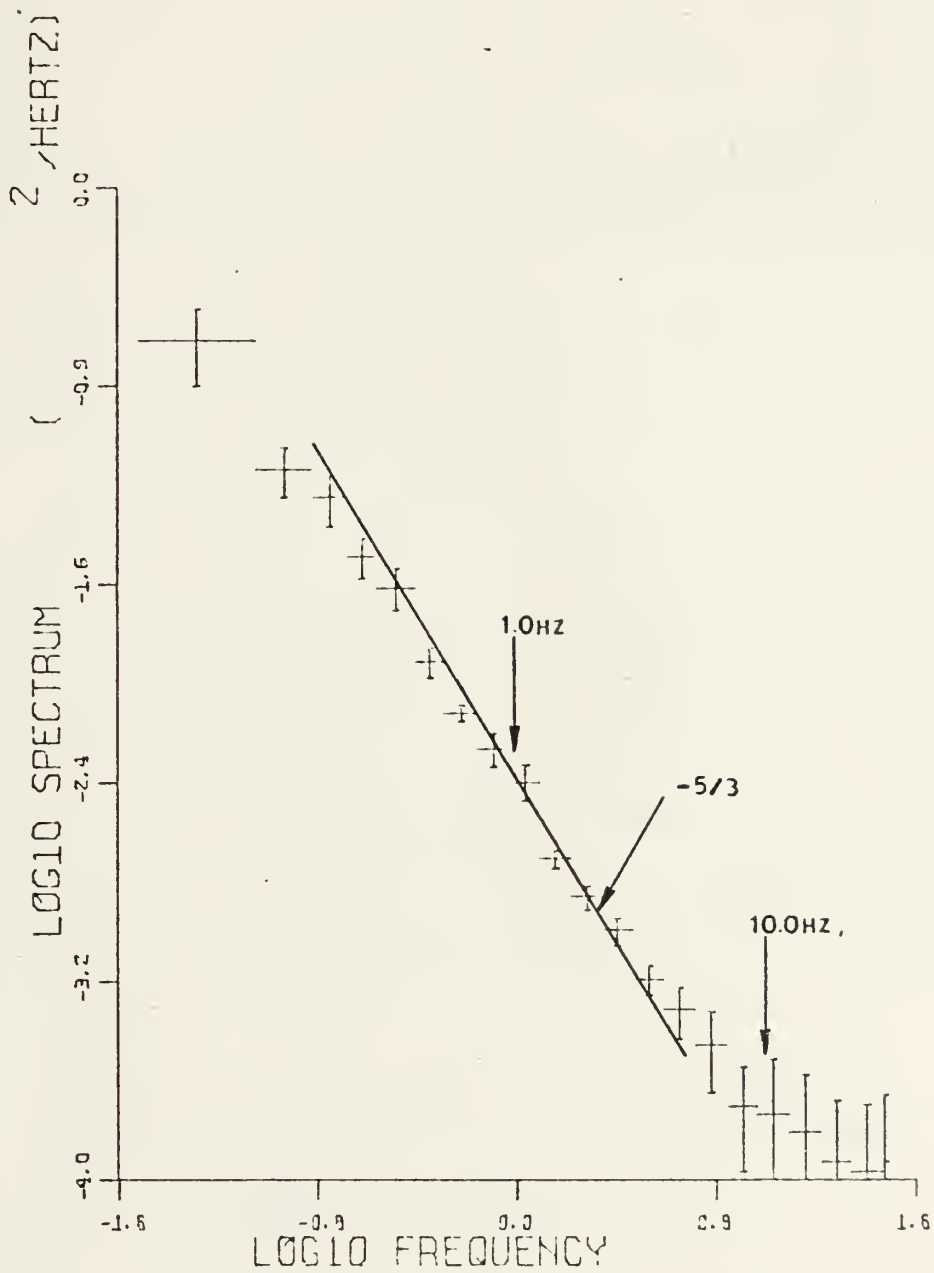


Figure 50. Sonic "W" Channel Data Observed 28 February 1973 3rd Period (Experiment II).



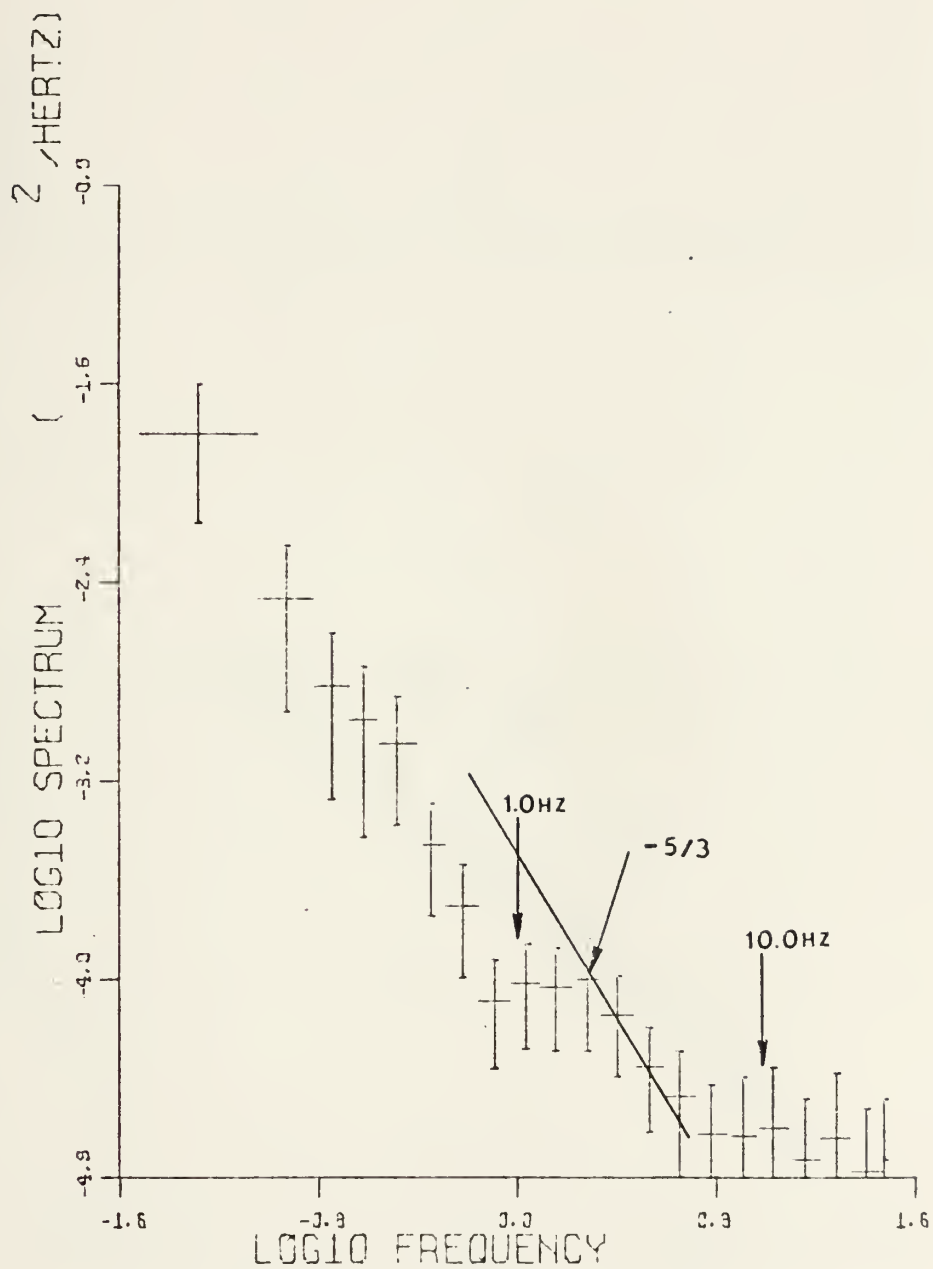


Figure 51. Sonic "T" Channel Data Observed 28 February 1973 3rd Period (Experiment II).



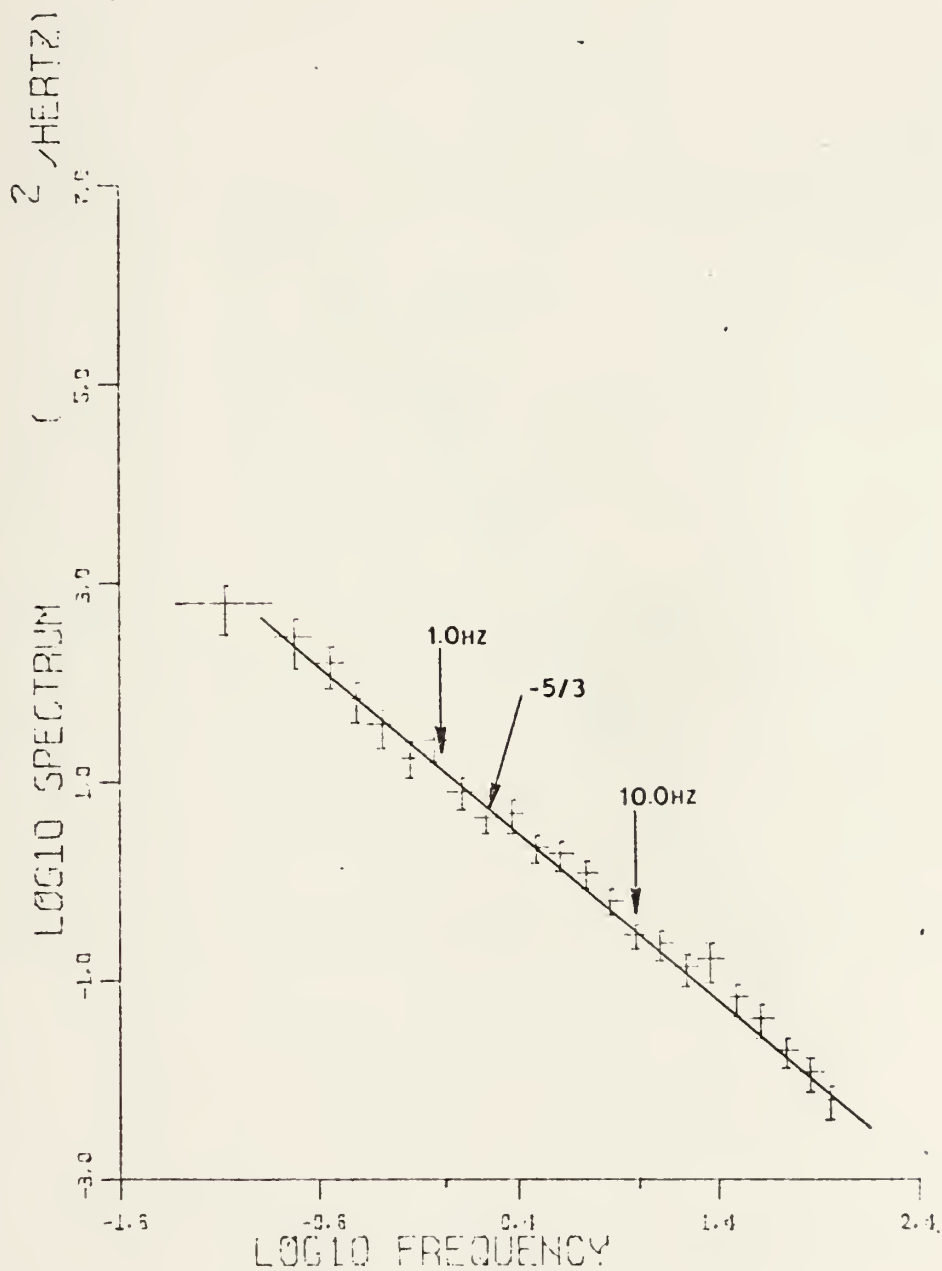


Figure 52. Hot Wire Data Observed 28 February 1973  
2nd Period (Experiment II).



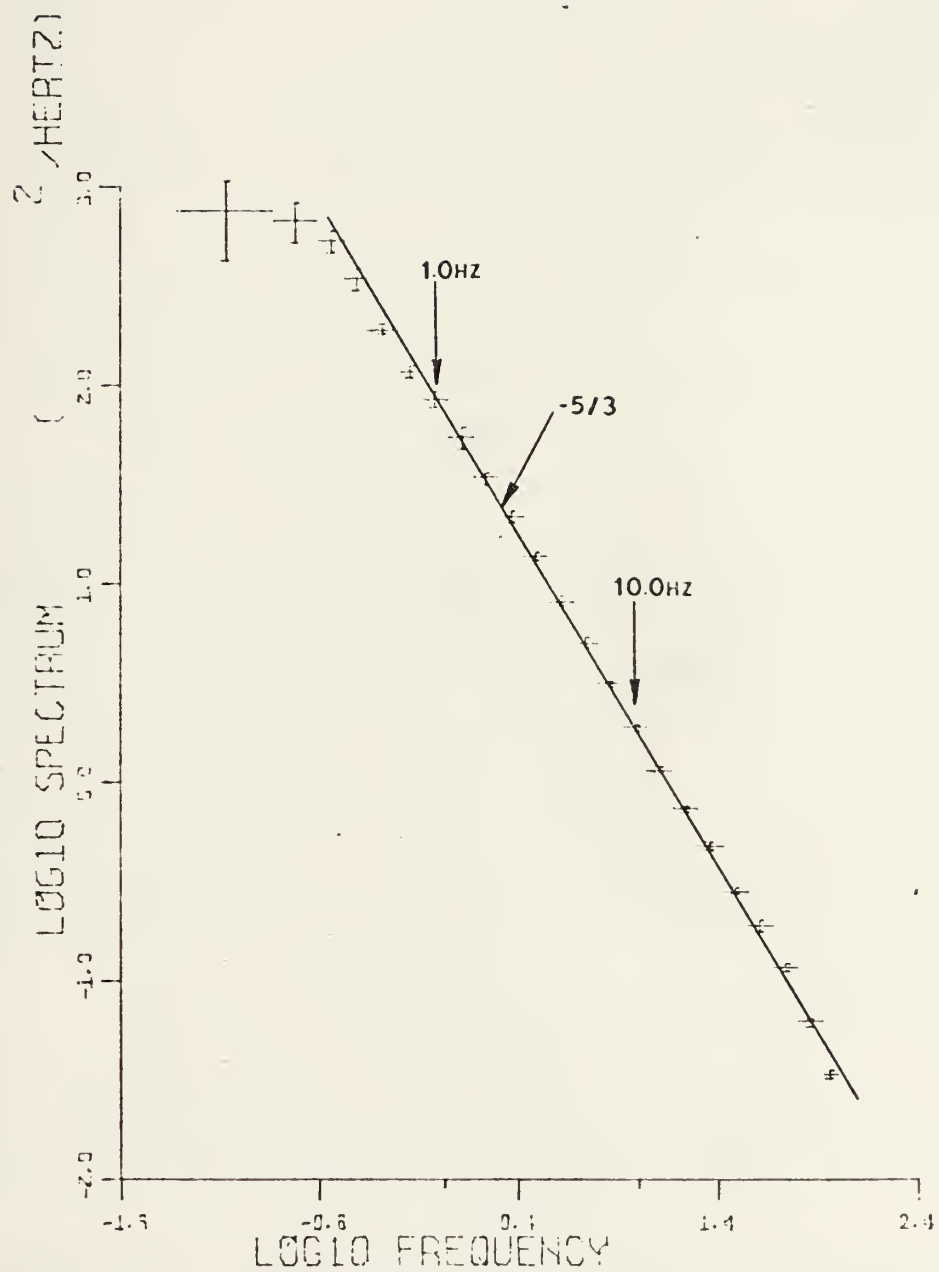


Figure 53. Hot Wire Data Observed 28 February 1973  
3rd Period (Experiment II).





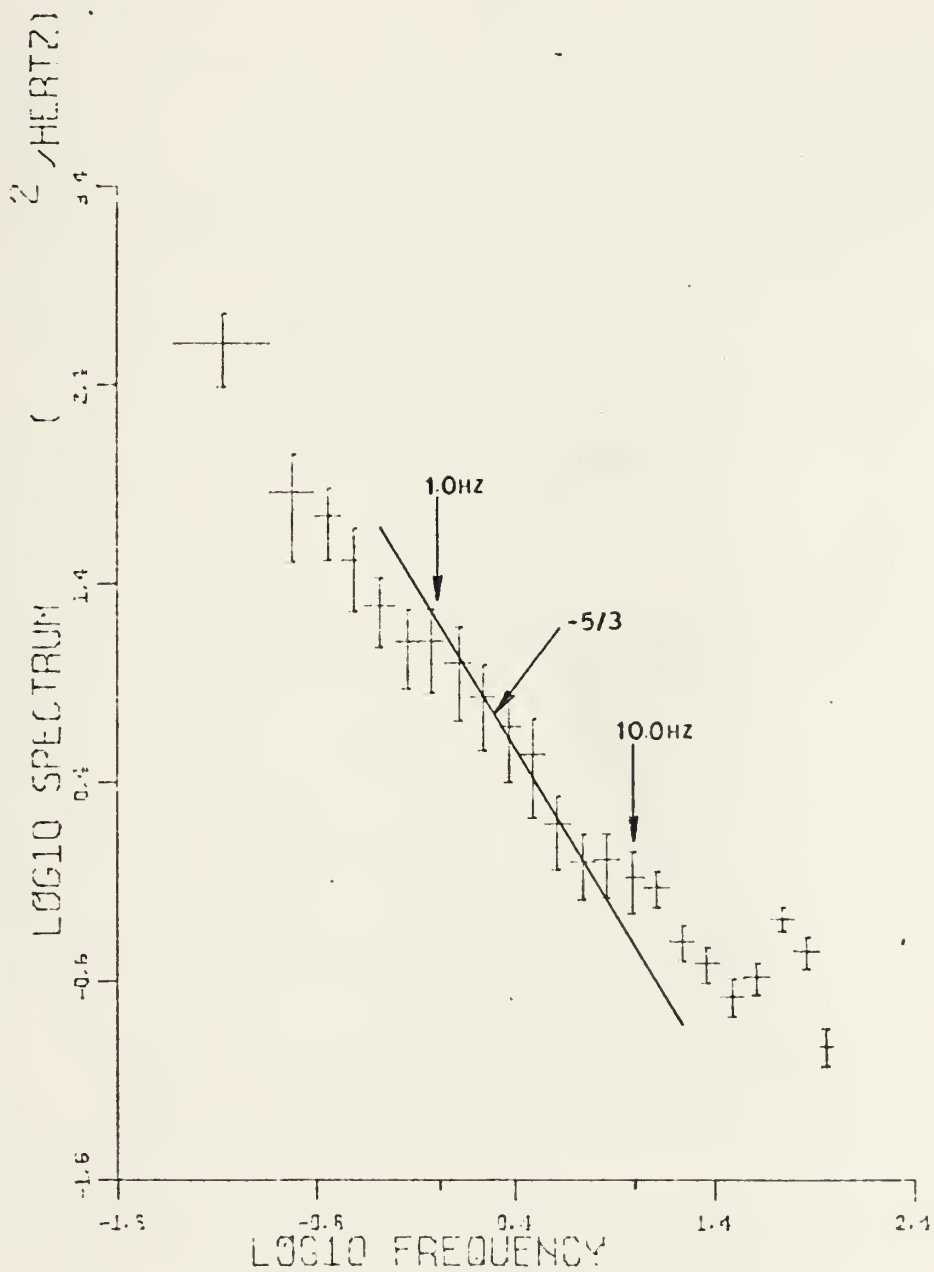


Figure 54. Thermocouple Data Observed 28 February 1973  
2nd Period (Experiment II).



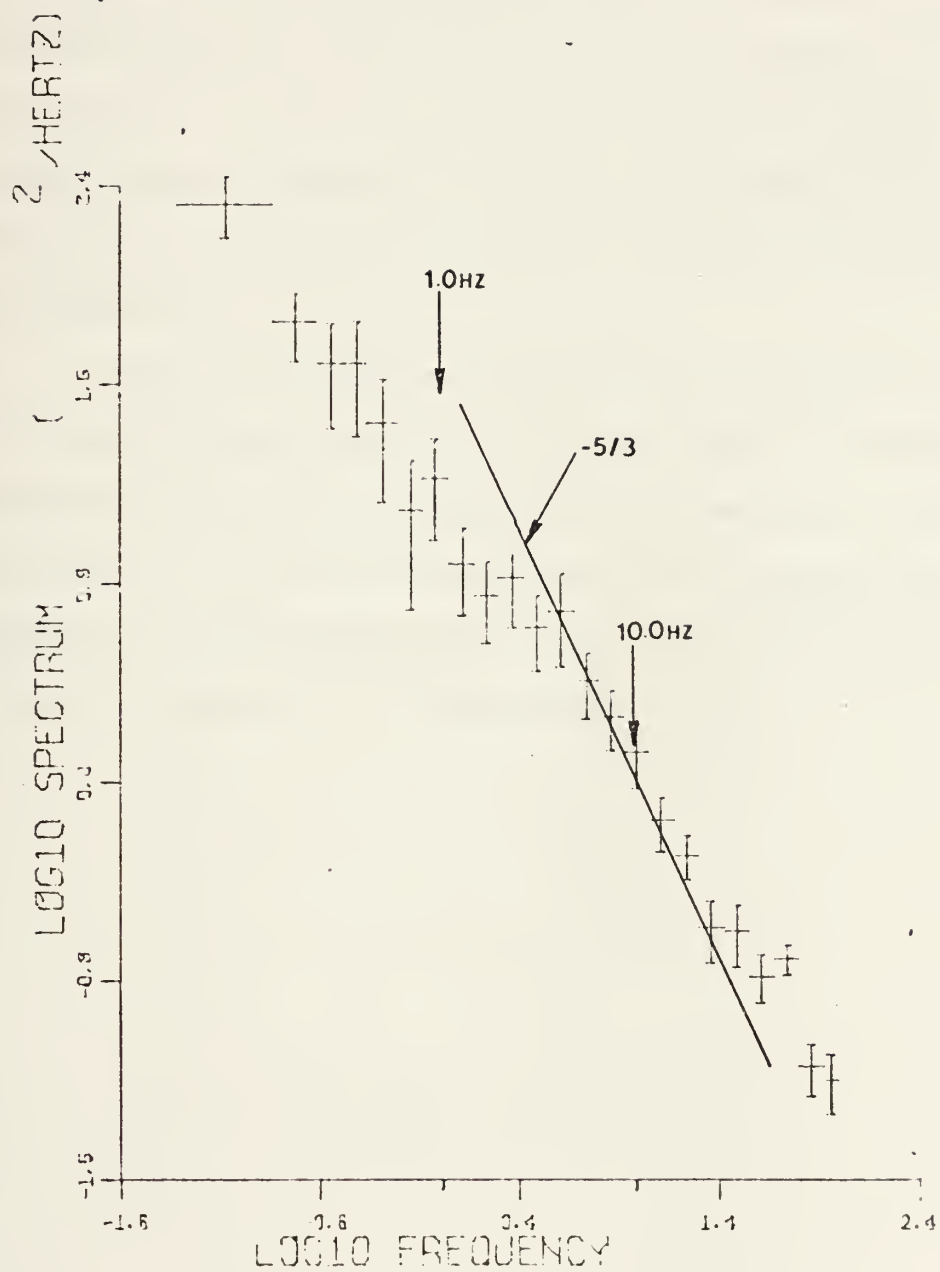


Figure 55. Thermocouple Data Observed 28 February 1973  
3rd Period (Experiment II).



measurement of the three components of the wind and also air temperature. Its frequency response was found to be from 0.0 Hz to approximately 12.0 Hz.

The sonic anemometer/thermometer measurements did not appear to be affected by weather elements and because it uses the speed of sound in air it has inherent calibration. The response of the sonic anemometer/thermometer is linear and so is its sensitivity. It is thus able to be used to describe vertical and horizontal transfers of energy, heat and momentum.

The  $-5/3$  slope of Kolmogorov's inertial subrange was easily recognizable on spectral plots of turbulence data measured by the sonic anemometer/thermometer. Thus the computation of the rate of dissipation of kinetic energy constant can be made which in turn means that heat and momentum transfer computations can be made.



## APPENDIX A

### Definition of Terms Used in Analog-Digital Data Processing

The terms used in the analog-to-digital process are defined here based on current usage in the Hybrid computer center and based on that utilized by the three time series programs for the spectral analysis of digitized data. There are some contradictions of terms between McKendrick (1971) and Jones (1971) and between what is currently used.

The word "record" is often used in both analog and digital discussions as meaning a finite length of data in seconds. In the analog sense, "record" means the entire length of data which is to be digitized. In the digital sense, "record" means a short length of data based on the sampling rate and the number of samples per record selected by the programmer. In McKendrick (1971) and Jones (1971), digital "record" is referred to as "block". The word "block" is not used in this thesis as "record" is what is utilized in all three programs (although the print outs use blocks). A digital "record" is limited in the number of samples it can contain because of Hybrid computer memory limitations. This limit is that the number of samples times the number of channels simultaneously digitized must be equal to or less than 6144 channel-samples. As an example, consider the following hypothetical problem:

record





Analog record length = 3,000 secs

Number of analog channels containing data = 5 channels

Sampling rate =  $100 \frac{\text{samples}}{\text{sec}}$

Number of channels digitized  
simultaneously = 5 channels

Samples per record selected =  $1024 \frac{\text{samples}}{\text{record}}$

$1024 \frac{\text{samples}}{\text{record}} \times 5 \text{ channels} = 5120 \frac{\text{channel-sample}}{\text{record}} \leq 6144$

$1024 \frac{\text{samples}}{\text{record}} \times \frac{1 \text{ sec}}{100 \text{ samples}} = 10.24 \frac{\text{seconds}}{\text{record}}$

Digital record length =  $10.24 \frac{\text{seconds}}{\text{record}}$

Note that the value for samples for record was chosen as an integral power of two , i.e.  $2^{10}$ . The reason is that the maximum number of data points (samples) that can be stored in the IBM 360/67 computer memory under the FTOR program are 8192 or  $2^{13}$  samples. Therefore, for efficiency purposes the FTOR program was designed to read in samples per record which contain integral powers of two.

One other commonly used word is "file." A "file" is a finite length of digital data containing any number of records from one on up. The length of a "file" is predetermined during the digitization phase and is based on the number of records desired per "file." An "end of file" mark is placed on the seven track tape after the desired number of records have been computed.



## BIBLIOGRAPHY

1. Cooley, J. W. and Tukey, J. W., "An Algorithm for the Machine Calculation of Complex Fourier Series," Mathematics of Computations, 19 (90), p. 297-301, 1965.
2. Jones, R. D., Time Series Analysis of Analog Data by Analog-to-Digital and Digital Data Processing Methods at the Naval Postgraduate School, M. S. Thesis, Naval Postgraduate School, Monterey, California, March 1971.
3. Kaijo Denki Company Ltd., Instruction Manual for Model PAT-313-1 Ultrasonic Anemometer Thermometer, Tokyo, Japan, 1969.
4. Kaimal, J. C. and others, An Improved Three-Component Sonic Anemometer for Investigation of Atmospheric Turbulence, paper presented at Symposium on Flow--Its Measurement and Control in Science and Industry, Pittsburgh, Pennsylvania, 9-14 May 1971.
5. Kainal, J. C., Wyngaard, J. C. and Haugen, D. A., "Deriving Power Spectra from a Three-Component Sonic Anemometer," Journal of Applied Meteorology, v. 7, p. 827-837, October 1968.
6. Lumley, J. L. and Panofsky, H. A., The Structure of Atmospheric Turbulence, Interscience Publishers, 1964.
7. McBean, G. A., "Instrument Requirements for Eddy Correlation Measurements," Journal of Applied Meteorology, v. 11, p. 1078-1084, October 1972.
8. McKendrick, J. D., An Investigation of Digital Spectral Analysis Programs and Computer Methods Utilized at the Naval Postgraduate School in the Analysis of High Frequency Random Signals, M.S. Thesis, Naval Postgraduate School, Monterey, California, March 1972.
9. Suomi, V. E. and Businger, J. A., "Variance Spectra of the Vertical Wind Component Derived from Observations of the Sonic Anemometer at O'Neill, Nebraska in 1953," Archiv fur Meteorology und Klimat, v. 10, p. 415, 1958.
10. Wilson, J. R., Boston, N.E.J. and Denner, W. W., Digital Analysis of Turbulence Data on the IBM 360/67 at the Naval Postgraduate School, NPS-58DW9071A, 1969.



INTERNALLY CLASSIFIED  
REPORT

INITIAL DISTRIBUTION LIST

No. Copies

<del>1. Defense Documentation Center</del>	<del>2</del>
<del>    Cameron Station</del>	
<del>    Alexandria, Virginia 22314</del>	
2. Library, Code 0212	2
Naval Postgraduate School	
Monterey, California 93940	
3. Professor Kenneth L. Davidson, Code 51Ds	5
Department of Meteorology	
Naval Postgraduate School	
Monterey, California 93940	
4. Professor Noel E.J. Boston, Code 58Bs	1
Department of Oceanography	
Naval Postgraduate School	
Monterey, California 93940	
5. Professor Charles Taylor, Code 51Ta	1
Department of Meteorology	
Naval Postgraduate School	
Monterey, California 93940	
6. Professor Thomas E. Houlihan, Code 59Hm	5
Department of Mechanical Engineering	
Naval Postgraduate School	
Monterey, California 93940	
7. Lieutenant Commander Peter D. Quinton, USN	3
390-B Ricketts Road	
Monterey, California 93940	
<del>8. Naval Weather Service Command</del>	<del>1</del>
<del>    Naval Weather Service Headquarters</del>	
<del>    Washington Naval Yard</del>	
<del>    Washington, D. C. 20390</del>	



## DOCUMENT CONTROL DATA - R &amp; D

(Security classification of title, body of abstract and indexing annotation must be entered when the overall report is classified)

ORIGINATING ACTIVITY (Corporate author)

Naval Postgraduate School  
Monterey, California 93940

2a. REPORT SECURITY CLASSIFICATION

Unclassified

2b. GROUP

REPORT TITLE

Turbulence Measuring System Utilizing  
a Sonic Anemometer/Thermometer

DESCRIPTIVE NOTES (Type of report and, inclusive dates)

Master's Thesis; March 1973

AUTHOR(S) (First name, middle initial, last name)

Peter Douglas Quinton

REPORT DATE

March 1973

7a. TOTAL NO. OF PAGES

99

7b. NO. OF REFS

10

10. CONTRACT OR GRANT NO.

9a. ORIGINATOR'S REPORT NUMBER(S)

b. PROJECT NO.

9b. OTHER REPORT NO(S) (Any other numbers that may be assigned  
this report)

10. DISTRIBUTION STATEMENT

Approved for public release; distribution unlimited.

11. SUPPLEMENTARY NOTES

12. SPONSORING MILITARY ACTIVITY

Naval Postgraduate School  
Monterey, California 93940

13. ABSTRACT

The general characteristics and the bandwidth responses of the Kaijo Denki PAT 313-1 sonic anemometer/thermometer were examined. Measurements were compared to those of a hot wire anemometer system and a one mil thermocouple system. Turbulence data were obtained by all three systems simultaneously in two experiments conducted at a beach site. The sonic anemometer/thermometer system proved to be a reliable, rugged, easily installed system with a bandwidth response of from 0.0 Hz to approximately 12.0 Hz.





### KEY WORDS

LINK A

LINK B

LINK C

ROLE

WT

ROLE

WT

ROLE

WT

### Sonic Anemometer/Thermometer

## Anemometer System



CONFIDENTIAL

Thesis  
Q725  
c.1

Quinton

Turbulence measuring  
system utilizing a  
sonic anemometer/  
thermometer.

143845

6 JUN 84

30069

Thesis  
Q725  
c.1  
-

Quinton

Turbulence measuring  
system utilizing a  
sonic anemometer/  
thermometer.

143845

INTERNALLY  
DISTRIBUTED REPORT

thesQ725

Turbulence measuring system utilizing a



3 2768 001 93089 4

DUDLEY KNOX LIBRARY